CNP-expressing progenitors display strikingly differential oligodendroglial or multipotent fates, as assessed by two Cre reporter lines

Dissertation

Zur

Erlangung des Doktorgrades (Dr. rer. nat.)

der

Mathematisch-Naturwissenschaftlichen Fakultät

der

Rheinischen Friedrich-Wilhelms-Universität Bonn

vorgelegt von

Reshmi Tognatta

aus

Neu Delhi

India

Bonn, 2012

Angefertigt mit Genehmigung der Mathematisch-Naturwissenschaftlichen
Fakultät der Rheinischen Friedrich-Wilhelms-Universität Bonn

Referent 1:   Prof. Dr. Dirk Dietrich
Referent 2:   Prof. Dr. Klaus Willecke

Tag der Promotion: 18.12.12

 Erscheinungsjahr: 2012

Acknowledgement

Table of contents

Abbreviations

AAV	adeno-associated virus
AEP	anterior entopeduncular area
AMPA	alpha-amino-3-hydroxy-5-methyl-4-isoxazole propionic acid
BBB	blood brain barrier
bHLH	basic helix loop helix
BLBP	brain lipid binding protein
BMP	bone morphogenetic protein
BrdU	5-bromo-2-deoxyuridine
CA	cornu ammonis
CC	corpus callosum
CGE	caudal ganglionic eminence
CNP	2',3'-cyclic nucleotide-3'-phosphodiesterase
CNS	central nervous system
Cre	cyclization recombination enzyme
D.Ctx	dorsal cortex
DNA	deoxyribonucleic acid
EGFP	enhanced green fluorescent protein
EPSC	excitatory postsynaptic currents
EYFP	enhanced yellow fluorescent protein
FCS	fetal calf serum
Fim	fimbrae
GABA	gamma-amino butyric acid
GFAP	glial fibrillary acidic protein
GFP	green fluorescent protein
GLAST	glutamate aspartate transporter
GluR	glutamate receptor
KO	knockout

LGE	lateral ganglionic eminence
MAG	myelin associated glycoprotein
MBP	myelin basic protein
MGE	medial ganglionic eminence
MOG	myelin/oligodendrocyte glycoprotein
mRNA	messenger ribonucleic acid
NeuN	neuronal nuclei
NG2	neuron-glia antigen: chondroitin sulphate proteoglycan
NMDA	N-methyl-D-aspartate
NPC	neural precursor cell
n.s	non-significant
O-2A	oligodendrocyte-type-2 astrocyte
OPC	oligodendrocyte precursor cell
PBS	phosphate-buffered saline
PDGFRα	platelet derived growth factor receptor
PFA	paraformaldehyde
Piri.Ctx	piriform cortex
PLP	proteolipid protein
pMN	progenitor motor neuron
RMS	rostral migratory stream
RT	room temperature
SEM	standard error mean
SGZ	subgranular zone
SVZ	subventricular zone
TN-C	tenascin
VZ	ventricular zone
V.Ctx	ventral cortex
WT	wildtype
Z/EG	*lacZ*/EGFP

1   Introduction

Cellular constituents of the mammalian central nervous system (CNS) consist of neurons and glia. While neurons are known to be the principal signalling cells, glial cells were historically considered merely inert supportive cells. The past two decades have seen a dramatic evolution in this concept, and glial cells are today recognized as active participants in the neural circuitry.

The multitude of neuronal and glial cell types of the mature CNS are generated from a homogenous pool of neural precursor cells in the embryonic neural tube, called the neuroepithelial precursors (NEPs). During initial embryonic developmental stages, NEPs display multipotency and have the ability to give rise to both neurons and glia; however with time their potential becomes more restricted towards either a neuronal or glial fate. A key question in developmental biology is whether specialised glial fate-restricted precursor cells display lineage plasticity.

I shall now provide a brief overview to the types of glial cells in the CNS for us to appreciate the diversity of these complex glial subtypes. Furthermore, I will then focus on the origin and development of perhaps the most intriguing glial cell type: the oligodendroglia.

1.1   Glial cells of the CNS

The major glial cell population can be divided into two sub-groups: microglia and macroglia based on their developmental origin (Figure 1).
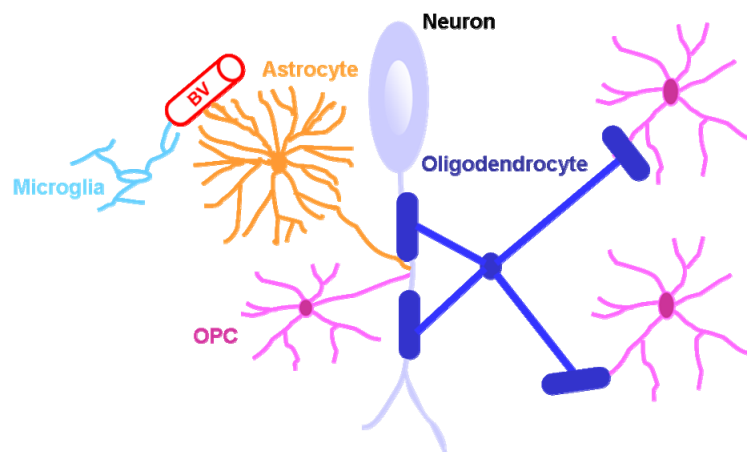
Figure 1. Schematic representation of glial cells in the CNS, their interactions with neurons and amongst themselves. BV, Blood Vessel; OPC, Oligodendrocyte Precursor Cell**.**

Microglial cells are descendants of haemopoietic precursors and macroglial cells that include oligodendrocytes and astrocytes are derived from neural tube precursors.

1.1.1 Microglia

In 1932 Rio-Hortega described these resident macrophages of the brain parenchyma. Ramified or resting microglia have a crucial scavenger function in the developing brain by removing away large number of cells in the neocortex that die in the course of normal remodelling of the fetal brain (Voyvodic, 1996). Each individual microglial cell covers a large area of 50,000 μm^3, never coming in contact with another microglial cell. Within the gray matter, microglial cells extend their processes in all directions; while white matter microglia align their processes perpendicular to white matter tracts.

In the healthy brain, resting microglia have a typical ramified morphology consisting of a small cell body, long slender processes with secondary branching and lamellipodia. During CNS insult, microglial morphology changes; the ramified microglia processes retract, become more amoeboid-like, and transform into the reactive microglia which contribute to defence of the compromised system (Xiang et al., 2006).

1.1.2 Astrocytes

Astrocytes were discovered by Ramon y Cajal; they occupy 25% to 50% of brain volume. Their functions include regulating extracellular ion concentrations, maintaining the blood brain barrier and providing trophic support as well as nutrients to neurons and oligodendrocytes. In the adult CNS, astrocytes are uniformly distributed across the parenchyma where they associate with blood vessels, the pial surface, neurons, oligodendrocytes and other astrocytes. Astrocytes communicate with each other via calcium signals at connexin-constituted gap junctions; they also invest neuronal cell bodies, dendrites and synapses (Kosaka and Hama, 1986; Ventura and Harris, 1999).

Astrocytes, like oligodendrocytes and neurons arise from embryonic precursors of the neural tube via radial glial cells starting from E13-E15 and continuing into late embryonic ages (Chan-Ling et al., 2009; Fogarty et al., 2005; Voigt, 1989; Malatesta et al., 2003). Radial glia transformation into astrocytes also occurs postnatally in some regions of the rodent brain (Kriegstein and Alvarez-Buylla, 2009).

Astrocytes display diverse morphology based on their structural and functional interactions with their microenvironment. In the gray matter, astrocytes are described as proto-

plasmic, owing to their compactness, profuse short stubby processes and a dense network of lamellar side processes extending from primary processes. Astrocytes in the white matter have a relatively simple morphology. They are more elongated, with 50-60 long processes extending from the cell body and oriented in parallel to axons (Miller and Raff, 1984). However, common features in both protoplasmic and fibrous astrocytes are presence of thick primary processes and the formation of processes which bear so-called end feet projections on blood vessels. *In vitro* studies also categorise astrocytes as type I- having a fibroblast-like morphology and being present in both white as well as gray matter cultures, and type II- having a neuron-like morphology and being present only in white matter cultures (Raff et al., 1983a).

The astrocytic cytoskeleton is constituted by 9 nm intermediate filaments composed of a unique glial fibrillary acidic protein (GFAP) (Bignami et al., 1972), as well as a less cell-specific filament protein- vimentin (Dahl, 1981).

1.2   The oligodendroglial lineage

1.2.1 Oligodendrocytes

Rapid conduction of nerve impulses is a priority for the nervous system of animals constantly challenged with life and death situations. The strategy adopted by invertebrates for faster conduction of action potentials involved increasing the axonal diameter to decrease electrical resistance. For instance, the giant squid axons are upto 1 mm in diameter and have rapid nerve conduction velocities. The need for a compact, powerful and energetically frugal nervous system in vertebrates did not allow for *"axonal gigantism"* and therefore a major evolutionary step was wrapping axons in insulating membranes of myelin sheathes: myelination (Hartline and Colman, 2007).

Discovery of the myelinated nerve fibre is credited to Ehrenberg in 1833. Myelin ensheathes the axon with periodic interruptions at the Nodes of Ranvier, such that the action potential jumps from one node to the other. Such a *"saltatory"* mode of impulse conduction greatly increases conduction velocity as well as efficiency (Bunge, 1968; Hirano, 1968). Disruption of myelin due to injury or pathological degeneration causes severe loss of neurologic functions (Fancy et al., 2011).

Oligodendrocytes are the cellular components of the CNS responsible for the production of myelin.

The term *"oligodendroglia"* was coined by Rio-Hortega in 1921 to refer to neuroglial cells with few processes. Characteristic morphological features of oligodendrocytes include a high density of nucleus and cytoplasm, absence of intermediate filaments and of glycogen and a high number of microtubules (25 nm) in their processes, which contact the axonal length (Lunn et al., 1997). Oligodendrocyte/myelin markers such as 2',3'-cyclic nucleotide-3'-phosphodiesterase (CNP), proteolipid protein (PLP), myelin associated glycoprotein (MAG), myelin/oligodendrocyte glycoprotein (MOG) and myelin basic protein (MBP) have been used to study oligodendrocyte function and subsequent myelin defects (Baumann and Pham-Dinh, 2001).

Progenitor cells of the oligodendroglial lineage give rise to the mature myelinating oligodendrocyte via an intermediate premyelinating oligodendrocyte stage (explained in section 1.2.3.4). The oligodendrocyte precursor cells (OPCs) are regarded as the fourth glial cell population of the CNS. OPCs persist within the brain throughout life, long after developmental myelination ceases; thereby suggesting that these cells have other functions in the CNS in addition to their progenitor role. OPCs arise in specialised ventral domains of the spinal cord and forebrain around embryonic day (E) 12.5 (Miller, 2002). The next section 1.2.2 is devoted to several aspects of OPC origin, development, morphology, physiology and fate choice.

1.2.2 Oligodendrocyte precursor cells (OPCs)

The immediate ancestor of the oligodendroglial cell is a precursor that *in vitro* has the ability to generate both oligodendrocytes and type-2 astrocytes, thus the name "O-2A" progenitor cell (Raff et al., 1983). The controversy whether during normal *in vivo* development these O-2A precursor cells give rise to astrocytes, has given way to a more acceptable term: the *"oligodendrocyte precursor cell* (Noble et al., 2005; Richardson et al., 2011).

Historical perspective: discovery of markers for OPCs

The story of the oligodendroglial precursor cells began almost 35 years ago with the discovery of what are considered the immediate ancestor of the oligodendroglial cell- the "O-2A" progenitor cell, that *in vitro* had the ability to generate both oligodendrocytes and type-2 astrocytes (Raff et al., 1983). Several molecular markers such as the Nerve/Glial antigen- 2 or NG2 and platelet derived growth factor receptor (Pdgfrα), were shown to be expressed by O-2A progenitors (Stallcup and Beasley, 1987; Levine

and Stallcup, 1987; Richardson et al., 1988). Using these markers, the natural history of O-2A progenitors began to be revealed. It was shown that as these cells differentiate, they downregulate the expression of NG2 prior to the appearance of mature oligoden-drocyte/myelin antigens. A small fraction of cells weakly co-express NG2 and early oligodendrocyte antigen galactocerebroside (GalC), implying a transition from a precursor state to a mature oligodendrocyte state.

1.2.2.1   Morphology and distribution

Embryonic NG2 glia in the rodent CNS possess a large oval or polygonal cell body with one to three unbranched processes (Levine et al., 1993; Nishiyama et al., 1996), while postnatal OPCs are characterised by a small (10-15 μm) polygonal cell soma and a mul-tipolar arbor of fine processes with a thickness of 0.2 to 0.5 μm (Nishiyama et al., 1996; Kukley et al., 2008, 2010). During development, as NG2 cells differentiate into mature oligodendrocytes via transitory stages, they undergo a series of morphological changes: an increase in the complexity of process branching, in number and length of processes, alongwith an increase in the total area covered by processes (Trapp et al., 1997; Kukley et al., 2010). Following development, OPCs in the aged CNS undergo a shortening of their processes and display simple arborisation (Chen et al., 2008).
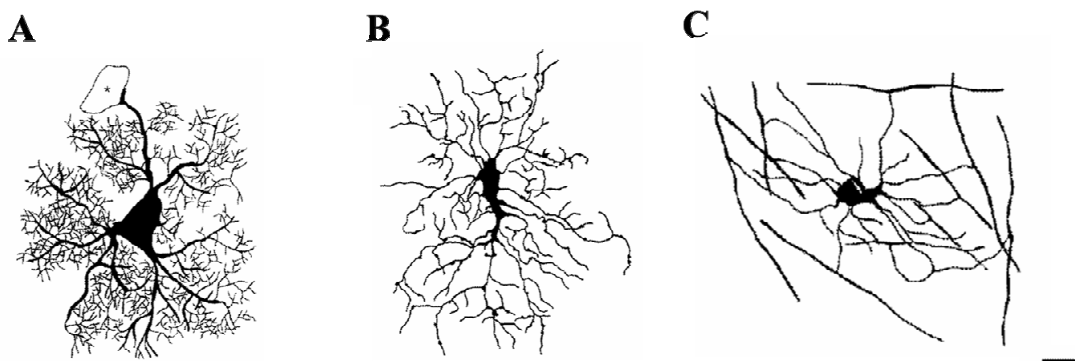
Figure 2. Morphological comparison between a gray matter astrocyte, OPC and a mature myelinating oligodendrocyte. A, Drawing of a gray matter astrocyte, the asterix represents a blood vessel and an end foot on it. B, Drawing of an NG2 cell. Note the difference between the size of the cell soma and thickness and size of fine processes. C, Drawing of a mature myelinating oligodendrocyte. Note the association with the myelin sheath. Scale bar: 10 μm applied to all (modified from Fröhlich et al., 2011).

The morphology of NG2 cells also differs depending on their location in the brain. In gray matter, the cells have a centrally located soma with several long bi- or tri-furcating primary processes to form a symmetrical process field (Bergles et al., 2000), and on the other hand white matter NG2 cells have a more polarized appearance with processes extending along the axonal axis (Kukley et al., 2007).

OPCs are morphologically quite distinct from other glial cell types in the CNS (Figure 2). Although astrocytes and NG2 glia both possess a multipolar tree of processes, NG2 cells are quite distinct with their smaller soma, fewer and less fine secondary processes, finer primary processes; clearly lacking the bushy astrocytic appearance (explained in section 1.1.2), as well as end feet projections (Nishiyama et al., 2005). Also, in absolute contrast to oligodendrocytes, NG2 cells do not bear myelin sheath endings (Trapp et al., 1997).

The predominance of NG2+ OPCs restricted to ventral columns of the embryonic spinal cord and forebrain is lost during development. The peak in density of OPCs is reached during the first postnatal week and by this time the entire CNS becomes uniformly populated with these cell types (Nishiyama et al., 1996).

Figure 3. Distribution of OPCs in the hippocampus during postnatal development. A-C, Frontal sections of the rat hippocampus at (A) P7, (B) P21 and (C) P97 immunoperoxidase labelled with anti-NG2 antibody. At P7, NG2 cells were densely distributed in non-neuronal layers, but by P97, NG2+ cells were uniformly distributed throughout the hippocampus (adapted from Nishiyama et al., 2002).

Not all oligodendrocyte precursors differentiate during the developmental period and well after the early postnatal period when oligodendrocyte production is in full swing, OPCs persist as a uniformly distributed population in the mature CNS and make up 4 to 9% of all cells in the adult rodent CNS (Nishiyama et al., 1999; Dawson, 2003; Reynolds and Hardy, 1997). While OPCs are uniformly distributed throughout the gray and white matter in the adult CNS, their distribution in the neuronal layer of the hippocampus is scarce during late embryonic and early postnatal periods (Figure 3) (Nishiyama et al., 2002). The persistence of OPCs long after developmental myelination has occurred, raises exciting prospects about their role in myelin repair, giving rise to other cell types in the adult brain and synaptic signalling.

1.2.2.2   Physiology

Ion channels

OPCs in gray and white matter express a wide range of voltage-gated channels that lead to active membrane properties. Depolarising voltage steps from the resting potential

elicit both rapidly inactivating as well as sustained outward K^+ currents (Chittajallu et al., 2004; Kukley et al., 2010). In addition to outward K^+ currents, NG2 cells have also been shown to exhibit inward K^+ currents to a variable degree (Lin and Bergles, 2003). It has been speculated that expression of potassium channels by OPCs has a role to play in their proliferation (Gallo et al., 2008). OPCs in the gray and white matters of the developing brain have also been shown to express voltage-gated sodium channels, although there is a disagreement on the proportion of NG2 cells expressing Na^+ channels (Fröhlich et al., 2011). It has also been demonstrated that Ca^{++} influx into the NG2 cells is mediated by Na^+ channels through Na^+/Ca^{++} exchangers (Tong et al., 2009).

Neuron-OPC synapse

Electrophysiological studies revealed that gray matter and white matter NG2+ OPCs have been shown to express alpha-amino-3-hydroxy-5-methyl-4-isoxazole propionic acid (AMPA)/kainate and/or gamma-amino butyric acid (GABA) neurotransmitter receptors (Bergles et al., 2010). The expression of voltage-gated channels and neurotransmitter receptors by OPCs provided the first clues about their communication with neighbouring neurons. Evidence of a novel neuron-NG2 cell synapse was shown by generation of AMPA receptor-mediated fast excitatory postsynaptic currents (EPSCs) in OPCs of the hippocampal CA1 region in response to schaffer collateral stimulation (Bergles et al., 2000; Jabs et al., 2005). Since then, neuron-OPC synapses have been widely reported in the cerebellum (Lin et al., 2005), cortex (Chittajallu et al., 2004) and corpus callosum (Kukley et al., 2007; Ziskin et al., 2007). It has been shown in the cerebellum and white matter that single NG2 cells form hundreds of synaptic contacts (Lin et al., 2005; Kukley et al., 2007; Ziskin et al., 2007).

The two major neurotransmitters- glutamate and GABA mediate synaptic transmission onto OPCs (Kukley et al., 2007, 2008; Ziskin et al., 2007). In the absence of any neuronal targets, the mechanism of glutamate transmitter release onto OPCs has been shown to consist of dedicated molecular machinery reminiscent of neuron-neuron synaptic transmission. Glutamate release from a pool of readily releasable vesicles following highly synchronous fusion events is triggered by Ca^{++} microdomains in the axons. This quantal transmission on OPCs results in inward currents in them, termed as axoglial currents (Kukley et al., 2007).

The irrelevance of N-methyl-D-aspartate (NMDA) receptor signalling for oligodendroglial development and myelination (De Biase et al., 2011; Guo et al., 2012), alongwith

the minimal expression of kainate receptors in OPCs (Kukley and Dietrich, 2009) suggests that the AMPA receptor is the key mediator of neuron-OPC synaptic signalling. Finally it has been suggested that synaptic glutamate release might induce Ca^{++} elevation in OPCs via Ca^{++} permeable AMPA receptors (Ge et al., 2006).

It is therefore tempting to speculate that glutamate receptor mediated axo-glial currents in OPCs as a result of ongoing neuronal activity could serve as a cue to trigger several calcium dependent signalling cascades that could influence OPC physiology *in vivo*. Culture studies in the past have shown that glutamate-mediated activation of AMPA receptors inhibits proliferation and differentiation of OPCs, as well as stimulates their migration (Gallo et al., 1996; Yuan et al., 1998; Gudz et al., 2006). Downregulation of glutamate input onto differentiating oligodendroglial cells could also serve to influence the maturation of these cell types (Kukley et al., 2010).

AMPA receptors are channel tetramers which are assembled from a group of four subunits: GluR1-4 or GluRA-D, which are encoded by four different genes (Greger et al., 2007; Verkhratsky and Steinhäuser, 2000).
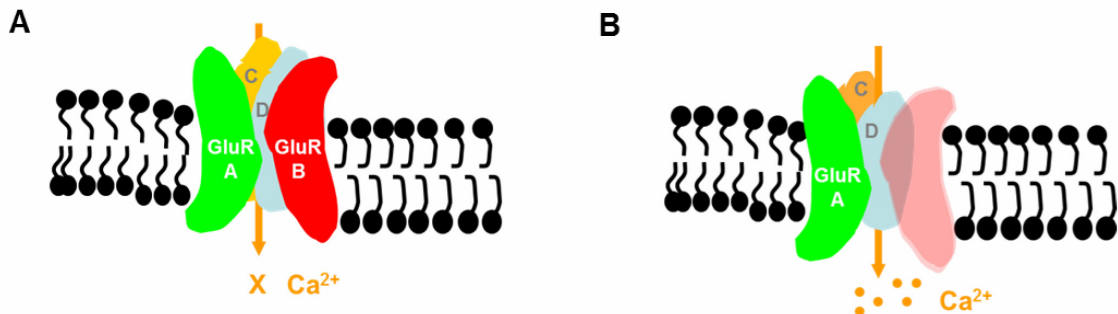
Figure 4. Expression of the GluRB subunit in OPCs. A-B, Illustration of the subunit composition of the glutamate receptor. Presence of the GluRB subunit renders the receptor calcium impermeable (A) and in the absence of the GluRB subunit, the receptor is calcium permeable (B).

The calcium permeability of the AMPA receptor depends critically on its subunit composition and the GluRB subunit is particularly important in this regard. In the presence of the GluRB subunit the receptor is Ca^{++} impermeable, while in its absence Ca^{++} influx can occur through the receptor (as shown in Figure 4). Ectopic expression studies revealed that the GluR heteromer is Ca^{++} impermeable due to the presence of an RNA editing site at the GluRB subunit (Burnashev et al., 1992; Hume et al., 1991).

OPCs in the postnatal brain during ongoing oligodendrogliogenesis and in culture have been shown to contain the GluRB subunit (Matthias et al., 2003; Kukley et al., 2007;

Stegmüller et al., 2003), whereas in the adult brain when the process of myelination is nearly completed, it has been reported that glutamate receptors in OPCs do not contain the GluRB subunit (Ziskin et al., 2007). This switch in subunit composition may indicate a particular importance of GluRB during the developmental period.

For this reason as well as for the pivotal role of this subunit in regulating calcium permeability, I chose to focus my interest on the role of the GluRB subunit in the development of OPCs by performing a loss of function analysis.

1.2.2.3 Cell cycle dynamics

OPCs represent the major cycling cell population in the adult mammalian brain parenchyma. Studies using 5-bromo-2-deoxyuridine (BrdU) labelling indicate that they comprise nearly 70% of all proliferating BrdU positive cells in the hippocampus, cerebral cortex, spinal cord and corpus callosum (Horner et al., 2000; Dawson, 2003; Polito and Reynolds, 2005; Bu et al., 2004). The proportion of actively cycling OPCs amongst the entire OPC cell population, also known as the growth fraction, is high in young (~2 weeks old) as well as in adult (~18-20 months) animals. Using proliferating cell nuclear antigen (PCNA) and BrdU labelling, the growth fraction of NG2 cells at early postnatal ages was estimated to be ~50% in the hippocampus, corpus callosum and cerebral cortex (Kukley et al., 2008; Psachoulia et al., 2009).

At adult ages the OPC growth fraction was also reported invariantly to be ~50% in both cortex and corpus callosum (Rivers et al., 2008; Psachoulia et al., 2009). This would imply that at any given time in both gray and white matter regions almost half of the OPC population is mitotically inactive. However, the existence of two separate dividing and non-dividing subpopulations of NG2 cells in CNS has been contested by recent studies which indicate that all NG2 cells regardless of region are dividing (Kang et al., 2010; Clarke et al., 2012). Interestingly, the decrease in rate of oligodendrocyte production from OPCs follows a close parallel with increase in cell cycle time of NG2 cells over development (Psachoulia et al., 2009).

1.2.2.4 Fate choice

Extensive cell culture studies have shown that OPCs can be induced to differentiate into type-2 astrocytes upon the application of fetal calf serum (FCS) (Raff et al., 1983) and certain cytokines, including the bone morphogenic protein (BMP) (Mabie et al., 1997). In a series of elegant experiments, Kondo and Raff (2000) showed that these type-2

astrocytes, generated by treatment of NG2 glia purified from postnatal day 6 rat optic nerve with FCS or BMP; could be re-programmed into multipotent CNS stem cells. These reverted cells had the capacity to self-renew, give rise to neurons, type-1 astrocytes and oligodendrocytes. Transplantation studies suggest NG2 cells represent the "type C" cells in the SVZ (Aguirre and Gallo, 2004), with a neurogenic potential in culture (Belachew et al., 2003) and upon transplantation (Aguirre et al., 2004).

Extensive *in vivo* studies utilising Cre-lox approach have also been used to elucidate OPC lineage.

Oligodendroglial Fate

Efforts to study the oligodendroglial progression of OPCs *in vivo* has been challenging since NG2 expression is lost during terminal differentiation of the precursor and appearance of mature oligodendroglial antigens. Pulse chase labelling of proliferating cells using BrdU revealed a decrease in the number of BrdU+NG2+ cells that followed in parallel an increase of BrdU+ oligodendrocytes over time (Polito and Reynolds, 2005), providing an indirect evidence of generation of oligodendrocytes from OPCs.

Direct evidence was required to solve the "conundrum" of the differentiation fates of OPCs and the breakthrough came with the use of Cre-lox fate mapping of OPCs in transgenic mice. Using constitutive Cre expression in NG2creBAC transgenic mice and inducible Cre expression in NG2creER^{TM}BAC mice to label the progeny of NG2 glia, a large number of myelinating oligodendrocytes were found among GFP-labelled progeny of OPCs (Zhu et al., 2008a, 2008b, 2011). Subsequently several other mouse lines were used to study the fate of NG2 cells in perinatal and adult ages - PdgfrαcreER^{TM} (Rivers et al., 2008; Kang et al., 2010), Olig2creER^{TM} (Dimou et al., 2008; Ono et al., 2008), PlpcreER^{TM} (Guo et al., 2009, 2010) all establishing the oligodendroglial fate of NG2 expressing cells. Apart from their oligodendroglial potential in the normal brain, fate mapping studies have also demonstrated that OPCs rise to oligodendrocytes during the process of remyelination, following a demyelinating insult (Zawadzka et al., 2010; Kang et al., 2010).

Astrocytic Fate

Failure to detect co-expression of GFAP and NG2 antigens in cell types in the CNS (Nishiyama et al., 2002), gave way to the view that generation of astrocytes from O-2A progenitors was merely a culture artefact and that OPCs and astrocytes were not lineally related.

Direct in-vivo of OPCs utilising Cre expression under the NG2 promoter reveal a significant population of GFP labelled protoplasmic astrocytes in the gray matter ventral forebrain region and spinal cord (Zhu et al., 2008a, 2008b). A follow-up study by the same group provided evidence that OPCs generate astrocytes only during embryonic CNS development (Zhu et al., 2011). The astrogliogenic fate of OPCs being restricted to the embryonic phase was inconsistent with other studies employing inducible Cre expression under *Olig2* and *Plp* promoters, in which reporter positive astrocytes were found upon postnatal Cre induction (Dimou et al., 2008; Guo et al., 2009, 2010).

In contrast to these observations, two separate studies with different *Pdgfrα* constructs used to drive inducible Cre expression in OPCs with TMX administration at postnatal ages (P30 and P45), do not report EGFP or EYFP labelling in astrocytes (Rivers et al., 2008; Kang et al., 2010). It has been postulated that the appearance of reporter positive white matter astrocytes in the Olig2creER^{TM} line is due to Olig2 expression in cells of the germinal zones and that these astrocytes may not be progeny OPCs (Ligon et al., 2006). Nevertheless, astrocytic differentiation from NG2 cells has also been reported in traumatic brain injury and experimental pathology models (Alonso, 2005; Tripathi et al., 2010).

Neuronal Fate

In vivo studies using the Cre-lox system undertaken to elucidate the neuronal fate of OPCs, have not been successful in providing an unequivocal answer to this question. Adult P45 TMX induction in PdgfrαcreER^{TM} mice to label NG2 glia reveal EYFP-labelled progeny of OPCs that co-label NeuN, and resemble projection neurons in the anterior piriform cortex. Upon BrdU labelling, no reporter positive neurons were found to be BrdU positive, suggesting that these neurons were formed by direct transformation of long term quiescent NG2 cell population (Rivers et al., 2008). In PlpcreER^{TM}, early postnatal NG2 cells (P7 Cre induction) were shown to generate few pyramidal neurons in the cerebral cortex and hippocampal interneurons (Guo et al., 2009, 2010).

However, other transgenic approaches have failed to arrive at a consensus vis-à-vis the neurogenic potential of OPCs. For example, also using PdgfrαcreER^{TM} mice Kang et al. (2010) did not observe any long term surviving EGFP labelled neurons in the forebrain upon P30 Cre induction, as was the case with the NG2creBAC transgenic study (Zhu et al., 2008a) and Olig2creER^{TM} mice (Dimou et al., 2008). However, GABAergic neurons have been reported to be progeny of early embryonic Olig2+ cells (Ono et al.,

2008) and groups have alluded to cases of reporter positivity in small number of NeuN positive neurons throughout the forebrain, particularly in the ventral regions following short times after Cre induction (Zhu et al., 2011; Kang et al., 2010; Dimou et al., 2008). Phenotypic analysis of the progeny of adult SVZ NG2 cells, also refute claims of the neurogenic potential of OPCs (Komitova et al., 2009).

While it is safe to say that the oligodendroglial potential of NG2-expressing OPCs has been well established, further experiments are needed to resolve the ambiguity of the astrocytic and neuronal fate choice of these cells and the local signals as well as environmental cues that control these differing fates.

1.2.3 Oligodendroglial development

1.2.3.1   Origin of OPCs

In the embryonic spinal cord where the scheme of oligodendroglial development is relatively simple as compared to the forebrain, the first committed cells of the oligodendroglial lineage arise in a column of the ventral ventricular zone. This ventricular zone column also generates motor neurons and is known as the progenitor motor neuron domain or the pMN domain (Jessell, 2000). Pringle et al. (1996) have suggested the existence of a common precursor for both oligodendrocytes and motor neurons known as the motor neuron/oligodendrocyte precursor cell or MNOP cell. In apparent contrast to lineage association between oligodendrocytes and motor neurons, studies indicate that OPCs develop from an immature cell restricted to give rise to only glial progeny (Rao et al., 1998). This tripotential glia restricted precursor (GRP) is restricted to the generation of oligodendrocytes, type-1 astrocytes and type-2 astrocytes. GRP cells do not give rise to neurons, which as per this hypothesis are generated from neuron restricted precursors (Miller, 2002). In light of the observed heterogeneity amongst oligodendroglial populations, a probable model consisting of both the GRP and MNOP cell pools of oligodendrocyte ancestory can be imagined to exist during oligodendroglial specification.

1.2.3.2   Multiple waves of oligodendrocyte production

Progenitor motor neuron (pMN) precursor cells complete motor neuron formation by E10.5 in mice, and this is followed by a phase of oligodendrocyte production. Activation of the basic helix loop helix (bHLH) transcription factors Olig1 and Olig2 through the sonic hedgehog (Shh) signalling is essential for both motor neuron and oligodendrocyte development (Lu et al., 2002).

OPCs arise in three distinct waves from different regions of the spinal cord (see Figure 5). In the first wave, OPCs arise ventrally from Olig2- expressing progenitor cells in the pMN domain at E12.5 and subsequently migrate to populate the entire neural tube. The development of these cells depends on Shh-mediated signalling, which serves as a "ventralizing" signal and its balance with the dorsally derived bone morphogenic proteins (BMPs) and molecules of the Wnt pathway are critical determinants of oligodendroglial specification. At later fetal stages ~E15.5, the second wave of OPCs emerges from dorsal sources in an Shh-independent manner (Cai et al., 2005; Vallstedt et al., 2005). The third and last wave occurs after birth. OPCs from ventral and dorsal regions are intermixed in the spinal cord, with a predominance of pMN-derived cells (Rowitch and Kriegstein, 2010).
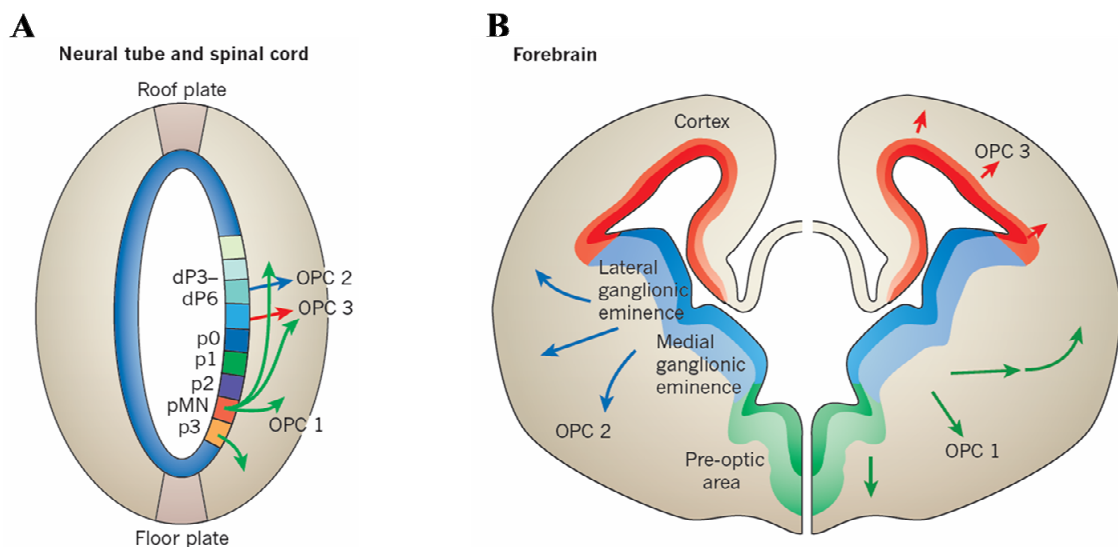
Figure 5. Illustration of generation of oligodendrocyte precursor cells (OPCs) in three distinct sequential waves in the mammalian CNS. A, Two sequential waves of OPCs: OPC1 and OPC2 arise from the ventral and dorsal regions of the Spinal Cord respectively. The third wave, OPC3 occurs after birth but its origin remains unclear. B, Similarly, three sequential waves of OPCs: OPC1, OPC2 and OPC3 arise in the telencephalon. OPC arise from *Nkx2.1*-expressing MGE precursors at E12.5; OPC2 from *Gsh2*-expressing LGE-CGE precursors at E15.5 and Emx1-expressing cortical precursors comprise the OPC3 wave at P0 (adapted from Kessaris et al., 2006).

The ventral foci of OPCs in the neural tube express Pdgfrα beginning E13-E14 (Pringle and Richardson, 1993) and mRNA for the myelin genes: 2',3' -cyclic nucleotide 3' – phosphodiesterase (CNP) and the DM-20 isoform of the proteolipid protein (PLP) from E12 onwards (Yu et al., 1994; Timsit et al., 1995).

Within a day or two after their appearance in the spinal cord ventricular zone (VZ), these Pdgfrα+ cells expand by local proliferation and eventually occupy the entire paren-

chyma at birth (Pringle and Richardson, 1993). NG2 expression by the Pdgfrα+ OPCs is acquired outside of the VZ around E15-E16 (Nishiyama et al., 1996).

An analogous, if not more complex, scheme of oligodendroglial development exists in the forebrain. Cre-lox fate mapping experiments have demonstrated multiple waves of OPC production from embryonic to postnatal ages emerging in a ventral-to-dorsal progression and populating the entire telencephalon- corpus callosum, motor cortex, lateral olfactory cortex, anterior commissure and preoptic area. The earliest cortical oligodendrocytes arise from *Nkx2.1*-expressing precursor cells originating in ventricular zone (VZ) of the medial ganglionic eminence (MGE) and the anterior entopeduncular area (AEP) starting E12.5, migrating to the entire telencephalon (both dorsal and ventral) and populating the cerebral cortex by E16. The second and the third populations of OPCs arise from *Gsh2*-expressing precursors in the lateral and caudal ganglionic eminence (LGE, CGE) at E16 and *Emx1*-expressing precursors in the postnatal dorsal and ventral cortex. Paradoxically, most of the early born OPCs disappear after birth, such that majority of oligodendrocytes in the adult dorsal cortex are derived from the *Emx1*-expressing precursors (Kessaris et al., 2006).

In the postnatal CNS and during adulthood, the subventricular zone (SVZ) plays an important role in the generation of OPCs. Retroviral studies show that NG2 cells in the corpus callosum and neocortex are generated from the neonatal SVZ (Levison et al., 1999). GFAP+ SVZ type B cells have also been identified as progenitors of oligodendrocytes in the adult CNS (Menn et al., 2006).

Cre-lox fate mapping studies using radial glial specific promoters show that radial glial cells go through OPC stages to generate oligodendrocytes throughout development (Fogarty et al., 2005; Casper and McCarthy, 2006).

1.2.3.3   OPC migration and proliferation

The origin of OPCs during early embryonic forebrain development has been shown to occur at highly restricted ventral foci from *Nkx 2.1* and *Gsh 2* expressing precursors (section 1.2.3.2). From their sites of origin, OPCs migrate through the developing forebrain to their final destinations in the gray and white matter regions. In more rostral regions of the CNS, OPCs have been shown to migrate from the MGE and LGE to the developing forebrain (Spassky et al., 1998). The migration of oligodendrocyte precursors throughout the developing CNS has been shown to be mediated by specific directional and substrate cues like netrins and semaphorins (Sugimoto et al., 2001). Evidence

for the dorsal to ventral migration of OPCs has also been shown in the spinal cord by cell tracing experiments (Warf et al., 1991).

Following commitment in the ventricular zone, OPCs undergo extensive proliferation and reach their maximum density during the first postnatal week. The early phases of this proliferation occur in the VZ and SVZ while the majority of oligodendrocyte precursor proliferation occurs after migration to the developing white matter (Miller, 2002). BrdU incorporation assay in the P5-P6 corpus callosum reveal that nearly 50% of OPCs were BrdU+ (Psachoulia et al., 2009). In the ventral spinal cord 40% of oligodendroglial precursors were BrdU+ between P3-P4 and 1 day later, this fraction increased to 50% (Miller et al., 1997). During this developmental period it has also been shown that minimal proliferation of glial precursors occurs in the VZ and SVZ (Hardy and Reynolds, 1991; Miller et al., 1997).

1.2.3.4   Oligodendroglial maturation: cellular markers

Co-expression of NG2 and mature oligodendrocyte antigens in a subset of cells indicated a transitory phase in OPC lineage progression. As they migrate from their sites of origin, OPCs settle along future white matter tracts or gray matter regions and transform into an intermediate, post-migratory pre-oligodendrocyte stage recognized by O4 immunoreactivity (Bansal and Pfeiffer, 1992). A schematic illustration of the different stages of OPC development into a mature myelinating oligodendrocyte is shown in Figure 6.

Premyelinating oligodendrocyte: The next step in oligodendroglial maturation is represented by a transient stage- the premyelinating oligodendrocyte stage. Studies with retroviral markers (Levison and Goldman, 1993) and immunohistochemistry (Hardy and Reynolds, 1991) have identified immature or premyelinating oligodendrocytes during development of the rodent brain.

DM20- an alternatively spliced product of the PLP gene has been detected in the developing brain before the appearance of myelin (Timsit et al., 1995) and is an established marker for premyelinating oligodendrocytes. The fact that these premyelinating oligodendrocytes originate from NG2+ precursors is demonstrated by cells that co-express both the NG2 and DM20/PLP antigens.

Premyelinating oligodendrocytes with DM20+ multiple-overlapping process arborisations have been shown to occupy 80 μm domain in cortex and 40 μm domains in the

corpus callosum (Trapp et al., 1997). Premyelinating oligodendrocytes differ in morphology as compared to OPCs in having a larger total process length, area covered by processes and soma diameter (Kukley et al., 2010).

Myelinating oligodendrocyte: Premyelinating oligodendrocytes either differentiate into mature myelinating oligodendrocytes upon axonal contact or undergo degeneration (Trapp et al., 1997). The majority of myelinating oligodendrocytes have appeared in the mouse brain by four weeks after birth, with peak myelinogenesis occurring around the second postnatal week (Miller, 2002; Sturrock, 1980). Fully differentiated oligodendrocytes express markers such as CNP, MBP, PLP and MOG to name a few.
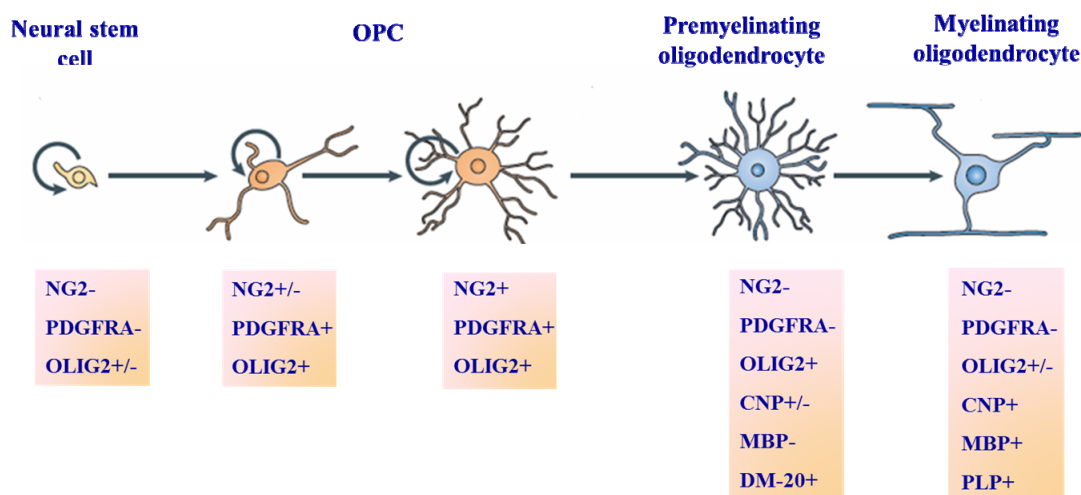
Figure 6. Schematic representation of oligodendrocyte development. NG2 and PDGFRα are not expressed by OLIG2 positive neural stem cells, but are expressed by proliferating OPCs derived from them. Proliferation is depicted by circular arrows. Next, OPCs differentiate into DM-20 positive premyelinating oligodendrocytes and cease to express the NG2 and PDGFRα antigens. Terminal differentiation into the mature myelinating oligodendrocyte state initiates expression of PLP, MBP and CNP myelin proteins. OPC, oligodendrocyte precursor cell; PDGFRα, platelet derived growth factor alpha; PLP, proteolipid protein; MBP, myelin basic protein; CNP, 2',3' -cyclic nucleotide 3' –phosphodiesterase.

The mature oligodendrocyte/myelin marker- CNP and its utility in my study is explained in great detail in the following section.

1.2.4 2′,3′ -Cyclic Nucleotide 3′ -Phosphodiesterase (CNP)

Drummond et al. (1962) provided the first evidence of an enzymatic activity in the brain that hydrolyses 2′,3′–cyclic nucleotides exclusively to nucleoside 2′ –phosphates. In the five decades following the discovery of these unusual phosphodiesterases, innumerable studies have been undertaken to characterise and purify CNP, as well as to elucidate its localization, physiological activity and functional significance.

Gene structure

The gene encoding for CNP is located on chromosome 17 in humans and chromosomes 11 and 3 in mice (Sprinkle et al., 1992; Douglas et al., 1992; Bernier et al., 1988). The second CNP locus on the mouse chromosome 3 is considered dysfunctional (Braun et al., 2004). It has been demonstrated that the 6 to 9 kb long CNP gene, consisting of four exons and three introns (Monoh et al., 1989, 1993), encodes two known CNP isoforms: CNP1 and CNP2. The larger 48 kDa CNP2 protein is identical to the 46 kDa CNP1 except for an additional 20 amino acids at its amino terminus. The transcripts encoding these two separate isoforms differ at their 5′ ends and are under the control of separate promoter regions, a 2.6 kb transcript encodes CNP1, while a 2.4 kb transcript encodes CNP2. The CNP1 mRNA is transcribed from the proximal promoter located between the first two exons, and contains only the open reading frame of the CNP1 isoform (Figure 7).
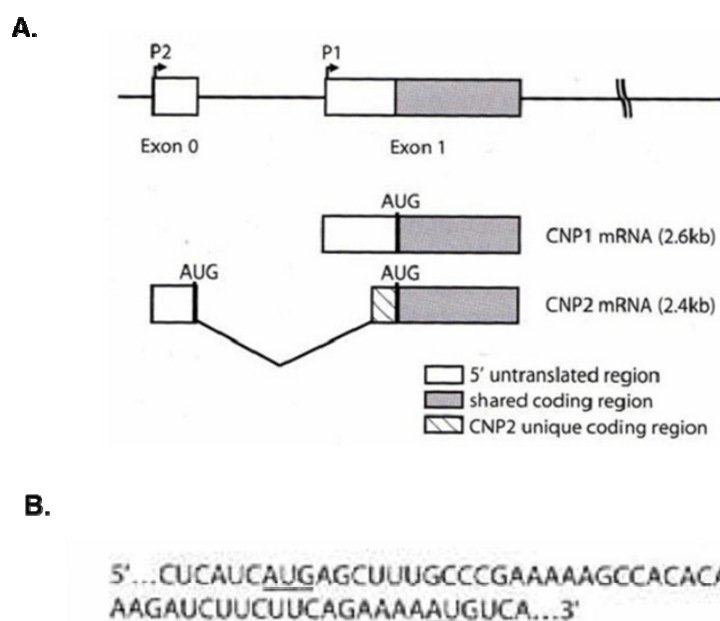
Figure 7. Schematic structure of the 5' end of mouse CNP gene and the resulting primary transcripts. A, The first two exons with the distal (P2) and proximal (P1) promoters are depicted. CNP1 mRNA is generated from P1 whereas transcription from P2, followed by an additional splicing event within the non-coding region of exon 1 gives rise to the CNP2 mRNA. B, Sequence of the bi-functional CNP2 mRNA surrounding the two in-frame initiation sites of AUG. Translational initiation at the first and second AUG generates CNP2 and CNP1 polypeptides respectively (adapted from Braun et al., 2004).

Transcription of the CNP2 mRNA is initiated 1 kb upstream at the distal promoter. The primary transcript originating from the distal promoter undergoes an additional splicing event to fuse sequences encoded by an upstream exon, including an AUG sequence and additional 60 base pairs of coding sequence, to sequences just upstream of the AUG of

the smaller protein, adding 20 amino acids (Kurihara et al., 1990; Gravel et al., 1994; O'Neill et al., 1997). Therefore, the CNP2 transcript has two AUG start and stop codons in frame, from the first and second exons and can thus give rise to both CNP isoforms.

This however does not preclude the fact that the two CNP isoforms are encoded by separate mRNAs that have been transcribed from two separate promoters located within the single CNP gene. Both polypeptides are synthesized on free ribosomes (Gillespie et al., 1990), are enzymatically active and are post-translationally modified by isoprenylation at the C-terminus (De Angelis and Braun, 1994, 1996; O'Neill and Braun, 2000).

1.2.4.1   CNP expression in the oligodendroglial lineage

CNPase is most prominent in the CNS and comprises 4% of the total myelin protein. Several studies report the close association of the CNPase protein with myelin sheaths (Kurihara and Tsukada, 1967; Kurihara and Tsukada, 1968; Drummond et al., 1962). *In vivo* and in culture, CNPase is expressed as early as GalC, which is considered to be a very early marker for differentiating oligodendrocytes (Brenner et al., 1986; Reynolds and Wilkin, 1988). The protein appears early in development, preceding myelination and is then maintained at high levels as myelin is produced (Snyder et al., 1983; Sprinkle et al., 1978). Although high levels of CNP are found to accumulate in differentiating and myelinating oligodendrocytes in parallel with the major structural myelin proteins: MBP and PLP, the onset of its expression occurs much earlier. In rat, CNP expression peaks around postnatal day 10, at a time when OPCs enter the phase of terminal differentiation (Amur-Umarjee et al., 1990; Bansal and Pfeiffer, 1985).

Immunohistochemical and *in situ* hybridisation studies indicate that CNP is concentrated within specific regions of the oligodendrocyte cell bodies, processes and myelin internodes (Nishizawa et al., 1981; Brenner et al., 1986; Reynolds and Wilkin, 1988; Trapp et al., 1988; Vogel and Thompson, 1988). Abundant CNP is visualised in the myriad filopodia of premyelinating oligodendrocytes, and upon their differentiation to mature oligodendrocytes, the protein is expressed in large processes that terminate on the myelin internode. Isoprenylation and Palmitoylation at the C-terminus mediate binding of CNP to membranes (Braun et al., 1991; De Angelis and Braun, 1994).

At the mRNA level, *in vitro*, the CNP2 -2.4 kb transcript was present specifically in O-2A progenitor cells, while the CNP1 mRNA was detected only in differentiating oligodendrocytes. *In situ* hybridisation studies in the developing ventral spinal cord of rat demonstrated that CNP expression regressed from being uniformly distributed at E12 to

a columnar cell population co-expressing Pdgfrα at E14, reinforcing its expression in precursor cells. The absence of co-localization of CNP and OPC-specific DM-20 transcripts was suggestive of the existence of two separate subsets of progenitor cells in the spinal cord (Yu et al., 1994). However, other studies reported patterns of expression of CNP transcripts being superimposable on that of DM-20, starting from E12.5 in the diencephalon and E14.5 in the rhombencephalon, postulating that these two mRNAs were expressed in the same cell (Peyron et al., 1997). Therefore, there seem to exist two different patterns of CNP expression in the spinal cord and brain. In CNP-lacZ transgenic mice where LacZ reporter gene is coupled with a 4 kb mouse CNP gene, transgene expression is detected in embryonic brain and spinal cord in immature oligodendrocytes and postnatally in the white matter (Gravel et al., 1998). While the above *in situ* studies employed full length CNP cDNA that did not discriminate between the two isoforms, the expression of CNP1 and CNP2 mRNA and protein has also been elucidated. Northern blot analysis revealed that the CNP1 mRNA is expressed by the brain and sciatic nerve, where as a 2.4-2.5 kb transcript similar to CNP2 is expressed additionally in the thymus and testes, indicative of the activity of the distal promoter in non-myelinating cells. The CNP2 mRNA can be detected embryonically as opposed to the postnatal expression of CNP1 mRNA. The CNP2 transcript and protein is expressed by oligodendrocyte precursors early in brain development, before the onset of myelination and eventually both protein isoforms accumulate during myelination in parallel with other myelin proteins (Scherer et al., 1994).

In addition to its expression in the CNS, Schwann cells in the peripheral nervous system (PNS) also express high amounts of CNPase (Sprinkle, 1989). Nonmyelin CNP is also shown to be expressed in vertebrate erythrocytes (Weissbarth et al., 1981), lymphocytes and platelets (Rastogi and Clausen, 1985; Sheedlo et al., 1984; Sprinkle et al., 1985), thymus (Bernier et al., 1987), liver (Dreiling et al., 1981) and photoreceptor cells of the retina (Giulian and Moore, 1980; Nishizawa et al., 1982). More recently, CNP has been reported in Leydig and Sertoli cells of the testis (Davidoff et al., 1997, 2002).

Functional Significance of the CNPase enzyme

CNP enzyme catalyses cleavage of the phosphodiester bond and exclusive production of 2′-nucleotide phosphates from 2′,3′-cyclic mono-nucleotides *in vitro* (Drummond et al.,1962; Sprinkle et al., 1978). The enzymatic activity was first demonstrated in bovine spleen and pancreas (Whitfeld et al., 1955; Allen and Davis, 1956).

Although the physiologically relevant substrates, 2´,3´ -cyclic nucleotides are not present in the brain, numerous cyclic phosphate-containing RNAs which occur as intermediates of RNA metabolism, suggest that CNPase may serve other functions than its enzymatic potential (Heaton and Eckstein, 1996). The association of CNP with myelin and its expression patterns in the OPCs (at the mRNA level) and differentiated oligodendrocytes suggests a crucial role for CNP in the process of myelination. CNP also governs co-ordinated cytoskeletal reorganisations during process formation and outgrowth in oligodendrocytes (Lee et al., 2005). Association of CNP with microtubules (MTs) and its MT polymerization activity classifies CNP as a microtubule-associated protein (MAP) (Dyer and Benjamins, 1989; Laezza et al., 1997; Bifulco et al., 2002). In mice over-expressing CNP, premyelinating oligodendrocytes extend redundant membranous process extensions and adult oligodendrocytes from these transgenic animals re-grow dramatically large processes in culture (Gravel et al., 1996; Yin et al., 1997). Interestingly, ectopic CNP expression in fibroblasts induces formation of filopodia and processes (De Angelis and Braun, 1994). On the other hand, in CNP-null mice the ultrastructure and periodicity of myelin and myelin assembly is not affected but adult mice experience a severe neurodegeneration causing a large microglial response, hydrocephalus and premature death. This is indicative that CNP clearly has a role in axonal survival (Lappe-Siefke et al., 2003). Furthermore, CNP deficiency also caused lapses in the paranodal loop structures of oligodendrocytes and failure to form proper axo-glial contacts at the paranodes directly leads to aberrant axo-glial signalling, resulting in axonal death or loss (Rasband et al., 2005; Salzer, 2003). Recently, the discovery of ATP/GTP binding sites on CNP indicate that it may be involved in signal transduction pathways (Stingo et al., 2007). CNP has also been shown to be an RNA-binding protein and a regulator of RNA function, processing and degradation (Gravel et al., 2009).

1.2.4.2   Selection of *Cnp*-dependent Cre driver line

Amongst the plenitude of oligodendroglial lineage-specific genes used in *in vivo* lineage studies of OPCs, the oligodendroglial lineage marker of interest in my study is 2',3' -cyclic nucleotide 3' –phosphodiesterase (CNP), which is detectable in all cells of the oligodendroglial lineage (Yu et al., 1994) and is maintained in mature oligodendrocytes throughout life.

The *Cnp* gene product- CNPase is expressed only in mature myelinating oligodendrocytes. Therefore, only relatively differentiated OPCs- those that had perhaps already

made the decision to mature into the oligodendroglial state will change their gene expression profile to initiate activity of the *Cnp* promoter. These OPCs in which the *Cnp* promoter is active do not express the CNPase protein yet, which will only be expressed upon terminal differentiation to the oligodendrocyte.

In my study, I chose to utilise a *Cnp* promoter driven Cre-lox approach to focus specifically on a later or advanced time point during the development of the OPC. I consider this subset of OPCs labelled by CNP-Cre mediated recombination, relatively differentiated as compared to their early stage counterparts and term these as *"late OPCs"*. These are OPCs that have perhaps already made the decision to differentiate into mature oligodendrocytes and will start expression of the *Cnp* promoter, unlike their more immature counterparts or the *"early OPCs"*.

1.3   Neurogenesis

An important question in the field of oligodendroglial biology is whether OPCs generate neurons, and therefore now I will give a brief overview into the process of neurogenesis in the CNS.

Neurogenesis or the birth of neurons is the process by which neurons are generated. Most active during embryonic development, neurogenesis which is responsible for populating the growing brain continues well into adulthood. There exist three distinct sets of progenitor cell pools in the embryonic telencephalon: neuroepithelial cells, radial glia and intermediate or basal progenitors (Figure 8). Since the neuroepithelial cells are the only cells present in the neural tube at early stages, it implies that they generate directly or indirectly, through progression to radial glia and basal progenitors, to all the neurons and glial cells of the adult CNS.

1.3.1   Embryonic neurogenesis

The basic terminology and events of the developing CNS were formulated almost 80 years ago by His, describing the idea that germinal cells divide at the ventricular surface of the CNS, giving rise to postmitotic neuroblasts that move outward to form a mantle layer. This historical terminology was modified as per rules of the Boulder Committee in 1969 to propose that the embryonic CNS consists of four fundamental zones from which the adult organisation is derived: *the ventricular zone, the subventricular zone, the intermediate zone and the marginal zone* (Angevine et al.,1970).

During early development, there is a dramatic surge in the neuroepithelial cells in the dorsolateral wall of the rostral neural tube. At the ventricular zone (VZ), the neural progenitor cells undergo characteristic interkinetic nuclear migration: alternate movement of the nucleus between the basal and apical surface (Sauer, 1935). This migration is synchronised with respect to the cell cycle, with the nucleus being at the apical surface during mitosis, moving towards the basal surface through G_1 and the S phase at the most basal location and then migrating back apically through G_2. Since at any given time the progenitor cells are not synchronised, with different cells being in various phases of the cell cycle, this gives a pseudostratified appearance.

The pseudostartified neuroepithelial cells undergo symmetric cell divisions to expand the pool of multipotent progenitors and around E10.5 the earliest born neurons arise from asymmetric divisions to form the layered preplate. The preplate splits into the superficial marginal zone and the deep seated subplate, and the cortical plate which will later give rise to the neocortex, begins to develop between these two layers.

Neurons populate the cortex in an "inside-out" manner, with the earliest born neurons settling into deeper laminae and later born neurons migrating past them to occupy more superficial layers (Angevine and Sidman, 1961; Bayer and Altman, 1991; McConnell and Kaznowski, 1991). Shortly after the appearance of the first neurons, neuroepithelial cells give rise to radial glial cells around E11, which in addition to serving as a scaffold for neuronal migration, also have a neuronogenic potential. Radial glial cells maintain a shape similar to neuroepithelial cells, with a long basal process extending upto the pial surface and a short apical process in contact with the ventricular lumen. Molecular features of radial glial cells are typical of the astroglial lineage, with expression of brain lipid binding protein (BLBP), glutamate transporter GLAST and the adhesion molecule TN-C. *In vivo* lineage tracing and time lapse studies have shown that radial glia are the source of postmitotic neurons in the cerebral cortex (Malatesta et al., 2003) and possibly in the entire telencephalon (Anthony et al., 2004; Noctor et al., 2002).

It is noteworthy that not all the neuroepithelial cells divide at the ventricular wall; around the time of radial glial appearance, some of these cells undergo mitosis at a distance from the apical surface, giving rise to basal progenitors, at a border between the VZ and the preplate known as the subventricular zone (SVZ). The SVZ is formed around E13.5 and expands during late corticogenesis, forming mainly upper-layer neurons. In some regions of the CNS, for example in the ventral telencephalon, the basal

progenitor cells alongwith the radial glia, which are far less in number, are the main source of neurons. However, at late fetal and early postnatal ages these basal progenitors become restricted to a glial lineage (Malatesta et al., 2008; Molyneaux et al., 2007).
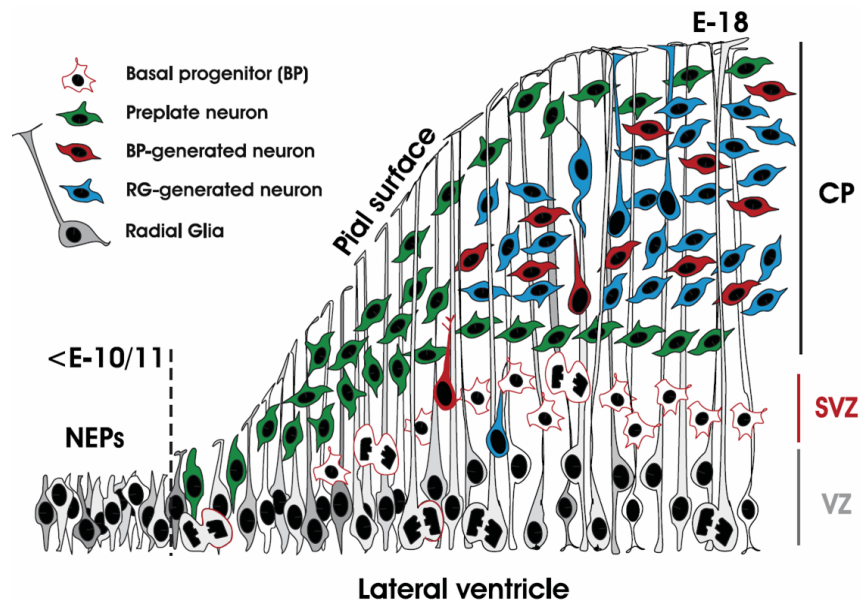
Figure 8. Progenitor cells in developmental neurogenesis. The neuroepithelial cells (white) give rise to the very first preplate neurons (green) and then progressively convert into basal progenitors (red) of the SVZ and radial glial cells (gray). Neurons are derived at early stages by basal progenitors and at later stages they are derived from both radial glia and basal progenitors (blue and green). CP, Cortical Plate; SVZ, Subventricular Zone; VZ, Ventricular Zone (adapted from Malatesta et al., 2008).

1.3.2 Postnatal neurogenesis

Adult neurogenesis is an intriguing feature and under unperturbed conditions occurs in two well-defined regions of the CNS: the SVZ of the lateral ventricles and the subgranular zone (SGZ) of the hippocampal dentate gyrus (Zhao et al., 2008). Neurons born in the adult SVZ migrate over a long distance through the rostral migratory stream (RMS) to become granule neurons and periglomerular neurons of the olfactory bulb. Neurons born in the adult SGZ migrate to the granule cell layer of the dentate gyrus to become dentate granule cells (Cameron and McKay, 2001).

The neural progenitor cells of the developing brain persist in these distinct regions of the postnatal brain and continue to produce glial cells, as well as neurons. In the late embryonic and early postnatal ages, the radial glial cells which were the precursor cells for neuronal cell types during embryonic development, now give rise to a discrete stem cell niche for postnatal neurogenesis. The neural stem cells of the SVZ is a relatively quiescent cell population known as type B cells, which give rise to actively proliferating

type C cells that function as intermediate or basal progenitors or transit amplifying cells in the adult SVZ. The type C cells in turn generate immature neuroblasts known as type A cells, which are directed towards the olfactory bulb by ensheathing glial tubes giving rise to the RMS (Doetsch, 2003).

While, neurogenesis occurs from specialised progenitor neural stem cells, several *in vivo* fate mapping studies in the recent past have also suggested that progenitor cells of the oligodendroglial lineage or OPCs possess a neuronogenic potential.

1.4   Aim of the study

Oligodendroglial precursor cells (OPCs) or NG2 cells are abundant in the developing and mature CNS. During development, it is accepted that these cell types serve as progenitors to oligodendroglial cells. However, culture studies have shown that OPCs could return to a multipotent state, suggesting that oligodendroglial lineage-restricted precursors might have a latent stem cell potential. A multitude of *in vivo* OPC lineage studies have in the past revealed contradictory results vis-à-vis their astrogliogenic and neuronogenic potential in the normal and compromised brain. Therefore, the primary objective of this study is to elucidate OPC fate choice and resolve the ambiguity in the field of oligodendroglial lineage development. Importantly, I will focus on a later timepoint during the development of an individual OPC. In order to preferentially study these relatively differentiated or *"late OPCs"*, a *Cnp*-based experimental approach will be employed, as the *Cnp* gene product- CNPase is expressed only in mature oligodendroglial cells. The main advantage of using CNP, instead of other oligodendroglial lineage-specific markers which are expressed starting from early OPC development is that *only* once an OPC has made the "decision" to differentiate, its pattern of gene expression undergoes change and it first starts to show *Cnp* promoter activity.

To eliminate any cell type-specific bias due to choice of reporter mice, Cre-lox strategy with two different Cre reporter lines will be employed to compare OPC cell fates.

In addition to their role as progenitor cells, OPCs also establish direct synaptic contact with neurons. It is speculated that glutamatergic synaptic input onto OPCs via AMPA receptors could influence their physiology by activating several Ca^{++} dependent signalling cascades. In my second research goal, I will investigate the influence of the GluRB subunit of the AMPA receptor on OPC behaviour *in vivo*: on its proliferation and differentiation.

2   Materials and Methods

2.1   Animals

Animal housing was performed according to the institutional guidelines at the animal facility of the University of Bonn. Animals were maintained with a continuous supply of food and clean drinking water.

2.1.1   C57BL/6 mice

"C57 black 6" or simply "black 6" is probably the most widely used of all inbred strains. It originated in the 1920's; substrain 6 was separated prior to 1937 and has gone through over 150 generations of full sibling matings. It has good breeding capacity and has been used as a genetic background for a large number of congenic strains covering both polymorphic and mutant loci. Its genome carries elements of Mus musculus and Mus spretus. C57BL/6 mice have a dark brown, nearly black coat, are easily irritable and have a tendency to bite. Mice were obtained from Charles River.

2.1.2   CD1 mice

Crl:CD1 (ICR) mice or CD1 mice were originally derived from a strain of Swiss mice that served as progenitors. These albino mice are widely used due to characteristics like easy handling, rapid growth, docile behaviour and high reproduction rate. Mice were obtained from Charles River and then bred in house.

2.1.3   CNP-Cre mice

Mice expressing Cre recombinase under control of the *Cnp1* regulatory sequence have been generated and characterised by Dr. KA Nave, MPI Göttingen (Lappe-Siefke et al., 2003), using a combined knockout and knock-in strategy. Utilizing homologous recombination, the coding region of *Cnp1* gene, encompassing most of exons 1 to 3 was replaced with C*re* recombinase gene. The targeted mutation was confirmed by showing complete loss of CNP enzymatic activity in homozygous mice and 50% reduction of enzymatic activity in heterozygous mutants; it was also shown that no other protein compensated for the enzymatic action of CNP. Onset of Cre expression begins in the spinal cord by embryonic day 13.5 (Genoud et al., 2002). CNP deficient mice show no

obvious abnormalities until 4 months of age, however after that mutant mice develop ataxia and hindlimb impairments. Homozygous CNP-Cre$^{+/+}$ mice develop axonal pathology at 3-4 months of age and have a reduced life span, with most animals dying between 7-11 months of age. Homozygous CNP-Cre$^{+/+}$ mice were obtained from MPI Göttingen, bred in house and maintained on a C57 black background. CNP-Cre$^{+/-}$ mice were inter-bred with other CNP-Cre$^{+/-}$ mice and also with wild type C57BL/6 mice to get CNP-Cre$^{+/+}$ and CNP-Cre$^{+/-}$ mice.

2.1.4 Z/EG mice

The lacZ/EGFP is a Cre double reporter line developed by Novak et al. (2000), and can be used to report Cre excision from embryonic to adult ages. The Z/EG transgene consists of a strong pCAGGS promoter, directing expression of a loxP-flanked βgeo fusion gene and three polyA sequences. Following that there is the coding sequence of the enhanced green fluorescent protein (EGFP) and a polyA sequence. In this configuration βgeo is expressed before Cre mediated excision and the expression of EGFP occurs after Cre excision. EGFP expression is strong enough in these mice and can be monitored in the live cells/slices. These mice were bred for three generations with CD1 mice by the donating investigator and for one generation with C57BL/6 mice. We obtained this strain from Jackson Laboratories as hemizygotes on a SV 129 background and then subsequently crossed them for atleast 4-6 generations with C57BL/6 mice.

2.1.5 ROSA26/EYFP mice

The ubiquitously expressed ROSA26 locus is subject to targeted insertion of the enhanced yellow fluorescent protein (EYFP) cDNA, preceded by a loxP-flanked stop sequence (Srinivas et al., 2001). The expression of EYFP ensues upon Cre-mediated excision of the stop sequence upon homologous recombination at the loxP sites which are oriented in the same direction. Mice were obtained from Dr. Martin Theis (IZN, Bonn) as heterozygotes, and maintained them against a C57 black background.

2.1.6 NG2creER^{TM}BAC transgenic mice

BAC modification technique is used to generate mice that express Tamoxifen-inducible Cre (CreER^{TM}) specifically in NG2-expressing cells. The nls-CreER^{TM} cDNA that contains the coding region of Cre with a nuclear localization signal was inserted in the first exon of the *ng2* gene. Upon crossing with the ROSA26/EYFP Cre reporter, no back-

ground reporter activity was observed in the absence of Tamoxifen (TMX). On the other hand, Cre induction resulted in reporter expression (see section 2.2.2). The NG2creER^{TM}BAC mice were obtained from Dr. Nishiyama (Zhu et al., 2011) and maintained as homozygotes against a C57 black background.

2.1.7 NG2DsRedBAC transgenic mice

These mice were obtained from Dr. Akiko Nishiyama as homozygotes. Here, DsRedT.1 (Bevis and Glick, 2002), which is a variant of the original red fluorescent protein DsRed1, was inserted into the first exon of the *ng2* gene in the BAC clone. The resulting transgenic mice express DsRed protein specifically in NG2+ cells (Zhu et al., 2008a). In our lab we maintained these mice on a C57 black background. The fraction of NG2 cells that were DsRed positive were examined in the adult NG2DsRedBAC line; in the Dorsal Cortex ~80% of all NG2 cells were DsRed+ and in the Corpus Callosum ~90% of all NG2 cells exhibited DsRed fluorescence.

2.1.8 PGK-Cre transgenic mice

The PGK-Cre mice (Lallemand et al., 1998) were obtained from Dr. Martin Theis (IZN, Bonn) and maintained on a C57 black background. The transgenic mice carry Cre recombinase controlled by the ubiquitously expressed PGK-1 promoter.

2.1.9 GluRB^{2lox} transgenic mice

Gene-targeted mice with loxP sites flanking the GluRB gene (*Gria2*) exon 11 (Shimshek et al., 2006), were obtained from Dr. R. Sprengel (MPI, Heidelberg) as homozygotes and we maintained these mice on a C57 black background. For experiments to generate NG2 cell specific GluRB knockouts, mice heterozygous for the GluRB allele (GluRB$^{2lox/wt}$) were inter-bred, such that a GluRB knock out (GluRB$^{2lox/2lox}$) and wild type mice (GluRB$^{wt/wt}$) were obtained from the same litter.

2.2 Cross-breeding of mouse lines

2.2.1 Generation of CNP-Cre:Z/EG and CNP-Cre:ROSA26/EYFP mice

The CNP-Cre line (CNP-Cre$^{+/+}$ and CNP-Cre$^{+/-}$) was inter-bred with the Z/EG and ROSA26/EYFP reporter lines (both homozygous and/or heterozygous), generating CNP-Cre:Z/EG and CNP-Cre:ROSA26/EYFP respectively.

For experiments in this study both double heterozygotes and double homozygotes were used at embryonic and postnatal ages as indicated, since no difference in reporter expression was observed between CNP-Cre:Z/EG and CNP-Cre:ROSA26/EYFP mice with CNP-Cre$^{+/+}$ or CNP-Cre$^{+/-}$ genotype. In cells that have undergone Cre-loxP mediated recombination, permanent expression of enhanced green fluorescent protein (EGFP) and enhanced yellow fluorescent protein (EYFP) occurs in CNP-Cre expressing cells and their progeny.
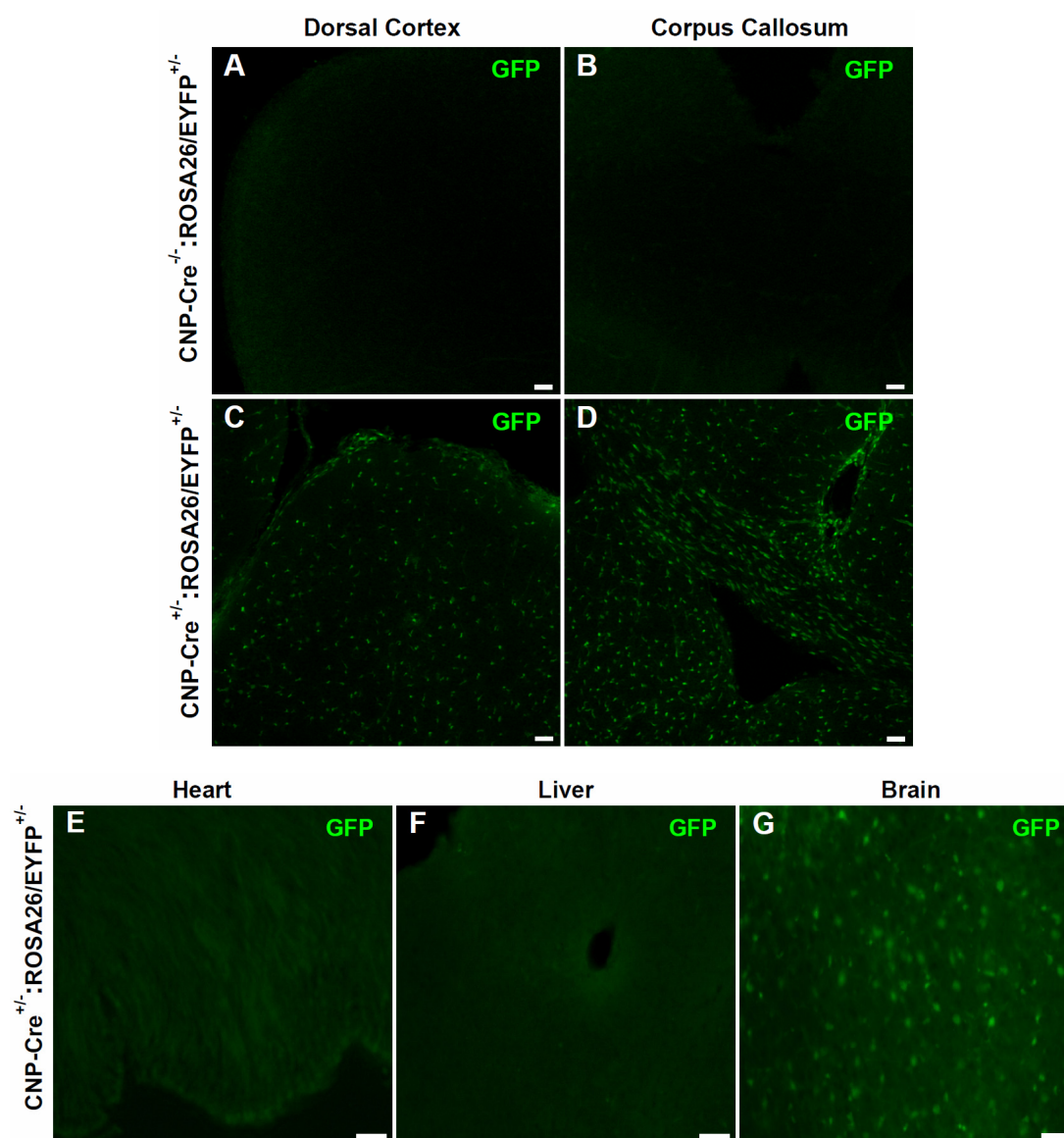
Figure 9. Specificity of CNP-Cre expression. A,B, Frontal sections through the Dorsal Cortex (A) and Corpus Callosum (B) of CNP-Cre$^{-/-}$:ROSA26/EYFP mice at P10 immunolabelled for GFP. C,D, Frontal sections through the Dorsal Cortex (C) and Corpus Callosum (D) of CNP-Cre$^{+/-}$:ROSA26/EYFP mice at P10 immunolabelled for GFP. E-G, Sections through the Heart (E), Liver (F) and Brain (G) of CNP-Cre$^{+/-}$:ROSA26/EYFP mice at P30, immunolabelled for GFP. GFP (green) is used to indicate EYFP fluorescence. Scale bars: 50 µm (applied to all).

2.2.1.1   Reporter expression is committed under the *Cnp* promoter

In the CNP-Cre:ROSA26/EYFP transgenic mice where I observed EYFP expression by non-oligodendroglial lineage cells, the Cre dependence of reporter expression was verified. For this control experiment, CNP-Cre:ROSA26/EYFP mice with CNP-Cre null homozygosity i.e. CNP-Cre$^{-/-}$:ROSA26/EYFP$^{+/-}$ were examined. With GFP immunolabellings at P10, no EYFP+ cells were seen throughout gray and white matter regions in 50 μm frontal sections of the forebrain (n=2 animals) (Figure 9A,B).

In my next set of experiments to check if the knock-in of Cre was stringently under the *Cnp* promoter, I checked the non-neural tissues of heart and liver where *Cnp* promoter activity is absent, for reporter positivity. I failed to observe any EYFP+ cells in the heart and liver tissues of P30 CNP-Cre$^{+/-}$:ROSA26/EYFP$^{+/-}$ animal upon GFP immunolabelling (Figure 9E,F), while reporter positive cells were observed in the forebrain frontal sections of the same animal (Figure 9G).

2.2.2   Generation of other transgenic lines

NG2creER^{TM}BAC:ROSA26/EYFP transgenic mice: Homozygous and/or heterozygous NG2creER^{TM}BAC mice were inter-bred with homozygous and/or heterozygous ROSA26/EYFP Cre reporter line. For experiments in this study both double heterozygotes and double homozygotes were used at embryonic ages for Tamoxifen injection. Using this strategy, NG2-expressing cells and their descendants will express enhanced yellow fluorescent protein (EYFP) upon Cre mediated recombination, only upon Tamoxifen induction.

To check for any "leaky Cre expression", control experiments were performed in which ~P9 NG2creER^{TM}BAC:ROSA26/EYFP mice were administered only 50 μl corn oil or NaCl (2 i.p injections per day for 3 days) and subsequently analysed ~24 hrs. after the last injection with GFP immunohistochemistry to identify any GFP-labelled cells. I did not observe any GFP+ cells in these control animals.

Upon embryonic (E16.5) and postnatal (P6) TMX administration at a dosage of 6 mg and 0.5 mg (explained in detail in section 2.6), a number of EYFP+ cells were observed in the adult gray (Dorsal cortex, Hippocampus and Ventral Cortex) and white matter regions (Corpus Callosum and Fimbrae). Reporter positive NG2+ cells were seen at E19.5 (TMX at E16.5) in the Dorsal Cortex and Ventricular Zone (see section 3.10).

NG2creER^{TM}BAC:GluRB^{2lox}:ROSA26/EYFP:NG2DsRed mice: To specifically knock out the GluRB subunit in OPCs an interbreeding strategy was employed, where mice heterozygous for the floxed GluRB allele (*GluRB$^{2lox/wt}$*) were inter-bred with homozygous and/or heterozygous NG2creER^{TM}BAC mice (described elsewhere in section 2.1.6).

Furthermore, the ROSA26/EYFP Cre reporter line is used to permanently label NG2 cells and their progeny that as a result of Cre-mediated recombination have either lost the GluRB subunit, in case of the GluRB$^{2lox/2lox}$ genotype: the GluRB knockouts and in NG2 cells that still possess the GluRB subunit, in case of the GluRB$^{wt/wt}$ genotype. For this, mice heterozygous for GluRB i.e. GluRB$^{2lox/wt}$ were cross-bred to each other, to yield both GluRB$^{2lox/2lox}$ and GluRB$^{wt/wt}$ genotypes.

These triple transgenic mice were additionally bred with the NG2DsRed line with an aim to easily identify all NG2 cells for future patch clamp experiments.

2.3   Tissue processing

Preparation of frontal brain sections of postnatal animals

Mice were anaesthetised in a small bell jar with a few drops of Isofluran, following which they were sacrificed by decapitation. The head was taken on a flat surface and using fine scissors the scalp was slit open and loosened, then the skull, along with the dura was opened. The brain was "scooped out" using a fine curved spatula into a glass beaker containing ice cold solution of sucrose preparation solution of the following composition (in mM): 87 NaCl, 2.5 KCl, 1.25 NaH$_2$PO$_4$, 7 MgSO$_4$, 0.5 CaCl$_2$, 25 NaHCO$_3$, 25 glucose, 75 sucrose, gassed with 95% O$_2$ and 5% CO$_2$ mixture.

Next, the brain was placed onto a pre-cooled metal dissection plate with sucrose solution to cut off the cerebellum- following which the trimmed brain was glued frontally onto a specimen disc using super glue (UHU®). This disc was fitted in the buffer tray containing ice cold sucrose solution and this set up was placed in the cooling bath (filled with crushed ice) of the vibratome (Leica VT1000 S, Leica VT1200 S and Thermoscientific Microm HM650V). 400 μm frontal slices were cut starting at the level of the olfactory bulb, using the vibratome with an amplitude of 1 mm and a speed of 0.22 mm/s.

Subsequent to slicing the entire brain, all the 400 μm slices were transferred to a beaker of sucrose preparation solution at 35° C. After the slices were incubated in warm su-

crose preparation solution for 25 minutes, they were allowed to cool in the same solution at room temperature after which the slices were fixed overnight in 8% paraformaldehyde (PFA) (in PBS; pH 7.44).

Preparation of frontal brain sections of embryonic animals

Embryos aged days 18, 16, 12.5, 10.5 and 8.5 were obtained by opening the abdominal cavity of the pregnant dam after decapitation. The embryos were separated from the placenta and the yolk sac was removed, after which the embryos were transferred to ice chilled pre-gassed sucrose preparation solution. The brains were carefully dissected out of the cranial cavity and embedded in 5% Agar to facilitate the slicing procedure. 400 μm slices were cut and processed pre-fixation as explained above for postnatal animals. At E12.5 and E10.5, whole embryos were fixed in 8% PFA.

After overnight fixation in 8% PFA, all tissue was re-sectioned to 50 μm, following 3 times 10 minute washes in PBS on a Leica VT1000 S vibratome. All sections were pre-embedded in agar to facilitate re-sectioning.
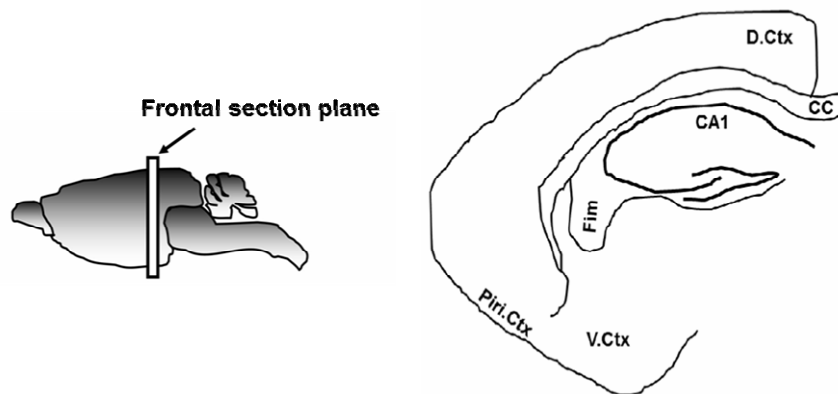
Figure 10. Schematic illustration of frontal forebrain slices. Frontal plane and a section of postnatal day 6 mouse brain, adapted from Atlas of the Developing Mouse Brain by Paxinos et al. (2007). D.Ctx, Dorsal Cortex; CA1 field of the Hippocampus; CC, Corpus Callosum; Fim, Fimbrae; V.Ctx, Ventral Cortex; Piri.Ctx, Piriform Cortex.

2.4   Immunohistochemistry

50 μm free-floating sections were first incubated with primary antibody in TBS containing 0.2% Triton X-100 overnight at 4° C. After 3 times 10 minute washes in TBS, antibodies and detection were each applied for 3 hrs. at 35° C with sections incubated in TBS containing 0.2% Triton X-100. Secondary detection was carried out by using biotinylated secondary antibodies, followed by incubation with streptavidin-conjugates. Dye-conjugated secondary antibodies were frequently used (see Table 1).

For counterlabelling of nuclei, I used Neurotrace fluorescent Nissl stain in the Cy5 emission range.

Table 1. The source and dilution of all antibodies used in this study.

Antibodies	Source	Dilution used
Primary		
Rabbit anti-NG2	Chemicon	1:500
Rabbit anti-GFAP	DakoCytomation	1:250 - 1:500
Mouse anti-NeuN	Chemicon	1:250
Goat anti-GFP FITC	Abcam	1:166.6
Chicken anti-GFP	Invitrogen	1:200 - 1:400
Rabbit anti-GFP	Invitrogen	1:200
Rat anti-BrdU	AbD Serotec	1:71.4 - 1:166.6
Mouse anti-APC (CC1 clone)	Chemicon	1:400
Rabbit anti-BLBP	Abcam	1:250
mouse anti-CNPase	Sigma Aldrich	1:100
Secondary		
Donkey anti-chicken Biotin	Jackson Immunoresearch	1:200
Goat anti-rabbit Biotin	Vector	1:200
Biotin anti-rat	Jackson Immunoresearch	1:100 - 1:500
Sheep anti-mouse Biotin	Serotec	1:200 and 1:4000
Goat anti-mouse Alexa 555	Invitrogen	1:200
Goat anti-rabbit Alexa 488	Invitrogen	1:200
Streptavidin DyLight 488	Jackson Immunoresearch	1:200
Goat anti-rabbit Rhodamine Red-X	Jackson Immunoresearch	1:200
Streptavidin Cy2	Jackson Immunoresearch	1:200
Streptavidin Cy5	Jackson Immunoresearch	1:200
Streptavidin Alexa 555	Invitrogen	1:200
Streptavidin Rhodamine Red-X	Jackson Immunoresearch	1:200
Streptavidin Cy3	Jackson Immunoresearch	1:200
Counterstain		
Nissl deep red	Invitrogen	1:100 - 1:200

NG2-GFP double immunohistochemistry: The two primary antibodies, rabbit anti-NG2 and chicken anti-GFP were applied simultaneously in TBS containing 0.2% Triton X-100 overnight at 4° C. Next, donkey anti-chicken biotin was applied for 3 hrs. at 35° C, following which in the last step, the sections were incubated with Streptavidin Dyelight-488 and goat anti-rabbit RRX.

GFAP-GFP double immunohistochemistry: The two primary antibodies, rabbit anti-GFAP and chicken anti-GFP were applied simultaneously in TBS containing 0.2% Triton X-100 overnight at 4° C. Next, donkey anti-chicken biotin was applied for 3 hrs. at 35° C, following which in the last step, the sections were incubated with Streptavidin Dyelight-488 and goat anti-rabbit RRX.

NeuN-GFP double immunohistochemistry: The two primary antibodies, mouse anti-NeuN and chicken anti-GFP were applied simultaneously in TBS containing 0.2% Triton X-100 overnight at 4° C. Next, donkey anti-chicken biotin was applied for 3 hrs. at 35° C, following which in the last step, the sections were incubated with Streptavidin Dyelight-488 and goat anti-mouse Alexa 555.

CC1-GFP double immunohistochemistry: Especially in this reaction, the CC1 and GFP labelling steps were carried out sequentially to avoid cross-reactivity (see below). Free floating 50 μm sections were incubated with the primary antibody, mouse anti-APC in TBS containing 0.2% Triton X-100 and 2% normal horse serum overnight at 4° C. Since primary antibody is raised in mouse and applied on mouse forebrain sections, this could result in highly unspecific labelling as the anti-mouse secondary antibody would recognise all endogenous epitopes in the mouse tissue. To reduce this unspecific epitope-antibody interaction (blood vessels, background etc.), the mouse primary Ab is applied alongwith horse serum. Horse serum would ensure that all unspecific binding sites have horse antibodies stuck to them and these unspecific epitopes will not be recognized by the anti-mouse secondary antibody. Next, sheep anti-mouse biotin was applied for 3 hrs. at 35° C, following which the slices were incubated with Streptavidin RRX for 3 hrs. at 35° C. Subsequent to CC1 labelling, the GFP labelling was performed. Rabbit anti-GFP was applied to the sections overnight at 4° C and then the slices were incubated with goat anti-rabbit Alexa 488 for 3 hrs. at 35° C.

CNP-NG2-GFP double immunohistochemistry: In this reaction, the CNP, GFP and NG2 labelling steps were carried out sequentially. First, free floating 50 μm sections were incubated with the primary antibody, mouse anti-CNPase in TBS containing 0.2%

Triton X-100 and 2% normal horse serum overnight at 4° C. As explained, horse serum was used to reduce unspecific epitope-antibody interaction, since the host species of the primary antibody for CNPase was mouse. This was developed with an Alexa conjugated secondary antibody-goat anti-mouse Alexa 555 for 3 hrs. at 35° C. Next, the GFP labelling was performed. Chicken anti-GFP was applied to the sections overnight at 4° C and then the slices were incubated with goat anti-chicken Alexa 488 for 3 hrs. at 35° C. Lastly, NG2 labelling was performed. Rabbit anti-NG2 was applied to sections overnight at 4° C, after which slices were incubated with goat anti-rabbit biotin for 3 hrs. at 35° C and then developed with Streptavidin Cy5 which was applied for 3 hrs. at 35° C.

BrdU-GFP double immunohistochemistry: Here, the GFP and BrdU labelling steps were performed sequentially since HCl pre-treatment for BrdU labelling leads to extreme denaturing of the tissue and loss of the other antigen- in this case GFP. Therefore, first the GFP immunoreaction was carried out. Slices were incubated with rabbit anti-GFP overnight at 4° C and then goat anti-rabbit Alexa 488 was applied for 3 hrs. at 35° C. After this slices were incubated in 2N HCl for 30 min. Following a more intensive washing out step i.e. 4 times 10 min with TBS, the primary antibody, rat anti-BrdU was applied overnight at 4° C. Next, slices were incubated with highly cross adsorbed biotin anti-rat for 3 hrs. at 35° C and then Streptavidin Cy5 was applied, again for 3 hrs. at 35° C. It is important to note that in this double labelling protocol only 0.06% Triton X-100 was used at each step, to preserve the antigens in the section since HCl pre-treatment for BrdU labelling strongly denatures the slice.

NG2-GFP-BrdU double immunohistochemistry: As explained above, to prevent the denaturing of the NG2 and GFP antigens by the strong HCl denaturing pre-treatment used for BrdU labelling, the NG2 and GFP labelling steps were performed before the BrdU labelling step. The two primary antibodies, rabbit anti-NG2 and chicken anti-GFP were applied simultaneously overnight at 4° C. For secondary detection, goat anti-rabbit RRX and goat anti-chicken Alexa 488 were applied for 3 hrs. at 35° C. After this slices were incubated in 2N HCl for 30 min. Following a more intensive washing out step i.e. 4 times 10 min with TBS, the primary antibody, rat anti-BrdU was applied overnight at 4° C. Next, slices were incubated with highly cross adsorbed biotin anti-rat cross SP for 3 hrs. at 35° C and then Streptavidin Cy5 was applied, again for 3 hrs. at 35° C. It is important to note that in this double labelling protocol only 0.06% Triton X-100 was used at each step, to preserve tissue condition.

BLBP-GFP double immunohistochemistry: The two primary antibodies, rabbit anti-BLBP and chicken anti-GFP were applied simultaneously in TBS containing 0.2% Triton X-100 overnight at 4° C. Next, donkey anti-chicken biotin was applied for 3 hrs. at 35° C, following which in the last step, the sections were incubated with Streptavidin Dyelight-488 and goat anti-rabbit RRX.

All immunolabelled sections were mounted in Vectashield (Vector Laboratories).

2.5   BrdU labelling

In order to perform proliferation assays in the three transgenic mouse lines, BrdU was administered to both embryonic and adult animals via different routes of delivery.

BrdU administration to CNP-Cre:ROSA26/EYFP mice

Intraperitoneal injections

P10 mice were administered 2 i.p injections of 100 mg/kg BrdU over a 12 hr. period for 4 days until P13 (Figure 11).
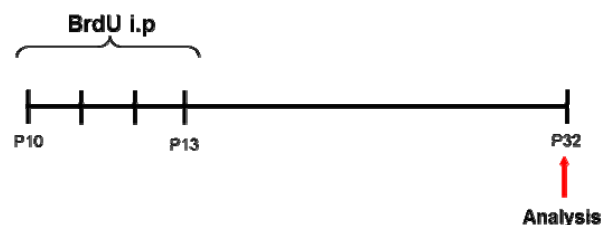
Figure 11. Postnatal BrdU administration protocol. BrdU was administered from P10 to P30 and animals were analysed at P30.

Wildtype mice were administered 100 mg/kg BrdU dissolved at 16.2 mg/ml in 0.9% NaCl, with 4 i.p injections per day for 4 days.

Oral gavage

BrdU was administered to timed pregnant dams at E12.5 orally at a dosage of 50 mg/kg of BrdU dissolved at 16.2 mg/ml in 0.9% NaCl, twice a day (4 hours apart) for one day only (Figure 12). This technique was established with the help of Gabriela Bodea (Institute of Reconstructive Neurobiology, UKB). The pregnant animal was held horizontally and the rounded rubber tipped animal feeding needle (Fine Science Tools; cat No. 9921, size: 20G x 1-1/2′′) was inserted in to its oral cavity, allowed to pass freely through the oesophagus up until the last rib cage. Great care was taken not to damage the trachea

and in case even minimum resistance was experienced, the needle was withdrawn and the procedure tried again. Subsequent to de-scruffing the animal, it was allowed to rest in a separate holding cage where it was monitored for 30 min for any changes in vital signs. The female was allowed to deliver normally and litters were prepared at P30 and subject to required immunolabellings. Pregnant wildtype mice were i.p injected at E16 with 50 mg/kg BrdU dissolved at 16.2 mg/ml in 0.9% NaCl, four times a day (over 12 hours) for one day only.
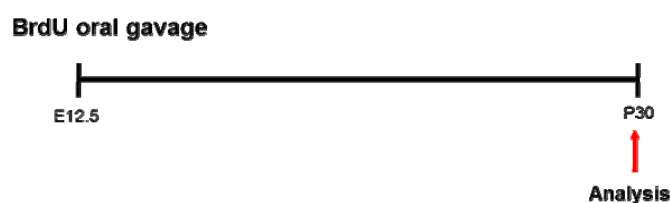
Figure 12. Embryonic BrdU administration protocol. BrdU was administered at E12.5 and animals were analysed at P30.

BrdU administration to NG2creER^{TM}BAC:GluRB^{2lox}:ROSA26/EYFP:NG2DsRed mice

Adult mice (P10-P32) which had already been injected with Tamoxifen to induce Cre recombination (read below) , were administered 1 i.p injection of BrdU 2-3 hours prior to sacrifice at a dosage of 300 mg/kg dissolved at 16.2 mg/ml in 0.9% NaCl). All mice were administered BrdU upon actual weighing to calculate the exact BrdU dosage.

2.5.1 Identification of EYFP+ cells as neurons based on morphological criteria

In the BrdU labelling experiments, reporter positive neurons were identified on basis of morphology, as having a large round to oval cell body, with a long axonic process and invariably a few dendrites. NeuN immunolabellings could not be used to ascertain the neuronal phenotype, since NeuN immunohistochemistry did not work well with HCl pre-treatment used for BrdU labelling. In order to substantiate that neurons were identified correctly based on their morphology, analogous scans were performed on NeuN-GFP labelled sections. I was blind to the channel used to scan the NeuN+ cells during the analysis procedure, so first I marked all EYFP+ cells that as per the criteria described above looked like neurons. Next, I saw using the NeuN channel if my identification of neurons based on morphology was correct and these cells indeed co-labelled

with NeuN. The fraction of NeuN+ neurons amongst those identified purely by morphology was 0.99 ± 0.004 (total of 208 EYFP+ neurons, n=3 animals), 0.97 ± 0.004 (total of 112 EYFP+ neurons, n=3 animals) and 0.98 ± 0.01 (total of 77 EYFP+ neurons, n=3 animals), in the dorsal, piriform and ventral cortices. This establishes that the stringent morphological characteristics criteria used to ascertain neuronal cells were indeed appropriate.

2.6   Induction of Cre-mediated recombination with Tamoxifen

Cre activity was induced in embryonic NG2creER^{TM}BAC:ROSA26/EYFP double transgenic mice by administering 6 mg of Tamoxifen to pregnant at E16.5 via gastric gavage using 20-gauge curved stainless steel feeding needles with round tips (Figure 13). Tamoxifen (TMX) (Sigma) was dissolved in corn oil preheated to 35° C, at a concentration of 20 mg/ml, mixed with 5mg/ml Progesterone, in a lengthy process of repetitive sonications at the same temperature. It is essential to note that no ethanol was used for dissolution. In postnatal NG2creER^{TM}BAC:ROSA26/EYFP mice, 0.5 mg TMX was administered at P6 at a concentration of 10 mg/ml (single i.p injection).
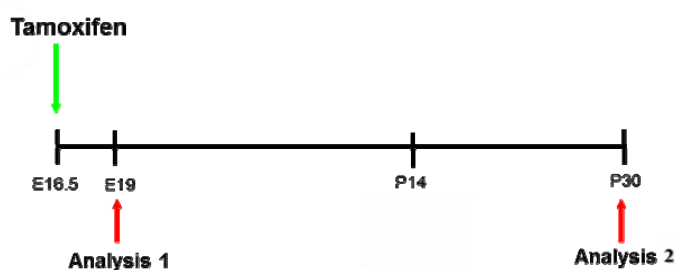
Figure 13. Embryonic Tamoxifen induction protocol. Tamoxifen was administered at E16.5 and the three time points of analysis were at E19, P14 and P30.

In NG2creER^{TM}:GluRB^{2lox}:ROSA26/EYFP:NG2DsRed transgenic mice, Cre activity was induced by administering 0.5 mg of TMX to postnatal mice at ages ranging from P5 to P20 via intraperitoneal injections using a disposable insulin syringe with a needle specification of 30G x ½˝ (0.3 mm x 12 mm) (single i.p injections for 1 or 6 days, see sections 3.11 and 3.12). A stock solution of 10 mg/ml was prepared by dissolving and sonicating Tamoxifen in 19.9:0.1 corn oil:ethanol.

2.7   Virus transfections

Viral vector production

Recombinant AAV1/2 and AAV8 genomes were generated by the working group of Dr. Susanne Schoch McGovern, with large scale triple transfection of HEK293 cells. The rAAV plasmids: **CMV Venus, Efa-doublefloxed reverse-hChR2-EYFP and Ef1a-DIO-EYFP-WPRE-pA**, helper plasmids encoding genes for serotype ½ and 8 specifications, and adenoviral helper pFΔ6 (Stratagene) were transfected using standard $CaPO_4$ transfection. Cells were harvested ~60 hrs. following transfection. Cell pellets were lysed in the presence of 0.5% sodium deoxycholate (Sigma) and 50U/ml Benzonase endonuclease (Sigma). rAAV viral particles were purified from the cell lysate by Hi-Trap^TM heparin column purification (GE Healthcare) for Serotype1/2 and by a centrifugation gradient for Serotype 8. Purity of the viruses was validated by coomasie blue labelling of SDS-polyacrylamide gels loaded with 7-15 µl of virus stock.

Virus injections

As in the CNP-Cre:Z/EG and CNP-Cre:ROSA26/EYFP lines, Cre-mediated reporter expression is constitutive, therefore a Cre reporter virus-based experimental strategy was employed. The rationale here was to transfect mice expressing Cre recombinase under the *Cnp1* promoter while lacking any reporter genes i.e. a CNP-Cre $^{+/-}$:ROSA26/EYFP$^{-/-}$ and CNP-Cre $^{+/-}$:Z/EG$^{-/-}$ genotype with Cre-dependent EYFP virus. Upon successful transfection of the virus, only transfected cells will be reporter positive under endogenous Cre expression, thus enabling one to follow fates of CNP-Cre expressing EYFP+ cells. To standardize the virus injection protocol, trials with varying volumes and frequency of injections were performed in neonatal mice.

Neonatal injections: P1 PGK-Cre mice expressing Cre recombinase in all cells under the PGK promoter were cryoanesthetized for 2-4 minutes. After which they were placed on a flat cool surface and one intraventricular injection of the Efa-doublefloxed reverse-hChR2-EYFP virus construct (Serotype 1/2) was made with a volume of 1 µl per ventricle in both hemispheres using a 5 µl (33 gauge) Hamilton syringe.

Next, the CMV-Venus virus construct (Serotype 8) was intraventricularly injected once a day with a volume of 1 µl in only one ventricle in P1 mice. I also injected 3 µl of the same CMV-Venus construct in the cerebral ventricle of P2 mice, twice a day for two days and then twice a day for one day. Postnatal day 3 CNP-Cre:Z/EG mice were intraventricularly injected with 1 µl (in only one ventricle) of the Ef1a-DIO-EYFP-WPRE-

pA virus construct. Additional to check the Cre dependent EYFP expression pattern of the above construct, 1 µl intraventricular injection in P2 wild type mice was performed.

2.8   Solutions

Sucrose preparation solution

87 mM	NaCl
2.5 mM	KCl
1.25 mM	Na_2HPO_4
7 mM	$MgCl_2$
0.5 mM	$CaCl_2$
25 mM	$NaHCO_3$
25 mM	Glucose
75mM	Sucrose

pH 7.0 at 5° C and 7.6 at 35° C with carbogen

Artificial cerebrospinal fluid (ACSF) for room temperature (RT)

124 mM	NaCl
3 mM	KCl
1.25 mM	Na_2HPO_4
2 mM	$MgCl_2$
2 mM	$CaCl_2$
26 mM	$NaHCO_3$

10 mM   Glucose

pH 7.4 with carbogen

Tris-buffered saline 0.1 mM
  100 mM   TRIS

  154 mM   NaCl

pH 7.6 with 1 M HCl and 1M NaOH

Phosphate-buffered saline 10 mM (1x)
  6.5 mM Na_2HPO_4

  1.9 mM NaH_2PO_4

  150 mM   NaCl

pH 7.4 with 1M HCl and 1M NaOH

Fixation medium 8% Paraformaldehyde (PFA)
  8 g   PFA

  100 ml   1 mM PBS

  12 drops   1 M NaoH

  6 drops   1 M HCl

pH 7.4 with 1 M HCl and 1 M NaOH

Cryostorage Glycol Solution
  1% (w/v)   PVP-40 Polyvinylpyrolidone

  30% (w/v)   Sucrose

30% (w/v)	Ethylene Glycol
0.2 M	PB

Phosphate Buffer 0.2 M

0.2 mM	Na_2HPO_4
0.04 mM	NaH_2PO_4

pH 7.4 with 1 M HCl and 1M NaOH

2.9 Image acquisition

Sections were scanned with a confocal laser scanning microscope (Leica TCS NT, equipped with an Argon-Krypton laser) and images with different dyes (eg. Dyl 488, RRX and fluorescent Nissl Cy5) were acquired sequentially. For Dyl 488 or Cy2, the following laser lines and filters were used: excitation 488 nm, triple dichroic (TD-488/568/633), pass through reflection short pass 580 nm, emission band pass 530/30 nm. For RRX or Cy3 we used: excitation 568 nm, triple dichroic (TD- 488/568/633), pass through reflection short pass 660 nm, emission band pass 600/30 nm. For Cy5 we used: excitation 647 nm, triple dichroic (TD- 488/568/633), emission long pass 665 nm. The majority of scans were acquired with a 63x objective (water; NA 1.2, correction ring, Leica) and the pinhole was set to 1 Airy unit. Laser power, detector gain and offset were adjusted such that in the final scan (4-10 averages) only a few pixels had zero or maximal (225) digital units. This means that few bright pixels in my sample signal were brought close to saturation (but not crossing it) i.e. close to white on a gray scale (blue pixels on pseudo glow over-under colour) and the darkest features were set to black (green pixels on pseudo glow over-under colour). Thus, the maximal and minimal detection was set such that section was not scanned with over-saturation or under-scanned, and all biological features remained unchanged. Typically detector gain and offset were set to ~60-70% and ~6 digital units, respectively. The beginning and end of the confocal stack to be scanned was set to z positions in the entire slice thickness where no EGFP+ or EYFP+ cells were seen. And the numbers of sections in each stack were decided so as to get a voxel depth of 1.5 μm between two adjacent sections. Detector gain and off-

set were set using the *"Glow over- under"* pseudo colour to ~70% and ~5-6 digital units, respectively. Photoshop was used to modify certain images: maximum brightness was rescaled to ~80% and a gamma correction factor of ~1-1.2 was introduced.

2.10 Cell count and quantification

To determine the postnatal phenotype EGFP+ or EYFP+ cells in the CNP-Cre:Z/EG mice and CNP-Cre:ROSA26/EYFP mice, frontal brain sections were investigated, around approximately -1.64 mm from Bregma at early postnatal, P6, P10 and late post-natal, P30 ages. For cell count analysis, areas were chosen randomly within the indicated brain regions (see Figure 10), all analysis were performed on 3-4 animals at each time point and 2-3 brain slices were used for each animal.

Brain regions under analysis

The regions of interest have been depicted in Figure 10. The dorsal cortex area under observation refers to the cerebral cortex above the corpus callosum that includes the primary and secondary motor cortex, primary somatosensory cortex and part of the retrosplenial granular cortex. The selective region of the corpus callosum under observation is directly under the Indusium griseum and the entire fimbrae was scanned. In the hippocampus, the stratum radiatum region of the CA1 was under observation and the ventral cortex region refers to the cerebral cortex located ventrally down across from the rhinal fissure, including the amygdala. The piriform cortex is the cerebral cortex extending from the rhinal fissure up until the cortex-amygdala transition zone.

Cell Counts

During scanning, volume under analysis was approximately 9.763×10^5 μm^3 (158.73 μm x 158.73 μm x 1.55 μm x 25 sections) and great emphasis was placed on the fact that the total number of confocal stacks made per region per animals should in total include atleast 20-30 EGFP+ or EYFP+ cells. It is important to note here that I considered two antigens as co-localized only if the co-localization pattern extended from top to bottom of the *z*-plane extent of the cell concerned. The image analysis processing software LSM 5 Image browser (Carl Zeiss) was used for cell identification and counts. The fractions presented in the results section as "fraction of EGFP or EYFP cells that were positive for a cell specific antigen" were calculated as follows: for each region, this fraction was calculated separately for each confocal stack, these fractions from different stacks were then averaged to obtain a value which represents the mean fraction for that

region for each animal. Final fractions for each region were calculated by averaging values across the number of animals. Standard error of mean (SEM) for each region has been calculated for fractions obtained from each animal. Fractions for each region are also mentioned alongwith total cell number which has been calculated for each region across all stacks and all animals. Absolute numbers of cells were all normalized to the "z-extent", which was calculated by multiplying the voxel size by the number of frames containing cells in each stack. The value for the number of frames containing cells in each stack was calculated by examining all frames of a stack and removing "empty or black" frames on the bottom and end of the stack. It is also important to note that absolute cell numbers were subject to correction for brain size, as the developing postnatal brain increases in volume from postnatal day 6 to postnatal day 30. Therefore, absolute cell numbers at P10 were all multiplied by a factor of 1.2 (volume of brain at P10/volume of brain at P6; i.e. 480 mm^3/400 mm^3) and absolute cell numbers at P30 were multiplied by a factor of 1.63 (volume of brain at P30/volume of brain at P6; i.e. 650 mm^3/400 mm^3). It is important to note that absolute cell numbers counted, include cells lying at the three defined borders of the slice (x,y,z), this may lead to an over esti-mation of cell numbers, but in my experiments this degree of over-sampling would be present across all groups being compared; thereby cancelling out this error in cell num-ber estimation. Moreover, the difference between absolute cell numbers between re-gions, groups and ages was always more than 10% in my experiments which maybe another reason to disregard the sampling error.

To determine Cre reporter expression, by the presence of EGFP+ or EYFP+ cells in the CNP-Cre:Z/EG and CNP-Cre:ROSA26/EYFP mice at both postnatal and embryonic ages, 400 µm live slices were first viewed before PFA fixation under the Nikon Eclipse TS-100 fluorescence microscope equipped with a DS Camera control unit DS-L2. It was imperative to view live slice first to ascertain the frontal plane where the maximum number of reporter positive cells were found and to first process these slices for 50 µm re-sectioning. Examination of live slices also ensured determination of reporter positiv-ity at the first instance, therefore saving time in the subsequent steps if no reporter posi-tive cells were found. Subsequent to this step, immunolabellings and confocal scans were taken on the Leica confocal scanning microscope.

3   Results

3.1   CNP-Cre mediated reporter expression in a subpopulation of NG2 cells

The CNP-Cre knock-in approach was used to label oligodendroglial lineage and explore their fates. Therefore, in order to ascertain the cell population labelled by CNP-Cre mediated recombination, the fraction of NG2 positive oligodendroglial precursor cells (OPCs) that were EGFP or EYFP positive was determined. I chose an early postnatal day 6 (P6) time point for this experiment as it is a developmental period before the onset of myelination in gray matter. Gray and white matter regions (Figure 14A) of the CNP-Cre:Z/EG and the CNP-Cre:ROSA26/EYFP mouse lines were examined with double immunolabelling with antibodies against GFP and NG2. It should be noted that the GFP antibody would also recognise the EYFP antigen owing to cross-reaction.

3.1.1   EGFP expression in a subset of NG2 cells in the CNP-Cre:Z/EG line

In P6 CNP-Cre:Z/EG mice, the proportion of NG2 cells that were EGFP+ in the gray matter regions of the dorsal cortex (Figure 14C, arrowhead), CA1 and ventral cortex was 0.22 ± 0.02 (total of 255 NG2+ cells, n=4 animals), 0.2 ± 0.03 (total of 234 NG2+ cells, n=4 animals) and 0.35 ± 0.03 (total of 159 NG2+ cells, n=3 animals) respectively (Figure 14B). In the white matter regions of corpus callosum (Figure 14E, arrowheads) and fimbrae, this fraction was 0.15 ± 0.06 (total of 344 NG2+ cells, n=4 animals) and 0.11 ± 0.06 (total of 505 NG2+ cells, n=4 animals) (Figure 14B) respectively. In both gray and white matter regions a number of NG2 cells did not display reporter positivity (Figure 14C,E, arrows; B).

3.1.2   EYFP expression in a subset of NG2 cells in the CNP-Cre:ROSA26/EYFP line

In CNP-Cre:ROSA26/EYFP mice at the same age (P6), a significantly higher fraction of recombined NG2 cells i.e. NG2 cells that were reporter positive, was observed. For instance, in the dorsal cortex, the proportion of NG2 cells that were EYFP+ cells was 0.64 ± 0.1 (total of 173 NG2+ cells, n=4 animals) (Figure 14D, arrowheads; B), and in
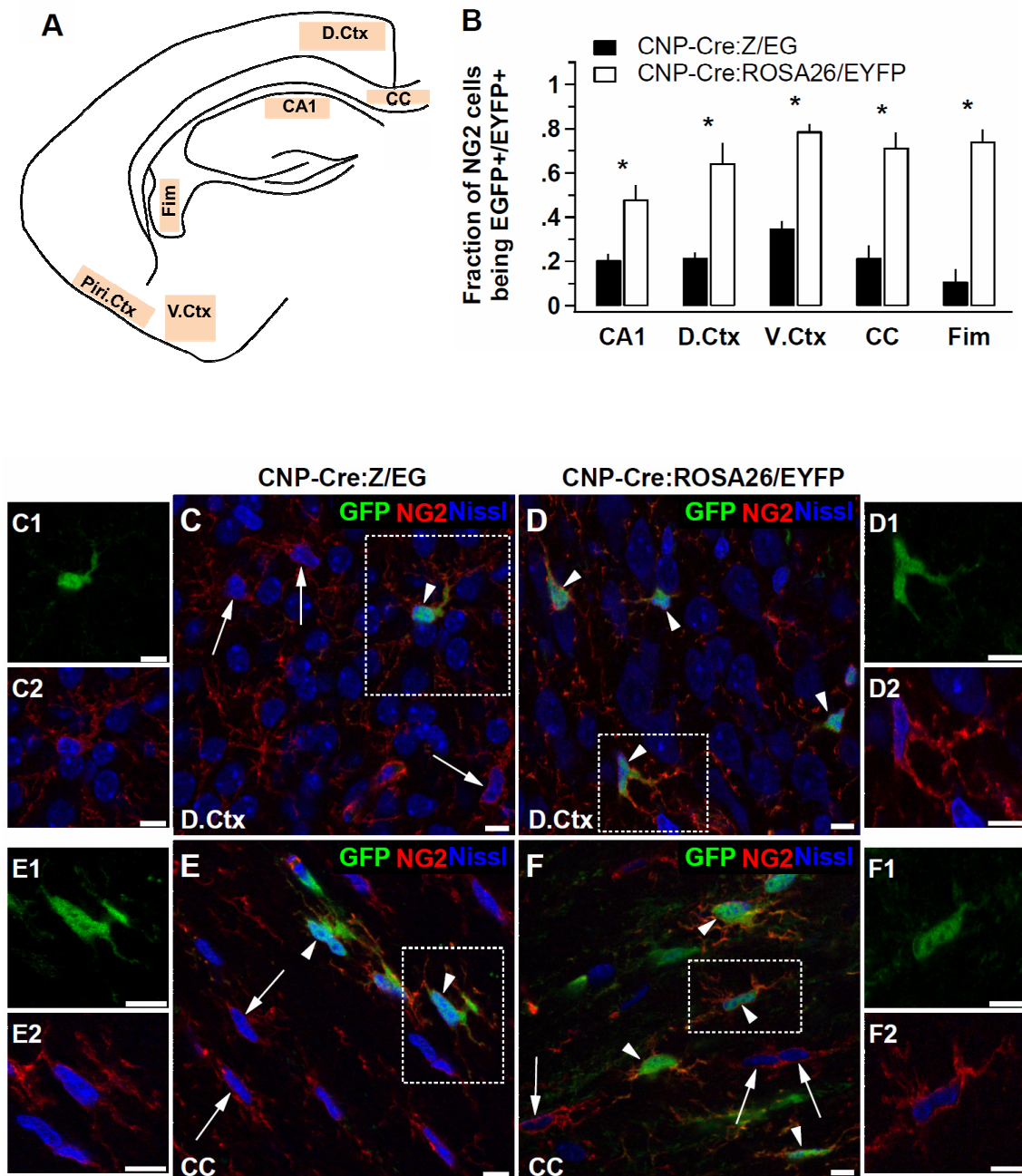
Figure 14. Reporter expression in NG2 cells in the CNP-Cre:Z/EG and CNP-Cre:ROSA26/EYFP lines. A, Illustration of postnatal day 6 murine brain partial frontal section with anatomical structures of interest in this study. Highlighted areas denote regions where analysis was performed. Gray matter: Dorsal Cortex, Hippocampal CA1, Ventral Cortex and Piriform Cortex. White matter: Corpus Callosum and Fimbrae. B, Fraction of NG2 cells that were EGFP+ or EYFP+. Error bars indicate SEM (±). Two-way Anova with Bonferroni post-hoc test used to indicate significant difference. For CA1, * indicates $p < 0.01$; for D.Ctx, V.Ctx, CC and Fim, * indicates $p < 0.0001$. C,D, Frontal sections through the Dorsal Cortex of CNP-Cre:Z/EG (C) and CNP-Cre:ROSA26/EYFP (D) mice at P6 immunolabelled for GFP (green), NG2 (red) and Nissl deep red (blue). C1-C2, D1-D2, represent maximum projections of the boxed areas in C,D at higher magnification. E,F, Frontal sections through the Corpus Callosum of CNP-Cre:Z/EG (E) and CNP-Cre:ROSA26/EYFP (F) mice at P6 immunolabelled for GFP (green), NG2 (red) and Nissl deep red (blue). E1-E2, F1-F2, represent maximum projections of the boxed areas in E,F at higher magnification. All arrowheads point to GFP+/NG2+ cells. All arrows point to GFP-/NG2+ cells. GFP (green) is used to indicate EGFP and EYFP fluorescence. Scale bars: 10 μm (applied to all). D.Ctx, Dorsal Cortex; V.Ctx, Ventral Cortex; CC, Corpus Callosum; Fim, Fimbrae.

the corpus callosum this fraction was 0.72 ± 0.07 (total of 286 NG2+ cells, n=4 animals) (Figure 14F, arrowheads; B).

It is noteworthy that at P6, in both experimental mouse lines a considerable population of NG2 cells that did not display any reporter positivity was observed (Figure 14C,E,F, arrows; B); and these NG2 cells represented a subset that was not labelled by CNP-Cre mediated recombination.

Taken together these findings suggest that with the CNP-Cre knock-in based experimental approach, a subpopulation of presumably relatively differentiated NG2 cells out of the entire OPC population, was selectively labelled. The next set of experiments were designed to elucidate the fate choice of precursor cells labelled by CNP-Cre mediated recombination, separately in the CNP-Cre:Z/EG and CNP-Cre:ROSA26/EYFP lines.

3.2   Analysis of reporter positive cells in the CNP-Cre:Z/EG line

3.2.1   EGFP expression in mature oligodendrocytes in gray and white matter forebrain

To ascertain whether CNP-Cre mediated EGFP expression was observed in mature oligodendrocytes, CNP-Cre:Z/EG animals were examined with double-labellings for GFP and oligodendrocyte stage specific markers: NG2 for labelling OPCs and mature oligodendrocyte specific adenomatosis polyposis coli (APC) clone CC1 (Bhat et al., 1996). In order to encompass the predominant developmental period, P10- a time point immediately prior to the onset of myelinogenesis in the gray matter and an adult P30 time point were chosen to examine the identity of reporter positive cells in the dorsal cortex and corpus callosum.

The absolute number of EGFP+ cells (per 1×10^{-3} mm^3) increased significantly from P10 to P30, both in the dorsal cortex (P10, 3.9 ± 0.3 per 1×10^{-3} mm^3; P30, 14.7 ± 2; $p < 0.05$) and corpus callosum (P10, 24 ± 2.5 per 1×10^{-3} mm^3; P30, 79 ± 10 per 1×10^{-3} mm^3; $p < 0.05$) (Figure 15E).

NG2-GFP co-labelling

In the dorsal cortex, concomitant with this increase in the number of reporter positive cells with age, there was a reduction in the fraction of EGFP+ cells that were NG2+. The fraction of EGFP+ cells that were NG2+ OPCs decreased significantly from $0.74 \pm$
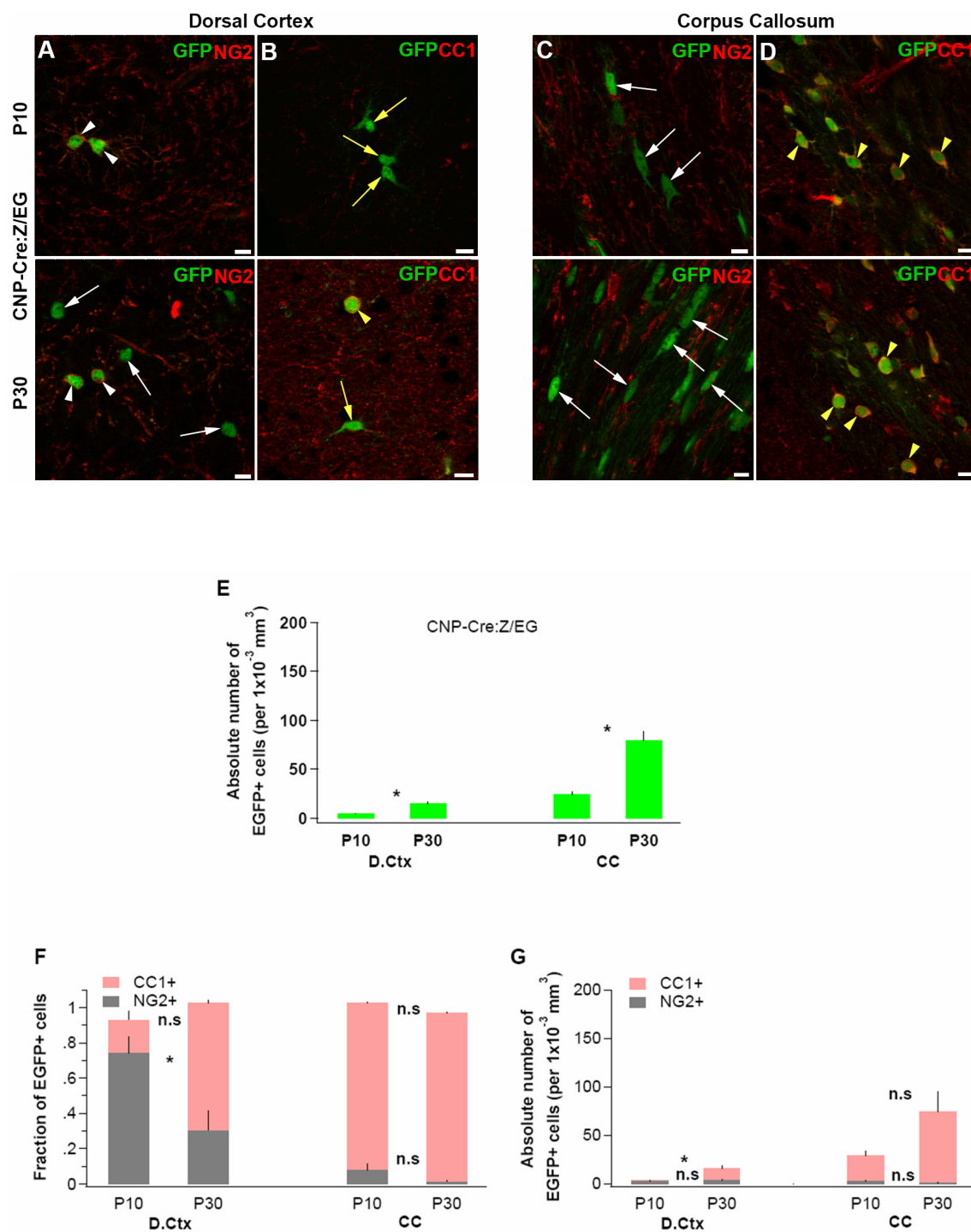
Figure 15. EGFP expression in mature oligodendrocytes in the CNP-Cre:Z/EG line. A-D, Frontal sections through the Dorsal Cortex (A,B) and Corpus Callosum (C,D) of P10 and P30 CNP-Cre:Z/EG mice, immunolabelled for GFP (green), NG2 (red) (A,C) and GFP (green), CC1 (red) (B,D). All white arrowheads point to GFP+/NG2+ cells. All white arrows point to GFP+/NG2- cells. All yellow arrowheads point to GFP+/CC1+ cells. All yellow arrows point to GFP+/CC1- cells. GFP (green) is used to indicate EGFP and EYFP fluorescence. Scale bars: 10 μm (applied to all). E, Histograms showing absolute numbers of EGFP+ cells in the Dorsal Cortex and Corpus Callosum at postnatal days 10 and 30 in the CNP-Cre:Z/EG line. F-G, Histograms showing fractions (F) and absolute numbers (G) of reporter positive cells that were NG2+ OPCs and CC1+ mature oligodendrocytes in the Dorsal Cortex and Corpus Callosum at postnatal days 10 and 30 in the CNP-Cre:Z/EG line. Error bars indicate SEM (±). Student's unpaired t-test used to indicate significant difference, * indicates $p < 0.05$. n.s, non-significant. D.Ctx, Dorsal Cortex; CC, Corpus Callosum.

0.09 (total of 76 EGFP+ cells, n=4 animals) at P10 to 0.3 ± 0.1 (total of 187 EGFP+ cells, n=4 animals) at P30 (Figure 15A, white arrowhead; F).

In the corpus callosum at P10 only a small fraction of EGFP+ cells that were NG2 cells existed, 0.08 ± 0.03 (total of 232 EGFP+ cells, n=4 animals), and this further reduced to 0.01 ± 0.01 (total of 1212 EGFP+ cells, n=4 animals) at P30 (Figure 15C,F). This is suggestive of differentiation.

Also, the absolute number of EGFP+NG2+ cells per $1x10^{-3}$ mm^3 decreased from P10 to P30. For instance, in the corpus callosum the number of EGFP+NG2+ cells decreased from ~2.2 ± 1 per $1x10^{-3}$ mm^3 at P10 (n=4 animals) to 1.1 ± 0.7 per $1x10^{-3}$ mm^3 at P30 (n=4 animals) (Figure 15G).

CC1-GFP co-labellings

In the dorsal cortex, CC1-GFP co-labellings revealed that the fraction of EGFP+ cells that were CC1+ mature oligodendrocytes increased from 0.19 ± 0.09 (total of 39 EGFP+ cells, n=2 animals) at P10 to 0.73 ± 0.01 (total of 127 EGFP+ cells, n=4 animals) at P30 (Figure 15B, yellow arrowhead; F).

In the P10 corpus callosum, a large fraction of EGFP+ cells that were CC1+ oligodendrocytes already existed: 0.95 ± 0.01 (total of 109 EGFP+ cells, n=2 animals), and this increased to 0.96 ± 0.01 at P30 (total of 609 EGFP+ cells, n=4 animals) (Figure 15D, yellow arrowheads; F). The absolute numbers of reporter positive cells that were CC1+ mature oligodendrocytes was also calculated. The EGFP+CC1+ cell population increased from 27 ± 5 per $1x10^{-3}$ mm^3 (n=2 animals) at P10 to 73 ± 20 per $1x10^{-3}$ mm^3 at P30 (n=4 animals) (Figure 15G).

3.2.2 Lack of EGFP expression in astrocytes in the ventral cortex

Next, I investigated whether CNP-Cre mediated EGFP expression was observed in astrocytes with double-immunolabellings for GFP to detect reporter positivity and for the astrocytic marker Glial fibrillary acidic protein (GFAP) (Bignami et al., 1972).

Early postnatal day 6 and 10, as well as adult P30 CNP-Cre:Z/EG animals were examined for the presence of reporter positivity in GFAP+ astrocytes. Both at P6 and P10, no EGFP+ cells that co-labelled GFAP were observed amongst 831 reporter positive cells examined in gray and white matter regions (total of 831 EGFP+ cells; n=8 animals).

In the adult P30 brain too, almost no reporter positive cells co-expressing GFAP were observed. For example in the ventral cortex, the majority population of EGFP+ cells did not demonstrate any GFAP immunoreactivity (~98%) (Figure 16A, arrows). Out of the 124 reporter positive cells examined in the ventral cortex of P30 CNP-Cre:Z/EG mice, only 2 EGFP+ cells (total of 124 EGFP+ cells; n=4 animals) were seen with a dense round cell body and a highly ramified bushy arbor of processes characteristic of protoplasmic astrocytes (Bushong et al., 2004), alongwith antigenicity for GFAP (Figure 16B,B´; arrowheads).
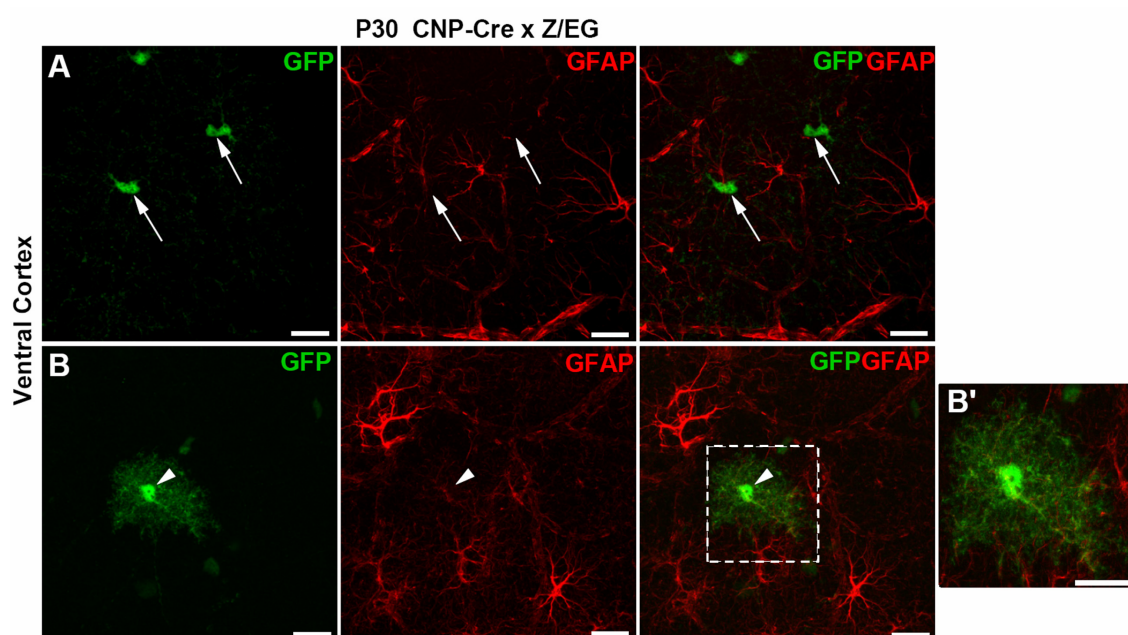
Figure 16. Absence of EGFP expression in ventral forebrain astrocytes in adult CNP-Cre:Z/EG animals. A,B, Frontal sections through the Ventral Cortex of P30 CNP-Cre:Z/EG mice double-immunolabelled for GFP (green) and GFAP (red). B´ depicts the cell shown in the white boxed area in B at higher magnification. All arrowheads point to GFP+/GFAP+ cells. All arrows point to GFP+/GFAP- cells. GFP (green) is used to indicate EGFP and EYFP fluorescence. Scale bars: 20 μm (applied to all).

Therefore, I did not find evidence of widespread astrocytic generation from CNP-expressing precursor cells labelled in the CNP-Cre:Z/EG line.

3.2.3 Absence of EGFP expression in neurons in the dorsal, ventral and piriform cortex

To determine if CNP-Cre mediated EGFP expression was observed in neurons, I performed GFP and the mature neuronal marker- NeuN (Mullen et al., 1992) at P30 in CNP-Cre:Z/EG mice.

In the P30 CNP-Cre:Z/EG mice, out of close to ~400 EGFP+ cells examined in four animals, only one or two EGFP+ cells with large cell bodies reminiscent of projection neurons and displaying NeuN immunoreactivity were seen. These negligible numbers of reporter positive neurons were observed only in the dorsal and piriform cortices.

Predominantly however, the dorsal (total of 173 EGFP+ cells, n=4 animals) (Figure 17A, arrows), ventral (total of 107 EYFP+ cells, n=4 animals) (Figure 17B, arrows) and piriform (total of 92 EYFP+ cells, n=4 animals) (Figure 17C, arrows) cortices were largely devoid of reporter positive cells displaying NeuN immunoreactivity.

Thus in the adult CNP-Cre:Z/EG line, I did not observe any CNP-Cre mediated EGFP reporter expression in NeuN+ neurons.
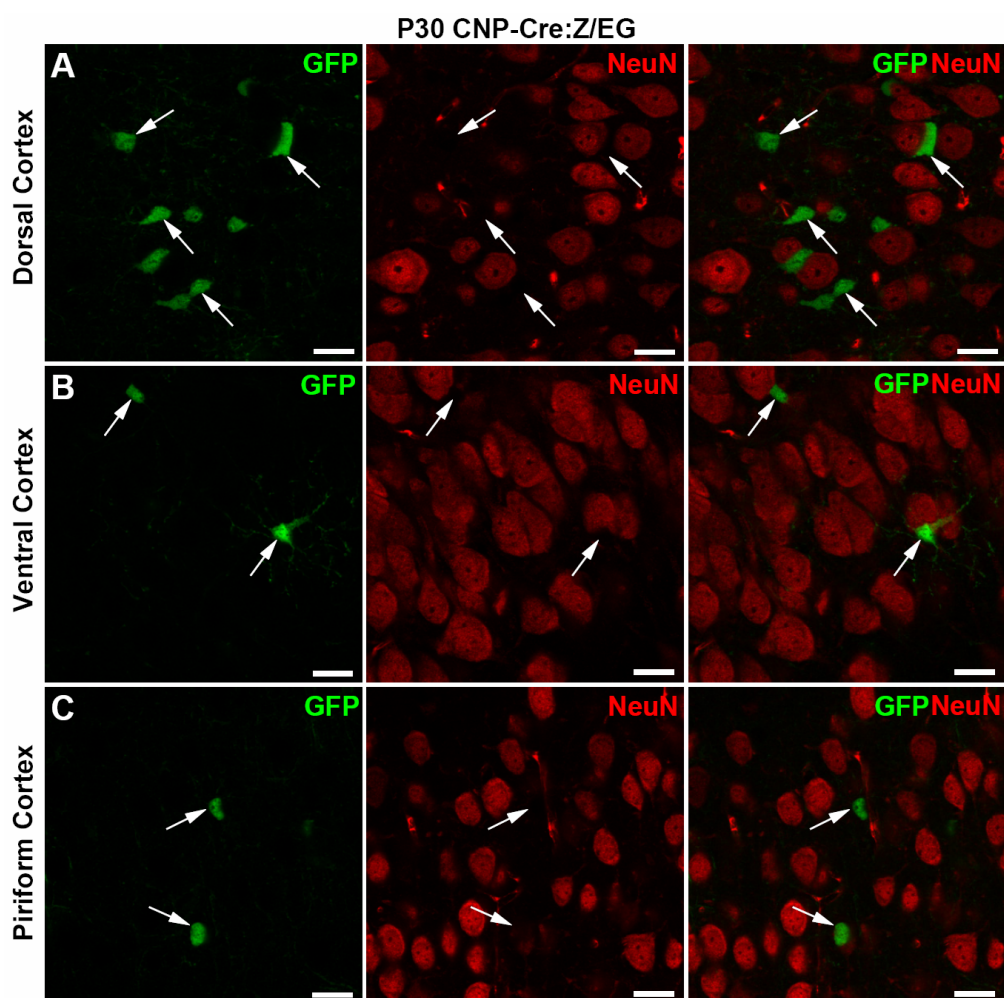
Figure 17. Absence of EGFP expression in neurons of the dorsal, ventral and piriform cortices in the adult CNP-Cre:Z/EG line. A-C, Frontal sections through the Dorsal Cortex (A) Ventral Cortex (B) and Piriform Cortex (C) of P30 CNP-Cre:Z/EG mice double-immunolabelled for GFP (green) and NeuN (red). All white arrows point to GFP+/NeuN- cells. GFP (green) is used to indicate EGFP and EYFP fluorescence. Scale bars: 20 μm (applied to all).

3.3 Analysis of reporter positive cells in the CNP-Cre:ROSA26/EYFP line

3.3.1 EYFP expression in mature oligodendrocytes in gray and white matter forebrain

Double immunolabellings of NG2-GFP and CC1-GFP were performed to determine if CNP-Cre mediated EYFP expression was observed in oligodendrocytes of the P10 and P30 CNP-Cre:ROSA26/EYFP line.

The absolute number of EYFP+ cells per $1x10^{-3}$ mm^3 increased significantly from P10 to P30, both in the dorsal cortex (P10, 23 ± 3.6 per $1x10^{-3}$ mm^3; P30, 50 ± 6 per $1x10^{-3}$ mm^3; $p < 0.05$) and corpus callosum (P10, 44 ± 6 per $1x10^{-3}$ mm^3; P30, 148 ± 20 per $1x10^{-3}$ mm^3; $p < 0.05$) (Figure 18E).

NG2-GFP co-labellings

In the dorsal cortex, the fraction EYFP+ cells that were NG2 cells decreased from 0.66 ± 0.13 (total of 358 EYFP+ cells, n=4 animals) at P10 to 0.3 ± 0.03 (total of 358 EYFP+ cells, n=4 animals) at P30 (Figure 18A, white arrowheads; F).

Similarly, in the corpus callosum, the proportion of EYFP+ cells that were NG2+ decreased from 0.28 ± 0.05 (total of 418 EYFP+ cells, n=4 animals) at P10 to 0.07 ± 0.02 (total of 853 EYFP+ cells, n=4 animals) at P30 (Figure 18C,F). This decrease in the fraction of EYFP+ cells that were NG2+ from P10 to P30 is indicative of differentiation.

CC1-GFP co-labellings

The fraction of EYFP+ cells that were CC1+ mature oligodendrocytes increased from P10 to P30 in the dorsal cortex (P10, 0.05 ± 0.01, total of 137 EYFP+ cells; P30, 0.24 ± 0.02, total of 592 EYFP+ cells; $p < 0.05$) and corpus callosum (0.65 ± 0.03, total of 318 EYFP+ cells; P30, 0.87 ± 0.01, total of 991 EYFP+ cells; $p < 0.05$). However, it is noteworthy that there was an accumulation of EYFP+ cells that were neither NG2+ OPCs nor CC1+ oligodendrocytes (Figure 18A-B, white and yellow arrows; F).

Therefore, although CNP-Cre mediated EYFP expression was observed in mature oligodendrocytes, there was a large population of EYFP+ cells which were distinct neither NG2+ OPCs or CC1+ oligodendrocytes and remained uncharacterised.
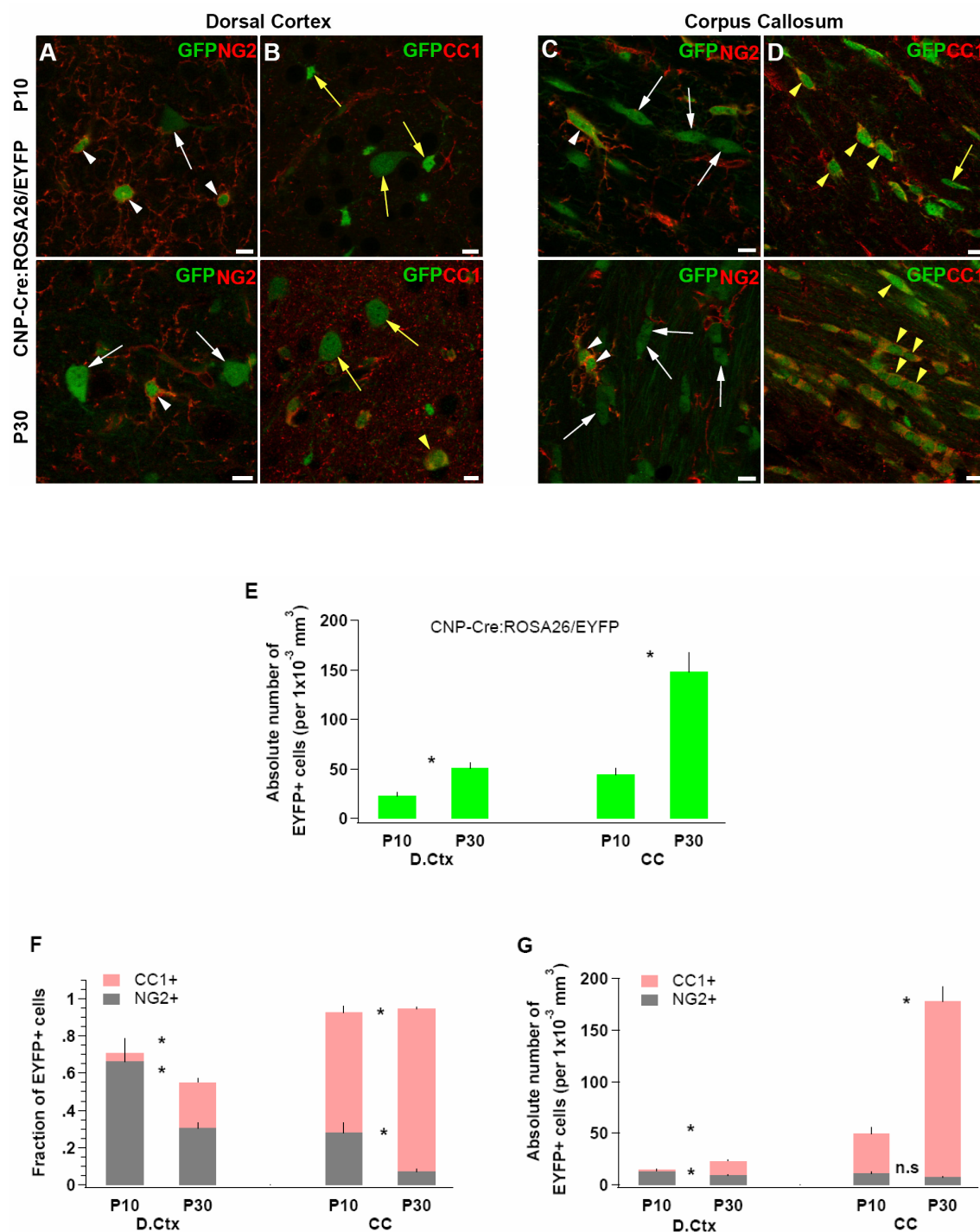
Figure 18. EYFP expression in mature oligodendrocytes in the CNP-Cre:ROSA26/EYFP line. A-D, Frontal sections through the Dorsal Cortex (A,B) and Corpus Callosum (C,D) of P10 and P30 CNP-Cre:ROSA26/EYFP mice, immunolabelled for GFP (green), NG2 (red) (A,C) and GFP (green), CC1 (red) (B,D). All white arrowheads point to GFP+/NG2+ cells. All white arrows point to GFP+/NG2- cells. All yellow arrowheads point to GFP+/CC1+ cells. All yellow arrows point to GFP+/CC1- cells. GFP (green) is used to indicate EGFP and EYFP fluorescence. Scale bars: 10 µm (applied to all). E, Histograms showing absolute numbers of EYFP+ cells in the Dorsal Cortex and Corpus Callosum at postnatal days 10 and 30 in the CNP-Cre:ROSA26/EYFP line. F-G, Histograms showing fractions (F) and absolute numbers (G) of reporter positive cells that were NG2+ OPCs and CC1+ mature oligodendrocytes in the Dorsal Cortex and Corpus Callosum at postnatal days 10 and 30 in the CNP-Cre:ROSA26/EYFP line. Error bars indicate SEM (±). Student's unpaired t-test used to indicate significant difference, * indicates $p < 0.05$. n.s, non-significant. D.Ctx, Dorsal Cortex; CC, Corpus Callosum.

The next set of experiments that I undertook in this study, were to ascertain the pheno-type of these non-oligodendroglial lineage reporter positive cells in the CNP-Cre:ROSA26/EYFP line.

3.3.2 EYFP expression in a small subset of astrocytes in the early postnatal and adult ventral cortex

Analysis of early postnatal brains (P6 and P10) of CNP-Cre:ROSA26/EYFP mice sur-prisingly revealed EYFP+ cells with astrocytic morphology and GFAP immunoreactiv-ity, especially in the ventral forebrain (Figure 19C,C′; arrowheads). The fraction of EYFP+ cells that displayed GFAP immunoreactivity was 0.09 ± 0.01 (total of 526 EYFP+ cells, n=8 animals).

In the ventral cortex region of adult P30 mice, a greater proportion of EYFP+ astro-cytes: 0.12 ± 0.02 (total of 179 EYFP+ cells, n=4 animals) were found (Figure 19A, arrowhead; D). In the P30 fimbrae (Figure 19B, arrowhead; D), a very miniscule frac-tion of GFAP+ fibrous astrocytes among EYFP+ cells were encountered: 0.01 ± 0.004 (total of 508 EYFP+ cells, n=4 animals). Also observed were EYFP+ GFAP+ cells that made end feet projections onto neighbouring blood vessels, a characteristic feature of astrocytes.

It is important to point out that I observed a few, 6 out of 526 EYFP+ cells in the ventral forebrain regions, with a typical bushy morphology characteristic of astrocytes: large soma and asymmetrically radiating processes that consist of several primary thick proc-esses, from which emanate multiple smaller collateral branching secondary processes. However, these cells lacked GFAP immunoreactivity.

The fraction of GFAP+ astrocytes that were EYFP+ in the P30 ventral cortex was 0.13 ± 0.01 (total of 155 GFAP+ astrocytes, n=4 animals).

Hence, the data presented here suggests that a small subset of GFAP+ astrocytes in the ventral forebrain is generated from precursor cells labelled by CNP-Cre mediated re-combination in the CNP-Cre:ROSA26/EYFP animals.

However, this fraction of EYFP+ cells being GFAP+ astrocytes was small and could not account for the large fraction of "unidentified" EYFP+ non-NG2+, non-CC1+ cells pre-sent in the P10 and P30 gray matter; therefore further experiments were performed to characterise these cell types.
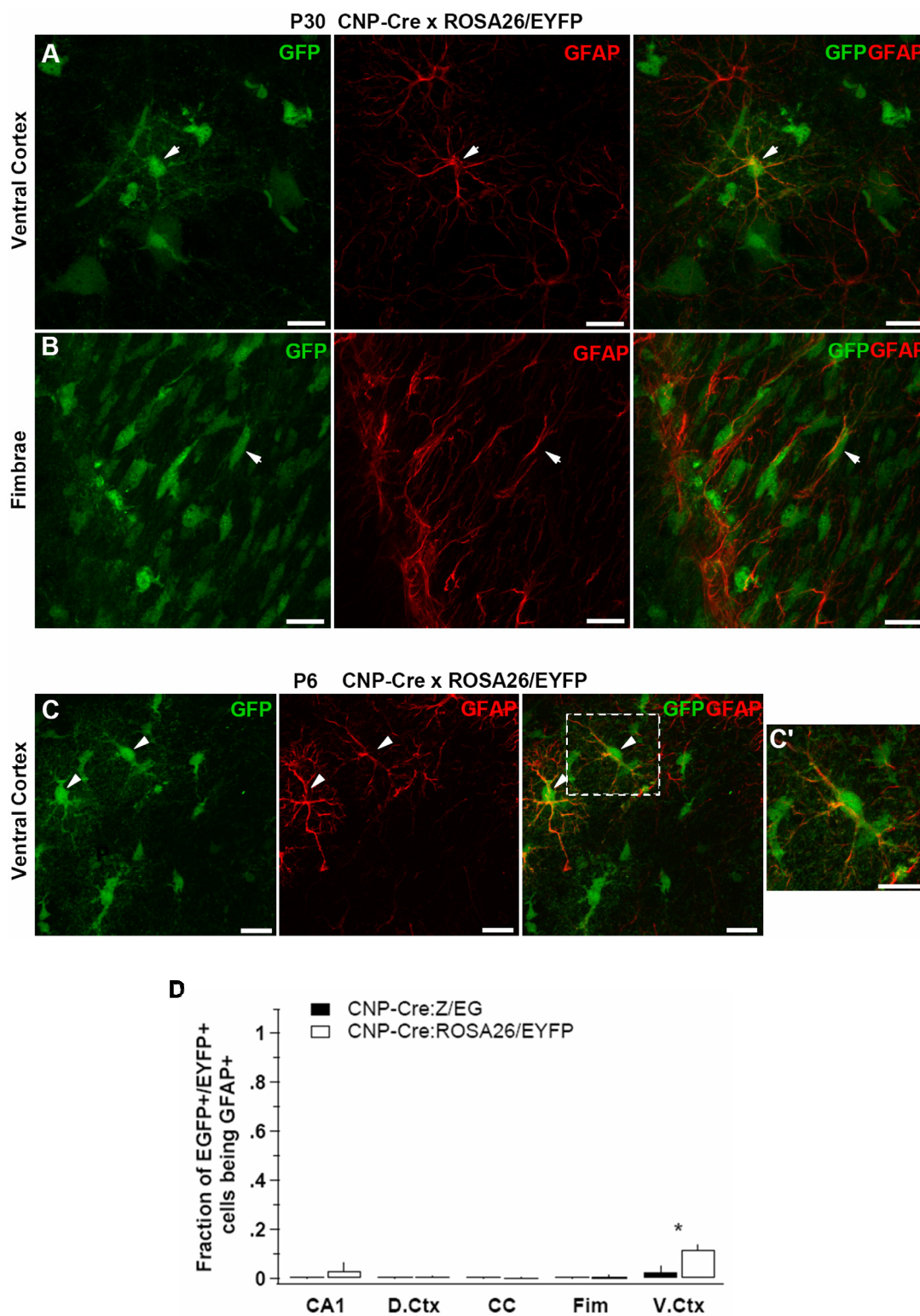
Figure 19. EYFP expression in a subset of ventral forebrain astrocytes in the CNP-Cre:ROSA26/EYFP line. A,B, Frontal sections through the Ventral Cortex (A) and Fimbrae (B) of P30 CNP-Cre:ROSA26/EYFP mice double-immunolabelled for GFP (green) and GFAP (red). C, Frontal sections through the Ventral Cortex of P6 CNP-Cre:ROSA26/EYFP mice double-immunolabelled for GFP (green) and GFAP (red). C´depicts the boxed are in C at higher magnification. All arrowheads point to GFP+/GFAP+ cells. GFP (green) is used to indicate EGFP and EYFP fluorescence. Scale bars: 20 µm (applied to all). D, Fraction of EYFP+ cells that were GFAP+ in the given regions of CNP-Cre:Z/EG and CNP-Cre:ROSA/EYFP lines. Error bars indicate SEM (±). Student's unpaired t-test used to indicate significant difference, * indicates p < 0.05. D.Ctx, Dorsal Cortex; CC, Corpus Callosum; Fim, Fimbrae; V.Ctx, Ventral Cortex.

3.3.3 EYFP expression in a large subpopulation of neurons in the adult dorsal, ventral and piriform cortex

A large number of reporter positive neurons were observed in CNP-Cre:ROSA26/EYFP mice.
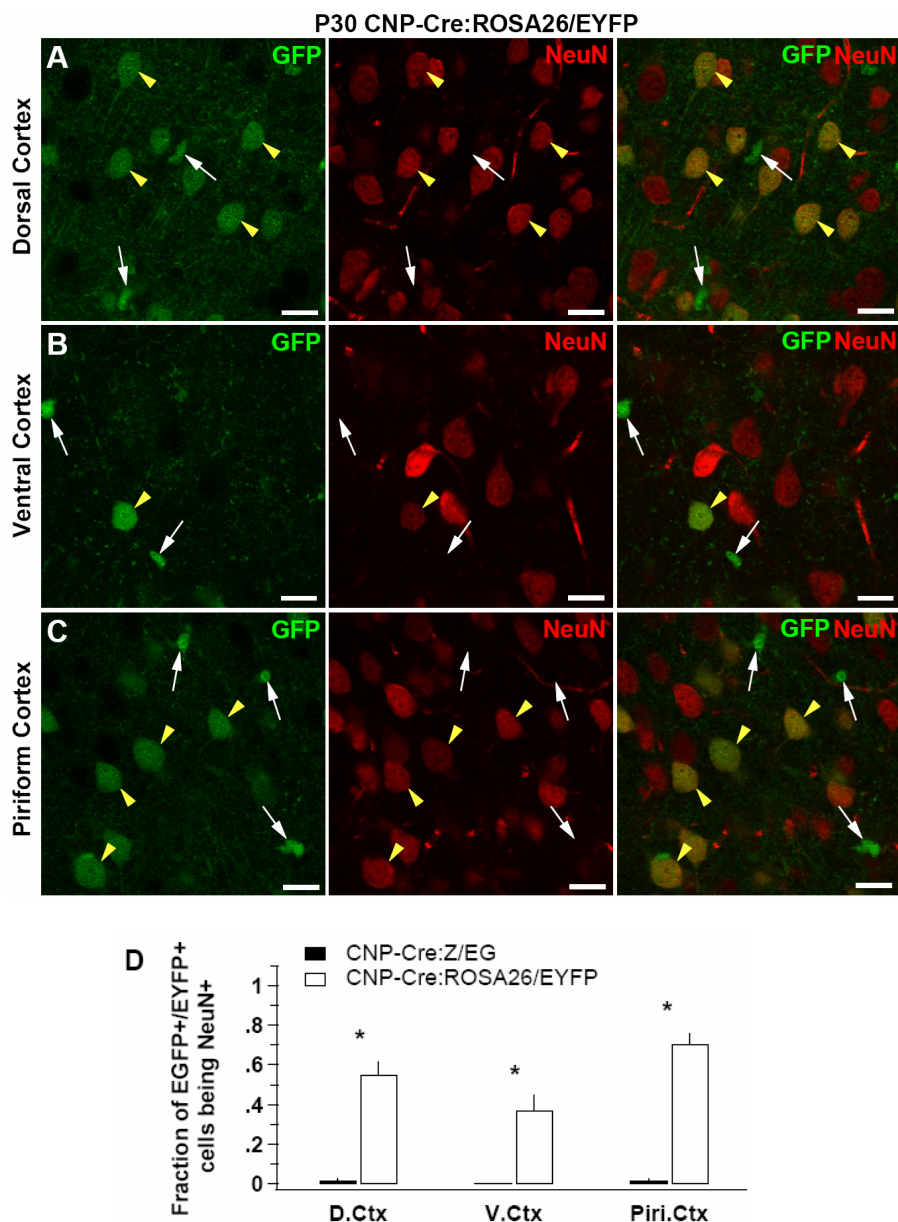
Figure 20. EYFP expression in a subset of neurons in the dorsal, ventral and piriform cortices of the adult CNP-Cre:ROSA26/EYFP line. A-C, Frontal sections through the Dorsal Cortex (A), Ventral Cortex (B) and Piriform Cortex (C) of P30 CNP-Cre:ROSA26/EYFP mice double-immunolabelled for GFP (green) and NeuN (red). All white arrows point to GFP+/NeuN- cells. All yellow arrowheads point to GFP+/NeuN+ cells. GFP (green) is used to indicate EGFP and EYFP fluorescence. Scale bars: 20 μm (applied to all). D, Fraction of EYFP+ cells that were NeuN+ neurons in given regions of the CNP-Cre:Z/EG and CNP-Cre:ROSA/EYFP mice. Error bars indicate SEM ($\pm$). Two-way Anova with Bonferroni post-hoc test used to indicate significant difference. * indicates $p < 0.0001$ for all three cortices. D.Ctx, Dorsal Cortex; V.Ctx, Ventral Cortex; Piri.Ctx, Piriform Cortex.

The fraction of EYFP+ cells being NeuN+ mature neurons was 0.55 ± 0.07 (total of 607 EYFP+ cells, n=4 animals), 0.37 ± 0.08 (total of 188 EYFP+ cells, n=4 animals) and 0.7 ± 0.05 (total of 353 EYFP+ cells, n=4 animals) in the dorsal (Figure 20A, arrowheads; D), ventral (Figure 20B, arrowheads; D) and piriform cortices (Figure 20C, arrowheads; D) respectively. Intriguingly, no EYFP+ neurons were observed in the CA1 hippocampal region and the dentate granule layer, suggestive of region specificity in neurogenesis.

The fraction of NeuN+ neurons that were EYFP+ was 0.23 ± 0.05 (total of 1462 NeuN+ neurons, n=4 animals) in the dorsal cortex, 0.08 ± 0.02 (total of 868 NeuN+ neurons, n=4 animals) in the ventral cortex and 0.22 ± 0.04 (total of 1264 NeuN+ neurons, n=4 animals) in the piriform cortex. Therefore these results indicate that large subset of neurons in the dorsal and piriform cortices were generated from precursors cells labelled by CNP-Cre mediated recombination.

The proportion of EYFP+ cells that were NeuN+ mature neurons in the CNP-Cre:ROSA26/EYFP line can be assumed to represent the large subset of NG2 and CC1 negative reporter positive cells observed in the adult cortex (section 3.3).

3.3.3.1   Age dependent distribution of EYFP+ neurons

In the CNP-Cre:ROSA26/EYFP animals, where a large subset of EYFP+ neurons had been observed in the dorsal and piriform cortices, the age dependence of reporter positive neuronal distribution was determined at varying time points ranging from P10 to P30. Subsequent to double-immunolabellings for GFP and NeuN to identify reporter positive mature neurons, GFP+NeuN+ cells in the postnatal days 10, 12, 15, 17, 22, 25 and 30 dorsal cortex and piriform cortices were counted. Animals were grouped in the P10-P12, P15-P17 and P22-P30 age groups. In the dorsal cortex, at P10-P12 age range there were $\sim 7 \pm 1.6$ per 1×10^{-3} mm^3 (n=3 animals) GFP+NeuN+ neurons. There was no significant difference in the number of EYFP+NeuN+ neurons present at the P15-P17 time point (9.3 ± 1.1 per 1×10^{-3} mm^3; n=4 animals). There were 15.5 ± 3.4 per 1×10^{-3} mm^3 (n=5 animals) EYFP+NeuN+ neurons in the P22-P30 age group and this did not represent a significant increase from the number of reporter positive neurons at P10-P12 or P15-P17 (Figure 21A). Similarly in the piriform cortex, the number of EYFP+NeuN+ cells at P22-P30 were 14.2 ± 3.3 per 1×10^{-3} mm^3 (n=5 animals). These were not significantly different in numbers from the EYFP+NeuN+ neurons present at either P10-P12 or P15-P17 time points (Figure 21B). These findings demonstrate that there is no sig-

nificant increase in the number of reporter positive neurons from P10 to P30 in the dorsal and piriform cortices.
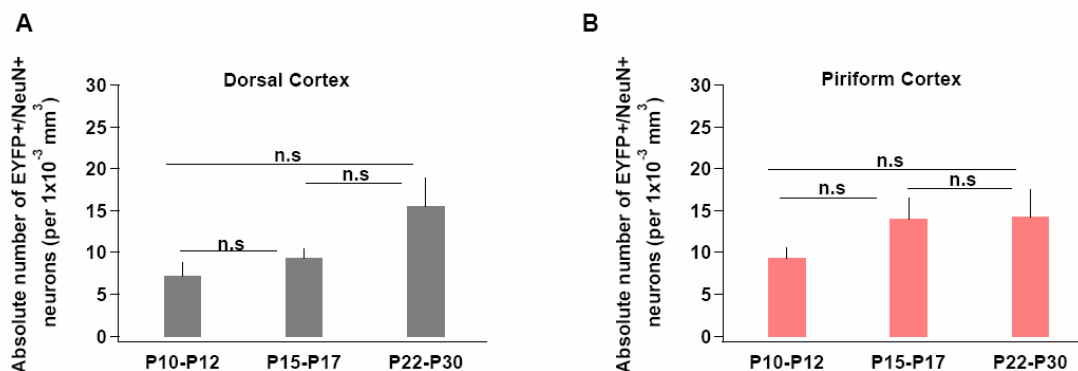
Figure 21. Age dependent distribution of EYFP+ neurons in the CNP-Cre:ROSA26/EYFP line. A,B, Absolute number of EYFP+/NeuN+ neurons at postnatal age groups P10-P12, P15-P17 and P22-P30, in the Dorsal Cortex (A) and Piriform Cortex (B). Error bars indicate SEM (±). One-way Anova with Tukey's post-hoc test used to indicate significant difference. D.Ctx, Dorsal Cortex; Piriform Cortex; n.s, non-significant.

3.4 Analysis of neurogenic time point

Having observed reporter expression by neurons in the CNP-Cre:ROSA26/EYFP line, it was essential to determine if they were generated postnatally from mitotic CNP-expressing cells or if there was an embryonic source of these EYFP labelled neurons, that was also labelled by the CNP-Cre knock-in approach. As a pilot study to ascertain the neuronogenic time point in the CNP-Cre:ROSA26/EYFP transgenic line, I decided to undertake BrdU pulse chase labelling at embryonic ages to first examine the time point of neurogenesis in wildtype mice and establish the BrdU pulse chase protocols and immunolabellings.

3.4.1 A large subset of neurons in the adult dorsal cortex co-label BrdU upon E16 pulse-chase

Upon BrdU injections to wild type mice at E16, double-immunolabellings for NeuN and BrdU were performed at P30, to examine the proportion of BrdU positive cells among NeuN positive mature neurons.

I concentrated the analysis in the layer II/III region of the cortices, as this was the layer where I had observed the highest number of reporter positive neurons in the CNP-Cre expressing mouse line. In the dorsal cortex, the fraction of NeuN positive cells that were BrdU positive was 0.67 ± 0.003 (total of 795 NeuN+ neurons, n=2 animals) (Figure

22A, arrowheads; C). However, the fraction of neurons that co-labelled BrdU in the ventral and piriform cortices was 0.04 ± 0.001 (total of 382 NeuN+ neurons, n=2 animals) (Figure 22B,C) and 0.04 ± 0.002 (total of 472 NeuN+ neurons, n=2 animals) respectively.

Having established postnatal and embryonic BrdU administration protocols in wildtype mice, targeting proliferating postnatal populations and dorsal cortex neurons respectively, I then undertook BrdU pulse chase labelling in CNP-Cre:ROSA26/EYFP mice to ascertain the time point of neurogenesis of the observed EYFP+ neurons.
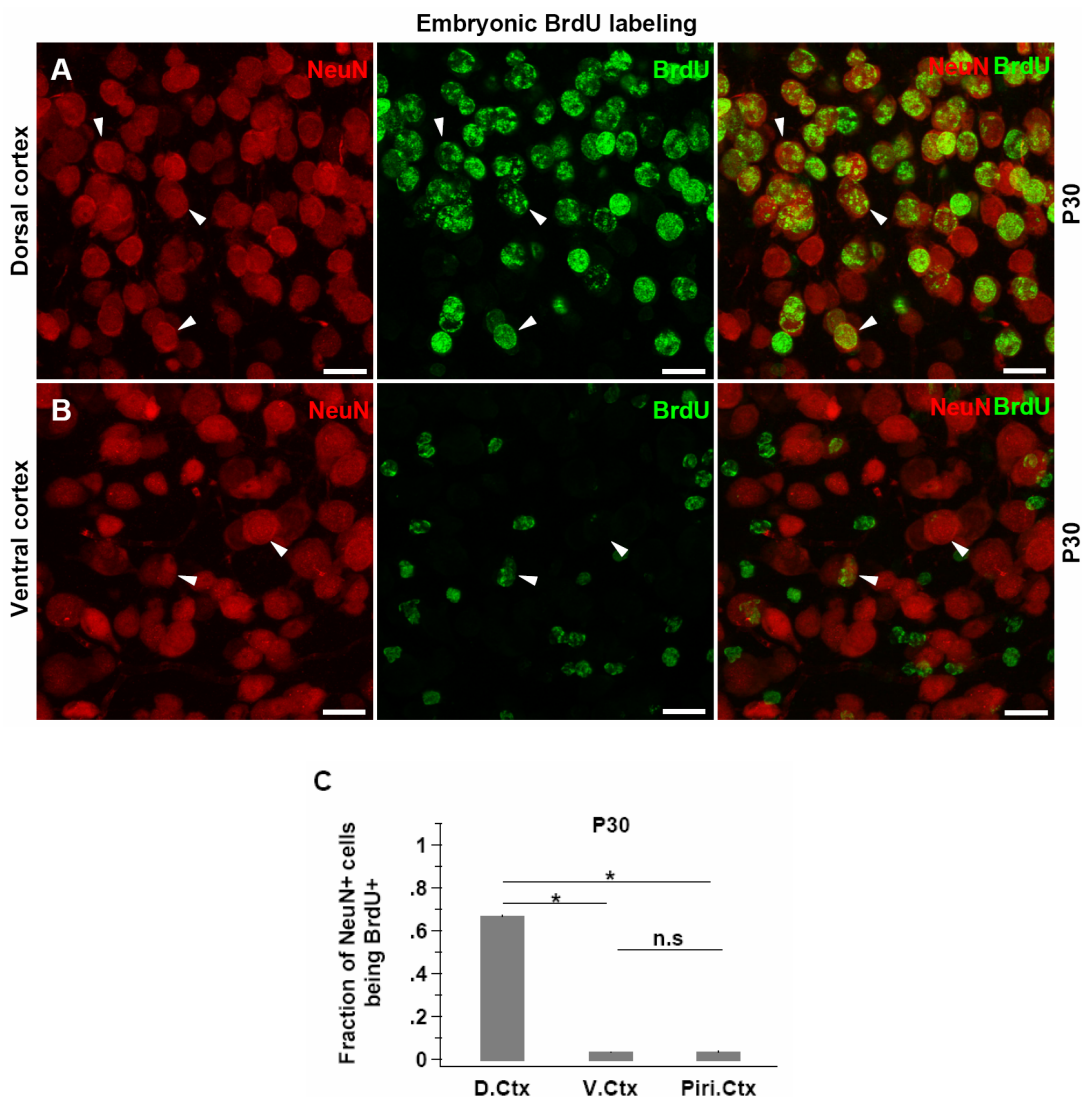
Figure 22. Time point of neurogenesis. A,B, Frontal sections through the Dorsal Cortex (A) and Ventral Cortex (B) of P30 wild type mice double immunolabelled for NeuN (red) and BrdU (green). All arrowheads point to NeuN+/BrdU+ mature neurons. Scale bars: 20 μm (applied to all). C, Fraction of NeuN+ neurons being BrdU+ at P30, upon E16 BrdU administration. All error bars indicate SEM (±). One-way Anova with Tukey's post-hoc test used to indicate significant difference. * indicates p < 0.05. n.s, non-significant; D.Ctx, Dorsal Cortex; V.Ctx, Ventral Cortex; CC, Corpus Callosum; Fim, Fimbrae.

3.5   Evidence of neurogenesis from embryonic EYFP+ precursors

In order to determine the time point of extensive neurogenesis observed in the ventral and piriform cortices of CNP-Cre:ROSA26/EYFP mice, BrdU labelling assays were performed at both postnatal and embryonic time points. The rationale here being that if EYFP+ neurons were derived from proliferation and differentiation of reporter positive precursors at a certain postnatal or embryonic time point, it is expected that they would incorporate BrdU label from their progenitor cell.

3.5.1   EYFP+ neurons in the ventral and piriform cortex co-label BrdU upon E12.5 pulse-chase

With E12.5 BrdU administration via oral gavage twice a day, four hours apart (Figure 23A), a significant population of EYFP+ neurons that were BrdU+ were observed in the ventral and piriform cortices at P30 (Figure 23C,D, arrowheads). The fraction of EYFP neurons being BrdU+ was 0.63 ± 0.1 (total of 468 EYFP+ neurons, n=6 animals) and 0.8 ± 0.04 (total of 250 EYFP+ neurons, n=6 animals) in the piriform and ventral cortex respectively (Figure 23I).

However, in the dorsal cortex this fraction was only 0.03 ± 0.01 (total of 393 EYFP+ neurons, n=6 animals) (Figure 23B, arrowhead; I); this low fraction of EYFP+ neurons that were BrdU labelled can be explained when seen in light of BrdU labellings in wild-type mice (see section 3.4.1) and other studies, where it was shown that in the dorsal cortex neurogenesis predominantly occurs around E16 (Bayer and Altman, 1990).

3.5.2   Lack of evidence for postnatal neurogenesis from EYFP+ precursors

In the postnatal BrdU labelling strategy, P10 CNP-Cre:ROSA26/EYFP mice were administered BrdU via 2 i.p injections, 12 hours apart for four days (Figure 23E). P32 immunohistochemical analysis of BrdU administered mice revealed that almost no EYFP+ neurons were BrdU+; with fraction of EYFP+ neurons that were BrdU+ being 0 both in the dorsal (total of 711 EYFP+ cells, n=4 animals) and piriform cortices (total of 387 EYFP+ cells, n=4 animals), and in the ventral cortex being 0.01 ± 0.01 (total of 355 EYFP+ cells, n=4 animals) (Figure 23F-H, arrows; I). Taken together these data suggest that in the ventral and piriform cortices, progenitors labelled by the CNP-Cre knock-in strategy serve as neuronal precursors during the early embryonic development.
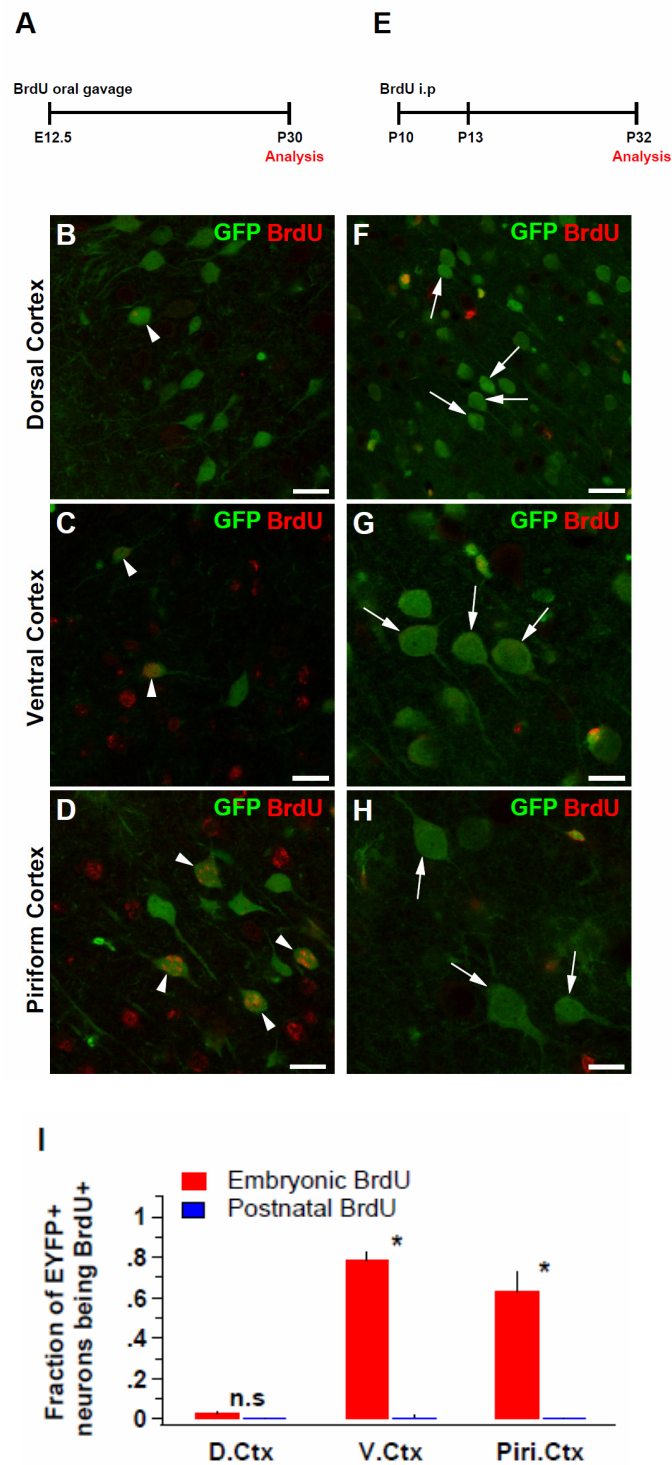
Figure 23. Neurogenesis from embryonic progenitors labelled by CNP-Cre mediated recombination. A, BrdU administration strategy to E12.5 CNP-Cre:ROSA26/EYFP mice via oral gavage. B-D, Frontal sections through the Dorsal Cortex (B), Ventral Cortex (C) and Piriform Cortex (D) of BrdU administered animals at P30 double immunolabelled for GFP (green) and BrdU (red). E, BrdU administration strategy to postnatal CNP-Cre:ROSA26/EYFP mice via i.p injections from P10-P13. F-H, Frontal sections through the Dorsal Cortex (F), Ventral Cortex (G) and Piriform Cortex (H) of BrdU injected animals at P32 double immunolabelled for GFP (green) and BrdU (red). All arrowheads point to GFP+/BrdU+ neurons. All arrows point to GFP+/BrdU- neurons. GFP (green) is used to indicate EYFP fluorescence. Scale bars: 20 μm (applied to all)**.** I, Fraction of EYFP+ neurons that were BrdU+ at both embryonic and postnatal BrdU administration time points in the given regions. Error bars indicate SEM (±). Two-way Anova with Bonferroni post-hoc test used to indicate significant difference. * indicates $p < 0.0001$ for the Ventral and Piriform Cortices. n.s, non-significant; adm, administration; i.p, intraperitoneal; D.Ctx, Dorsal Cortex; V.Ctx, Ventral Cortex; Piri.Ctx, Piriform Cortex.

3.5.3   Absence of BrdU labelling in EYFP+ OPCs upon E12.5 pulse-chase

Having found evidence with the BrdU pulse-chase experiments that embryonic CNP-Cre labelled precursor cells generate neurons, it was imperative to rule out the possibility that the BrdU+ neurons observed at P30 (after E12.5 BrdU injection) were the result of generation from postnatal reporter positive NG2 cells; which could have incorporated the BrdU label as they are generated from embryonic oligodendroglial lineage precursor cells. For this triple-immunolabellings of NG2, GFP and BrdU were performed on animals that had received BrdU at E12.5 and sacrificed at P30.
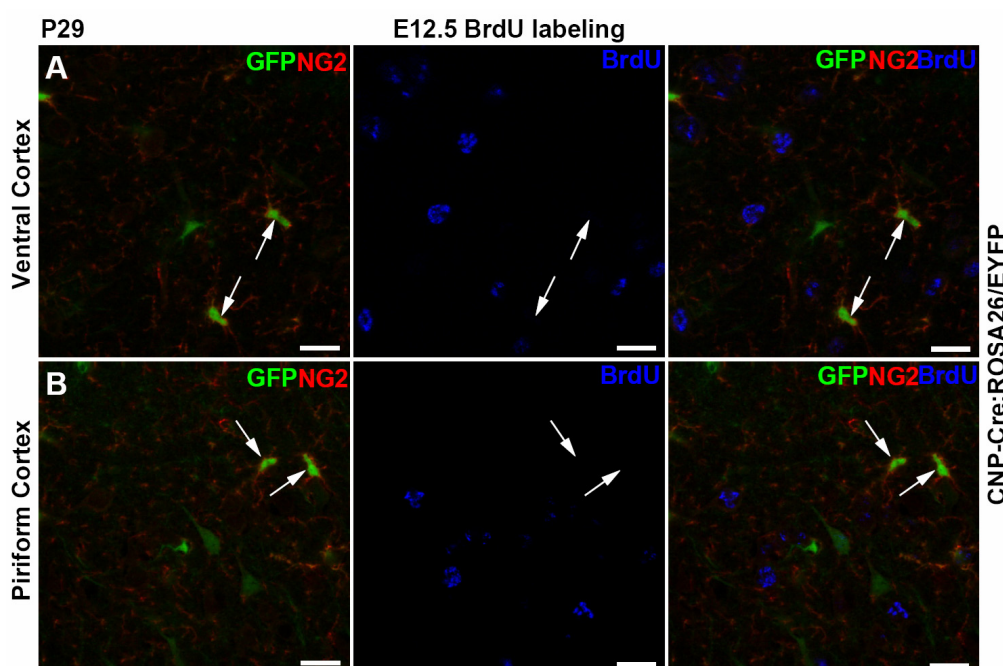
Figure 24. Reporter positive OPCs are not labelled by E12.5 BrdU pulse chase. A, Frontal sections through the Ventral Cortex (A) and Piriform Cortex (B) of P29 CNP-Cre:ROSA26/EYFP animals that were administered BrdU at E12.5 triple immunolabelled for GFP (green), NG2 (red) and BrdU (blue). All Arrows point to GFP+/NG2+/BrdU- cells. GFP (green) is used to indicate EYFP fluorescence. Scale bars: 20 μm (applied to all).

In the ventral and piriform cortices, the regions where a high fraction of reporter positive neurons showed co-labelling for BrdU (see Figure 23); I failed to report any NG2+GFP+ OPCs that displayed BrdU immunoreactivity. Out of 135 NG2+GFP+ cells analysed, each in the piriform cortex and ventral cortex of 50 μm thick frontal sections from four animals, no BrdU positivity was observed in any of them (Figure 24A-B). While the results of this experiment indicate that neurons were primarily generated from embryonic CNP-Cre expressing precursors, rather than from postnatal NG2 cells; however other explanation for this are discussed in section 4.3.

Embryonic BrdU labelling experiments performed in this study had revealed an embry-
onic source of reporter positive neurons observed in the CNP-Cre:ROSA26/EYFP line;
therefore the next set of experiments were dedicated to examining CNP-Cre mediated
reporter expression in the CNP-Cre:ROSA26/EYFP lines at embryonic time points.
CNP-Cre:Z/EG mice where I had not observed any reporter positive neurons (section
3.2.3) were also examined for the presence of EGFP+ cells at embryonic ages.

3.6 EYFP expression in non-oligodendroglial lineage cells in the embryonic forebrain

It has been already mentioned (in section 1.2.4), that *in situ* hybridisation studies
showed the presence of *Cnp* expression as early as E12.5; as reporter expression had
been thus far determined only in the postnatal ages in the CNP-Cre:Z/EG and CNP-
Cre:ROSA26/EYFP transgenic lines, the obvious next step was to verify the earliest
time point of reporter expression. Thus, to this end the CNP-Cre:ROSA26/EYFP and
CNP-Cre:Z/EG mice were analysed at embryonic ages.

In the CNP-Cre:ROSA26/EYFP mice at embryonic time points, a large number of re-
porter positive cells were observed throughout the CNS. EYFP+ cells were found in the
E18 ventricular and subventricular zones of the lateral ventricles and the cortex. Espe-
cially at the dorso-lateral and lateral ventricular wall, reporter positive cells appeared in
small cohorts of columns and seemed to be migrating towards the pial surface (Figure
25A-B, arrowheads). At E12.5 EYFP+ cells were observed at the cortical plate, ven-
tricular zone of the lateral ventricles and the ganglionic eminences; with expression lo-
calized at the anterior lateral ganglionic eminence (LGE) and a few scattered cells at the
medial ganglionic eminence (MGE) (Figure 25F-G).

Furthermore to examine the phenotype of these embryonic reporter positive CNP-Cre
expressing cells, I decided to perform an NG2-GFP double-immunolabelling at E16. A
large population of EYFP+ cells in the dorsal cortex and subventricular zone did not
display antigenicity for NG2 (Figure 25C-D, yellow arrowheads). The proportions of
EYFP+ cells that were NG2+ cells in the dorsal cortex and SVZ were significantly dif-
ferent at 0.14 ± 0.03 (total of 762 EYFP+ cells, n= 3 animals) and 0.04 ± 0.01 (total of
1264 EYFP+ cells, n= 3 animals) (Figure 25C-D, white arrowheads; E) respectively.
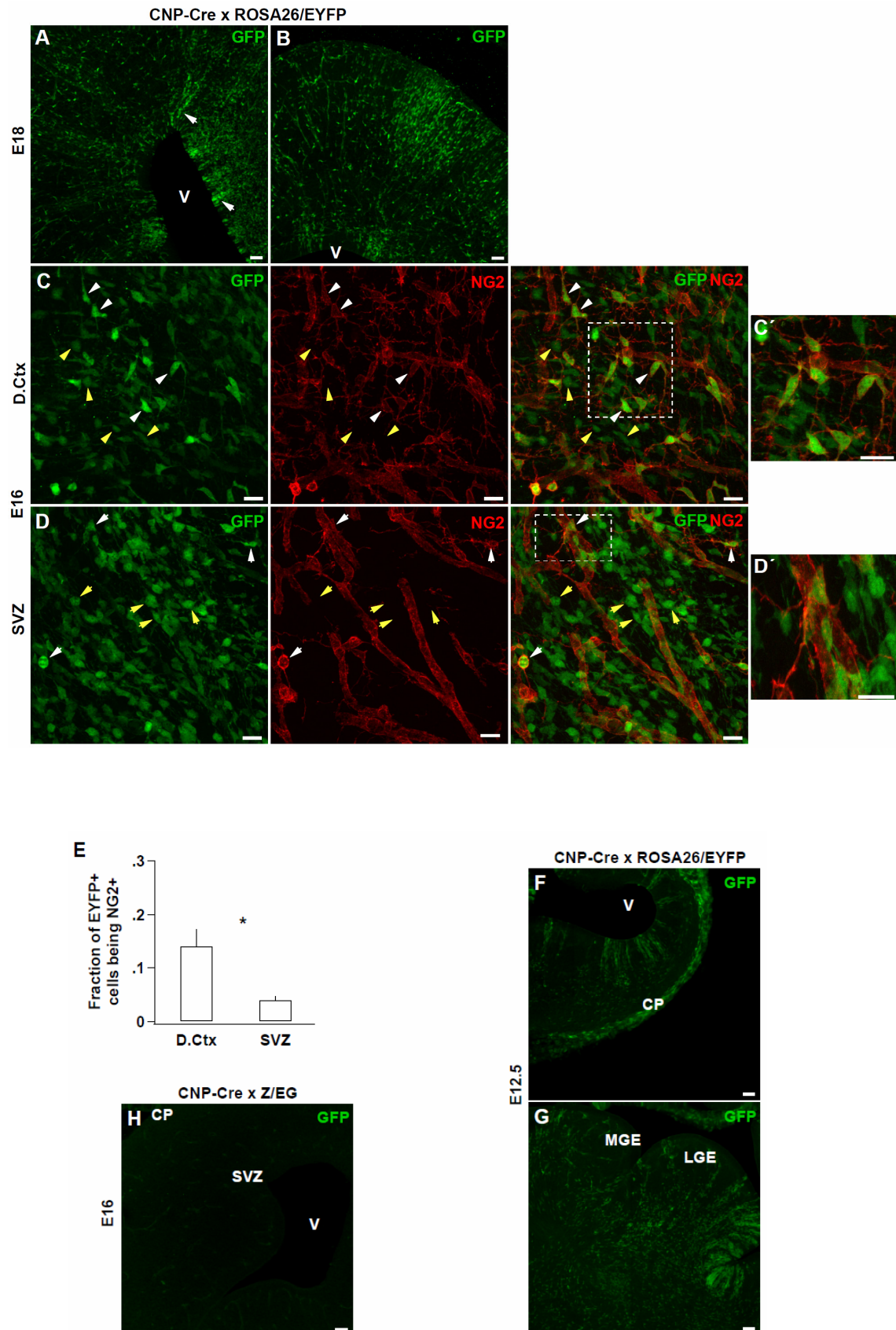
Figure 25. CNP-Cre driven reporter expression in the embryonic forebrain. A,B, Frontal sections through the Dorsal Forebrain of E18 CNP-Cre:ROSA26/EYFP mice immunolabelled for GFP (green). White arrowheads point to column of GFP+ cells at the Ventricular Wall. C,D, Frontal sections through the Dorsal Cortex (C) and Subventricular Zone (D) of E16 CNP-Cre:ROSA26/EYFP mice double immu-nolabelled with GFP (green) and NG2 (red). Boxed areas in C and D are shown at higher magnification in

Figure 25. (continued) C´and D´ respectively. All white arrowheads point to GFP+/NG2+ cells. All yellow arrowheads point to GFP+/NG2- cells. E, Fraction of EYFP+ cells that were NG2+ in the E16 CNP-Cre:ROSA26/EYFP Dorsal Cortex and Subventricular Zone. Error bars indicate SEM (±). Student's unpaired t-test used to indicate significant difference, * indicates p < 0.05. F,G, Frontal sections through the Dorsal (F) and Ventral (G) Forebrains of E12.5 CNP-Cre:ROSA26/EYF mice immunolabelled with GFP. H, Frontal section through the Dorsal Forebrain of the E16 CNP-Cre:Z/EG mouse immunolabelled for GFP. GFP (green) is used to indicate EYFP fluorescence. Scale bars: 50 µm (applied to A,B,F-H); 20 µm (applied to C,D). CP, Cortical Plate; D.Ctx, Dorsal Cortex; LGE, Lateral Ganglionic Eminence; MGE, Medial Ganglionic Eminence; SVZ, Subventricular Zone; V, Ventricle.

At the lateral ventricular wall only 4 out of 430 EYFP+ cells (n=2 animals) examined at the lateral ventricular wall exhibited NG2 immunoreactivity.

In contrast, I failed to observe any reporter positivity in the forebrain regions of the ventricular zone, subvbentricular zone and cortex in the embryonic CNP-Cre:Z/EG line (Figure 25H). Frontal sections through entire forebrain were devoid of EGFP+ cells (n=4 animals).

Together, these findings indicate that a difference in the time point of appearance of reporter positive cells was observed between CNP-Cre:ROSA26/EYFP and CNP-Cre:Z/EG mice, with EYFP expression starting from early embryonic ages, contrasting with the postnatal detection of EGFP+ cells.

3.7 EYFP expression in radial glia-like cells in the embryonic ventricular zone

Having observed numerous EYFP+ cells at E16.5, I sought to elucidate the phenotype of these cell types. Brain Lipid Binding Protein (BLBP) is a hydrophobic ligand binding protein and is expressed exclusively in radial glia and astrocytes throughout the developing CNS (Feng et al., 1994).

It has been well established that during embryonic development BLBP+ radial glial cells serve as neural progenitors and generate neurons as well as glial cells- both oligodendrocytes and astrocytes (Kriegstein and Götz, 2003; Malatesta et al., 2008; Kriegstein and Alvarez-Buylla, 2009).

To this end, I asked whether the EYFP+ precursors observed during embryonic stages displayed phenotypic properties reminiscent of radial glial cells. For this double immunolabellings with GFP and BLBP antibodies were performed. At E16, EYFP+ cells with typical radial glial morphology, a spindle-shaped elongated cell body and bipolar processes were found predominantly at the VZ seemingly migrating away towards the pial surface.
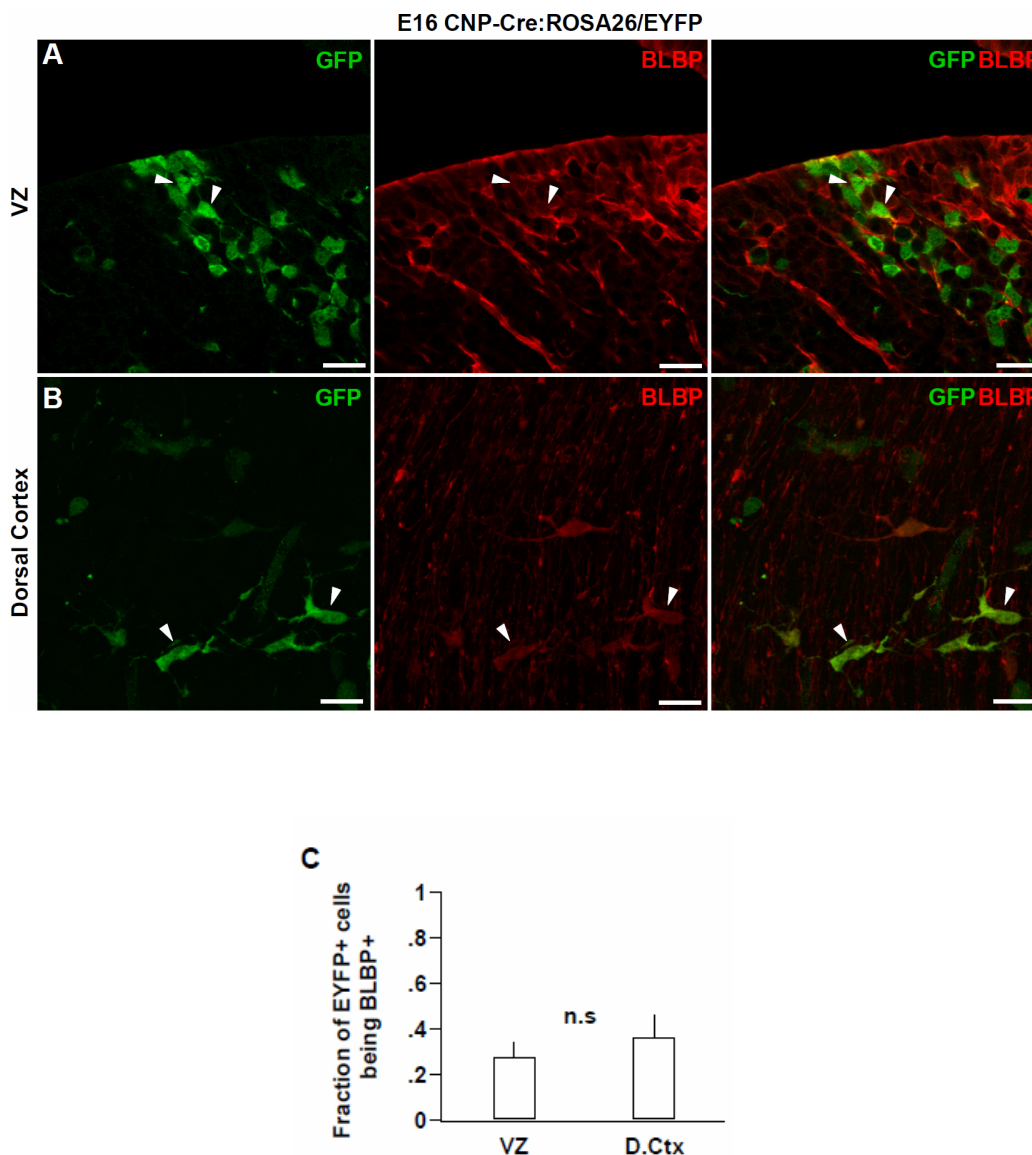
Figure 26. Radial glial phenotype of embryonic reporter positive cells labelled by CNP-Cre mediated recombination. A,B, Frontal sections through the Ventricular Zone (A) and Dorsal Cortex (B) of E16 CNP-Cre:ROSA26/EYFP mice double immunolabelled for GFP (green) and BLBP (red). All arrowheads point to GFP+/BLBP+ cells. GFP (green) is used to indicate EYFP fluorescence. Scale bars: 20 μm (applied to all). C, Fraction of EYFP+ cells being BLBP+ in the Ventricular Zone and Dorsal Cortex of CNP-Cre:ROSA26/EYFP mice. Error bars indicate SEM (±). Student's unpaired t-test used to indicate significant difference. n.s, non-significant; VZ, Ventricular Zone; D.Ctx, Dorsal Cortex.

In the E16 CNP-Cre:ROSA26/EYFP mice significant co-labelling was observed the fraction of EYFP+ cells co-expressing the radial glial marker BLBP was 0.36 ± 0.1 (total of 339 EYFP+ cells, n=3 animals) and 0.28 ± 0.06 (total of 435 EYFP+ cells, n=3 animals) in the dorsal cortex and ventricular zone respectively (Figure 26A-B, arrowheads; C).

3.8   Absence of CNPase protein in EYFP+ OPCs

In the CNP-Cre:Z/EG and CNP-Cre:ROSA26/EYFP lines, Cre-mediated reporter expression in OPCs is brought about by the activity of the *Cnp* promoter; thereby indicating that the *Cnp* gene is actively transcribed in these EGFP+ or EYFP+ OPCs. In the next set of experiments, I sought to investigate whether the *Cnp* gene product- CNPase was expressed in postnatal reporter positive NG2-expressing OPCs. Immunolabellings for CNPase, GFP and NG2 revealed that reporter positive NG2 cells in the dorsal cortex and subcortical white matter regions did not express the CNPase protein. This is in conjunction with studies that have shown that CNP expression occurs when OPCs enter terminal differentiation stages preceding myelination (Amur-Umarjee et al., 1990; Bansal and Pfeiffer, 1985).
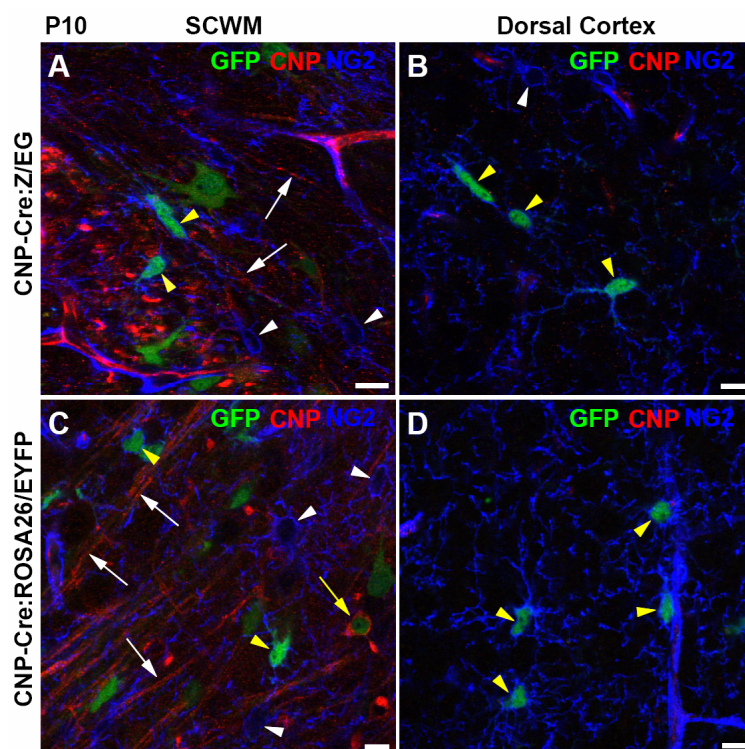
Figure 27. Absence of CNPase expression in reporter positive NG2 cells. A-D, Frontal sections through the Subcortical white matter (A,C) and Dorsal Cortex (B,D) of P10 CNP-Cre:Z/EG (A,B) and CNP-Cre:ROSA26/EYFP (C,D) mice triple-immunolabelled for GFP (green), CNP (red) and NG2 (blue). All white arrowheads point to NG2+/GFP-/CNP- cells. All yellow arrowheads point to NG2+/GFP+/CNP- cells. All white arrow points to NG2-/GFP-/CNP+ cell. Yellow arrowhead points to NG2-/GFP+/CNP+ cell. GFP (green) is used to indicate EYFP fluorescence. Scale bars: 20 μm (applied to all). SCWM, Subcortical white matter.

In the P10 CNP-Cre:Z/EG mice, 0 out of 28 NG2+EGFP+ cells in the dorsal cortex expressed the CNP protein (n=2 animals). Similarly the fraction of NG2+EGFP+ cell

being CNPase positive in the subcortical white matter was also 0 (total of 9 NG2+EGFP+ cells) (Figure 27A-B, yellow arrowheads).

In the P10 CNP-Cre:ROSA26/EYFP line, 0 out of 89 NG2+EYFP+ cells and 0 out of 80 NG2+EYFP+ cells each in the subcortical white matter and dorsal cortex respectively, expressed CNPase (n=3 animals) (Figure 27C-D, arrowheads). A few i.e. ~12 reporter positive displaying CNPase immunoreactivity (total of 473 EYFP+ cells, n=3 animals) were observed in the white matter, but these cells were negative for NG2, suggesting that these were more differentiated oligodendroglial lineage cells (Figure 27C, yellow arrow).

Taken together, these results indicate that a clear difference in CNP-Cre driven reporter expression and CNP protein expression was observed in OPCs.

3.9 Unspecific EYFP expression with postnatal Cre-dependent EYFP virus transfection

The experiments performed thus far provided substantial proof that precursor cells labelled by the CNP-Cre knock-in approach served as a precursor pool for neuronal phenotypes during embryonic time points. CNP-Cre mediated reporter expression was also observed in embryonic radial-glia like cells. Therefore, the next set of experiments were designed to "bypass" these embryonic precursor cells, thus selectively labelling only the postnatal CNP-Cre expressing cell population: presumably oligodendroglial lineage restricted precursors, to ascertain their progeny. This was done by employing a Cre-dependent EYFP virus transfection approach (see Methods section 2.7).

In order to first standardize the virus injection protocol, a Cre-independent approach was adopted. I administered a CMV-Venus virus construct in varying volumes and frequencies intraventricularly. From the transfection protocols: injections of 1 μl once a day for one day (1μl x 1 / 1 day) (n= 8 animals), 3 μl x 2 / 2 days (n= 6 animals) and 3 μl x 2 / 1 day (n= 6 animals), the best transfection rate depicted by the number of reporter positive cells was observed in the protocol with 3 μl injections of the virus twice a day for 1 day (Figure 28A,B,C).

The Cre-dependent EYFP virus was injected in the ventricles of P3 CNP-Cre $^{+/-}$:Z/EG$^{-/-}$ mice (n=4 animals) and there was a widespread transfection in the hippocampus, dorsal cortex and ventricles. A large number of oligodendrocytes and OPCs were in the cortex and corpus callosum.
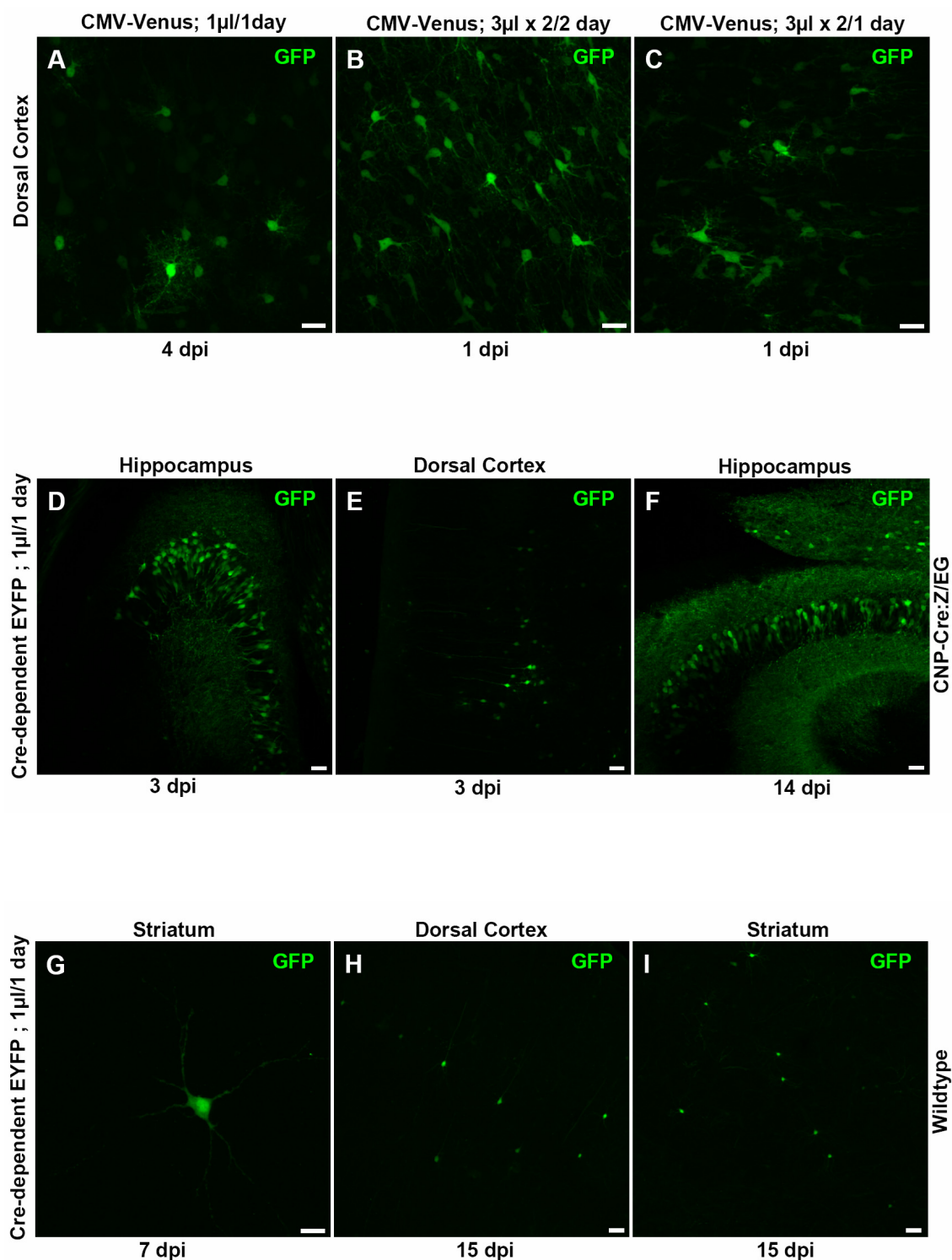
Figure 28. Cre-dependent EYFP virus transfection strategy to follow OPC lineage. A-C, Frontal sections through the Dorsal Cortex of wildtype mice with CMV-Venus virus construct injections 4dpi (1 μl per day for one day) (A), 1dpi (3 μl twice a day for two days) (B), 1dpi (3 μl twice a day for one day) (C) immunolabelled for GFP. D-F, Frontal section 3 dpi of Cre-dependent EYFP construct (1 μl per day for one day) through the Hippocampus (D), Dorsal Cortex (E) and 14 dpi through the Hippocampus (F) of CNP-Cre:Z/EG mice immunolabelled for GFP. G-I, Frontal section 7 dpi of Cre-dependent EYFP construct (1 μl per day for one day) through the Striatum (G), and 15 dpi through the Dorsal Cortex (H), Striatum (I) of Wildtype mice immunolabelled for GFP. GFP (green) is used to indicate EYFP fluorescence. Scale bars: 50 μm (applied to all). dpi, days post injection.

Also, neurons and astrocytes were observed in the hippocampus and dorsal cortex, with few premyelinating oligodendrocytes in the striatum at 3 dpi (n=2 animals) and 14 dpi (n=2 animals) (Figure 28D,E,F).

Intrigued by the sheer number of transfected cell types, I then decided to examine the Cre dependence of the Cre-dependent EYFP virus construct; therefore P2 wild type mice (n=10 animals) were injected with the Cre-dependent EYFP virus. Since reporter positivity is controlled by Cre recombination and with Cre recombinase being absent in this strategy, I expected to find no EYFP+ cells upon transfection. On the contrary, at 7 dpi (n=2 animals) I observed astrocytes in the striatum (~2 cells in 50 μm frontal section) (Figure 28G) as well as neurons in the dorsal cortex (1-2 cells in 50 μm frontal section) (Figure 28H). At 15 dpi (n=2 animals) around 15-20 EYFP+ neurons were seen in the region spanning the dorsal cortex all the way down till the ventral cortex (Figure 28I) and 8-10 reporter positive astrocytes were observed in the striatum.

With Cre-dependent EYFP virus injections in wildtype mice, reporter positive neurons and astrocytes were observed at locations in the dorsal, piriform and ventral cortices, in numbers that were comparable to those observed in the CNP-Cre:ROSA26/EYFP line. Thus, with this approach it would not be possible to determine if EYFP positivity observed in neurons and astrocytes was due to "leaky Cre" activity or were the progeny of CNP-Cre expressing cells; thereby making this approach un-usable.

3.10 EYFP expression in radial glia-like cells and neurons in the NG2creER^{TM}BAC:ROSA26/EYFP line

In previous experiments with the CNP-Cre:ROSA26/EYFP line, I observed reporter expression not restricted exclusively to NG2 cells but extending to a more widespread population of early neural stem cells (section 3.7). Therefore having labelled precursor cells not belonging exclusively to the oligodendroglial lineage with the CNP-Cre knock in, it was imperative to adopt an experimental strategy to label only OPCs to answer the question if OPCs have a neuronogenic potential. The Tamoxifen-inducible NG2creER^{TM}BAC transgenic mice were crossed with the ROSA26/EYFP Cre reporter, to accomplish lineage tracing of purely oligodendroglial lineage precursor cells.

Numerous reporter positive cells were observed in both gray and white matter regions of E19.5 NG2creER^{TM}BAC:ROSA26/EYFP mice subsequent to Cre induction at E16.5. NG2-GFP immunolabelling revealed a miniscule population of reporter positive cells

that were immunoreactive for NG2 throughout the entire ventral and dorsal forebrains. It should be remembered that at ~E11.5 upon specification in ganglionic eminences (section 1.2.3.2), OPCs acquire NG2 expression around ~E15 as they begin migrating from germinal zones (Nishiyama et al., 1996, 2007). The proportion of EYFP+ cells that were NG2 positive in the ventricular zone was only 0.07 ± 0.04 (total of 283 EYFP+ cells, n=3 animals) (Figure 29A, arrows).

Numerous EYFP+ cells seen at the lateral, dorsal and ventral ventricular wall, often found in clusters seen to be migrating away to the pial surface and depicting a typical radial glial morphology. Apart from morphological characterisation, BLBP-GFP co-immunolabellings to identify the radial glial phenotype of EYFP+ cells revealed that the proportion of EYFP+ cells which were BLBP+ radial glia-like cells was 0.16 ± 0.02 (total of 213 EYFP+ cells, n=3 animals) in ventricular zone (Figure 29B, arrowhead). It is worth mentioning that at this embryonic time point, a considerable subset of reporter positive cells reminiscent of a typical neuronal morphology were observed in the dorsal, ventral and piriform cortices.
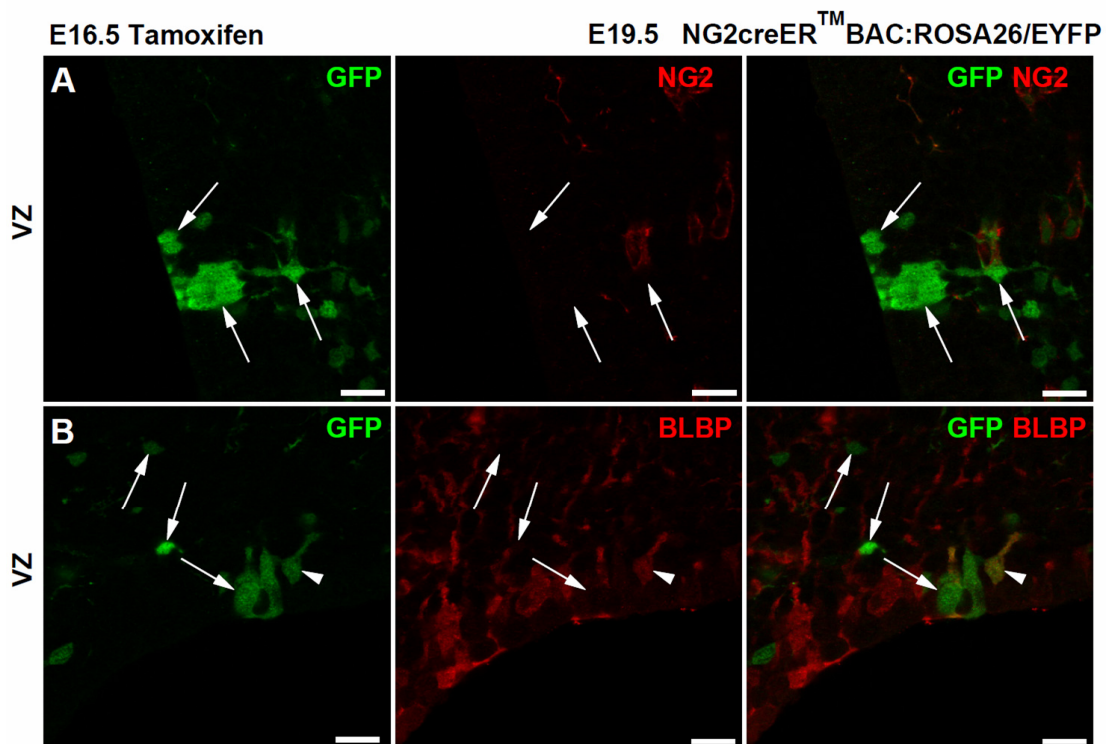
Figure 29. Phenotype of EYFP+ cells in the E19.5 NG2creER^{TM}BAC:ROSA26/EYFP line (E16.5 TMX administration). A, Frontal sections through the Ventricular Zone of E19.5 NG2creER^{TM}BAC:ROSA26/EYFP mice that were administered Tamoxifen at E16.5, immunolabelled for GFP (green), NG2 (red). All arrows point to GFP+/NG2- cells. B, Frontal sections through the Ventricular Zone of E19.5 NG2creER^{TM}BAC:ROSA26/EYFP mice that were administered Tamoxifen at E16.5, immunolabelled for GFP (green), BLBP (red). All arrows point to GFP+/BLBP- cells. All arrowheads point to GFP+/BLBP+ cells. VZ, Ventricular Zone.
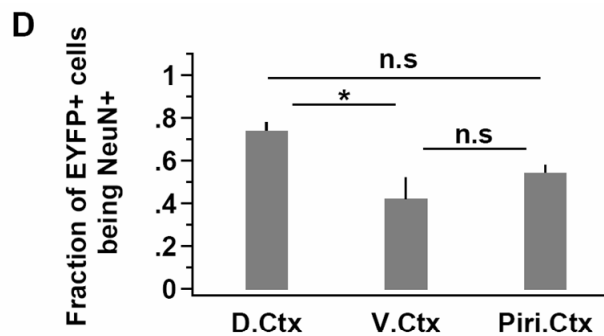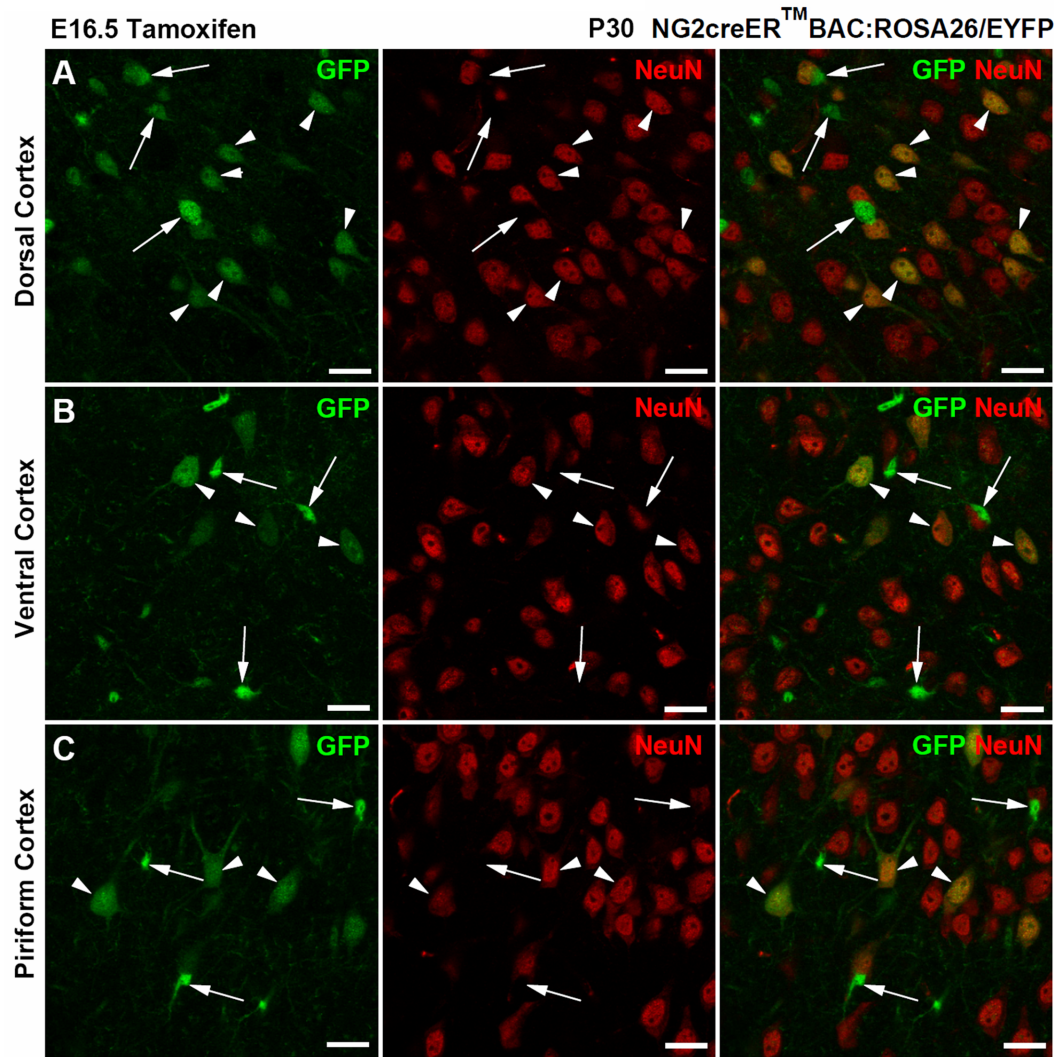
Figure 30. Extensive cortical neurogenesis in NG2creER^{TM}BAC:ROSA26/EYFP line. A-C, Frontal sections through the Dorsal (A), Ventral (B) and Piriform (C) cortices of P30 NG2creER^{TM}BAC:ROSA26/EYFP mice that were administered Tamoxifen at E16.5, double-immunolabelled for GFP (green) and NeuN (red). All arrows point to GFP+/NeuN- cells. All arrowheads point to GFP+/NeuN+ cells. GFP (green) is used to indicate EGFP and EYFP fluorescence. Scale bars: 20 μm (applied to all). D, Fraction of EYFP+ cells that were NeuN+ in the Dorsal, Ventral and Piriform Cortices of P30 NG2creER^{TM}BAC:ROSA26/EYFP mice that were administered Tamoxifen at E16.5. Error bars indicate SEM (±). One-way Anova with Tukey's post-hoc test used to indicate significant difference. * indicates $p < 0.05$. n.s, non-significant; D.Ctx, Dorsal Cortex; V.Ctx, Ventral Cortex; Piri.Ctx, Piriform Cortex.

Next, NG2creER^{TM}BAC:ROSA26/EYFP double transgenic mice that were administered Tamoxifen at late embryonic day E16.5, were analysed with GFP-NeuN double immunolabellings at P30 to inspect the occurrence of reporter positive cells that co-labelled NeuN.

At P30, a considerable population of EYFP+ cells with a characteristic neuronal morphology: large soma, fine dendritic processes and a long axon; were seen primarily in the dorsal, ventral and piriform cortices. These reporter positive neurons also displayed immunoreactivity for the mature neuronal marker NeuN (Mullen et al., 1992). The proportion of NeuN+ neurons among reporter positive cells in the dorsal, ventral and piriform cortex was 0.74 ± 0.04 (total of 458 EYFP+ cells, n=3 animals) (Figure 30A, arrowheads; D), 0.42 ± 0.1 (total of 264 EYFP+ cells, n=3 animals) (Figure 30B, arrowheads; D) and 0.54 ± 0.04 (total of 265 EYFP+ cells, n=3 animals) (Figure 30C, arrowheads; D) respectively.

Reporter positive neurons were also seen, although in considerably fewer numbers in the CA3 region of the hippocampus of the adult NG2creER^{TM}BAC:ROSA26/EYFP animals.

On the other hand, analysis of an adult (~P40) NG2creER^{TM}BAC:ROSA26/EYFP animal which was administered Tamoxifen at P6, did not reveal any EYFP+ cells that represented a neuronal morphology throughout 50 μm thick frontal sections.

3.11 Deletion of GluRB subunit in OPCs inhibits their proliferation

The time period around the second to third postnatal week is the peak period of myelinogenesis (Sturrock, 1980). Due to this reason OPCs were analysed at approximately this time point (2-3 weeks) to investigate the effect of GluRB deletion on the viability of OPCs, their cell number and proliferative potential. The dorsal cortex and corpus callosum were chosen as representative regions of gray and white matter respectively.

0.5 mg TMX was administered to NG2creER^{TM}BAC:GluRB$^{2lox/2lox}$:ROSA26/EYFP and NG2creER^{TM}BAC:GluRB$^{wt/wt}$:ROSA26/EYFP mice at P5 to P10 (single i.p injection/day for 1 or 3 days) for Cre induction. Importantly, it has been previously shown that with early postnatal TMX induction (similar to the one used in this study), majority of reporter positive cells were NG2 cells and a small fraction reporter positive cells were oligodendrocytes (Zhu et al., 2011).

Figure 31. Effect of GluRB removal on OPC cell number and proliferation. A,C, Frontal sections through the Dorsal Cortex (A) and Fimbrae (C) of Control: GluRB[wt/wt] mice immunolabelled for GFP (green) and BrdU (red). B,D, Frontal sections through the Dorsal Cortex (B) and Fimbrae (D) of Knock-out: GluRB[2lox/2lox] mice immunolabelled for GFP (green) and BrdU (red). All arrowheads point to GFP+/BrdU+ cells. GFP (green) is used to indicate EYFP fluorescence. Scale bars: 20 μm (applied to all). E-F, Absolute number of EYFP+ cells in the Dorsal Cortex (E) and Fimbrae (F) of GluRB[wt/wt] and GluRB[2lox/2lox] mice. G-H, Fraction of EYFP+ cells being BrdU+ in the Dorsal Cortex (G) and Fimbrae (H) of GluRB[wt/wt] and GluRB[2lox/2lox] mice. Error bars indicate SEM (±). Student's unpaired t-test used to indicate significant difference, * indicates $p < 0.05$. n.s, non-significant. CTRL, Control; KO, Knockout.

Subsequently, ~10 to 14 days post the last TMX injection, 300 mg/kg i.p injections of BrdU were given to these animals. These TMX and BrdU administered animals were then sacrificed three hours later and I further proceeded with GFP-BrdU double immunolabellings on 50µm sections.

GluRB KO mice i.e. animals in which the NG2 cells have presumably lost the GluRB subunit upon TMX induction were viable, survived into adulthood and did not exhibit any obvious behavioural alterations such as tremors or seizures associated with hypomyelination (Filley, 1998); although it must be stated that no behavioral tests were performed.

Next, absolute numbers of EYFP reporter positive cells were examined between the two experimental groups. No significant differences were observed in the cell density of EYFP+ cells per $1x10^{-3}$ mm^3 in the dorsal cortex and fimbrae between GluRB KO and control groups (CTRL) (Figure 31E,F), suggesting that the survival of these cells remains unaffected upon deletion of the GluRB subunit. In the dorsal cortex, the KO mice had ~20 ± 4 EYFP+ cells per $1x10^{-3}$ mm^3 (n=7 animals) and the CTRL mice had ~12 ± 2 EYFP+ cells per $1x10^{-3}$ mm^3 (n=5 animals) (p=0.12, non-significant); while in the fimbrae, the KO mice had ~73 ± 13 EYFP+ cells per $1x10^{-3}$ mm^3 (n=7 animals) and the CTRL mice had ~45 ± 11 EYFP+ cells per $1x10^{-3}$ mm^3 (n=5 animals) (p=0.15, non-significant).

However, even within each experimental group the density of EYFP+ cells per $1x10^{-3}$ mm^3 will greatly depend on the TMX injection. Due to this reason and since OPCs represent the most proliferative postnatal cell population (Dawson, 2003; Psachoulia et al., 2009), capable of compensatory mechanisms for reduction in their cell numbers (Kessaris et al., 2006); it was imperative to investigate for changes in the proliferative potential.

In the dorsal cortex, the fraction of EYFP+ cells that were BrdU+ (Figure 31A,B, arrowhead) was not significantly changed between the control and knockout groups (CTRL, 0.1 ± 0.06, total of 175 EYFP+ cells, n=5 animals and KO, 0.05 ± 0.01, total of 420 EYFP+ cells, n=7 animals; p=0.11, non-significant) (Figure 31G).

On the other hand, the fraction of EYFP+ cells being BrdU+ in the fimbrae was significantly reduced in the fimbrae of the GluRB knockouts (Figure 31C,D, arrowhead; H) as compared to the control group (CTRL, 0.1 ± 0.03, total of 465 EYFP+ cells, n=5 animals; KO, 0.03 ± 0.01, total of 1018 EYFP+ cells, n=7 animals; p=0.03, significant).

3.12 Lack of evidence for change in OPC differentiation upon GluRB subunit deletion

Synaptic input received by OPCs (Ziskin et al., 2007; Kukley et al., 2007) can also be speculated to regulate lineage progression vis-à-vis maturation and differentiation (Kukley et al., 2008; Etxeberria et al., 2010).
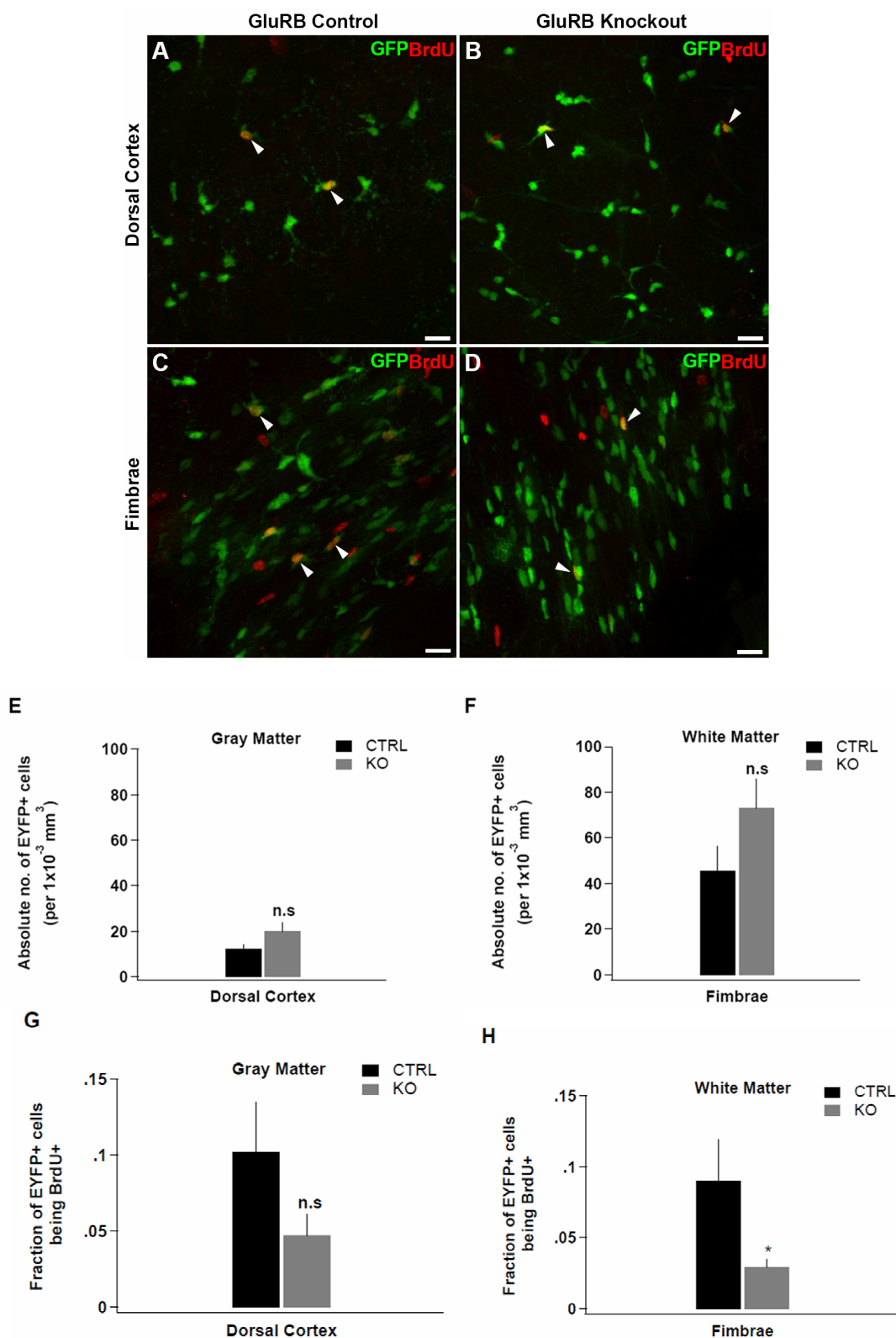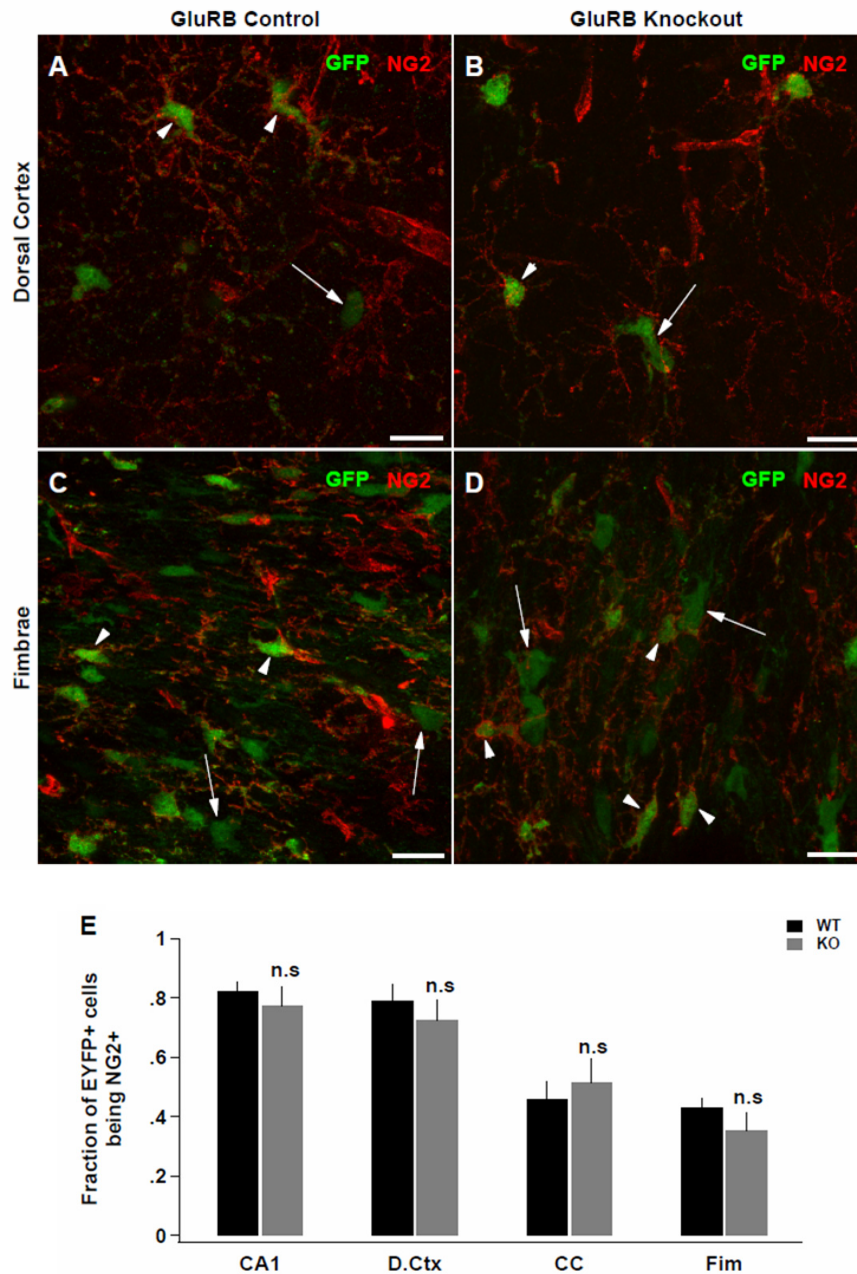

Figure 32. Effect of GluRB removal on OPC differentiation. A,C, Frontal sections through the Dorsal Cortex (A) and Fimbrae (C) of Control: GluRB$^{wt/wt}$ mice immunolabelled for GFP (green) and NG2 (red). B,D, Frontal sections through the Dorsal Cortex (B) and Fimbrae (D) of Knockout: GluRB$^{2lox/2lox}$ mice immunolabelled for GFP (green) and NG2 (red). All arrowheads point to GFP+/NG2+ cells. All arrows point to GFP+/NG2- cells. GFP (green) is used to indicate EYFP fluorescence. Scale bars: 20 μm (applied to all). E, Fraction of EYFP+ cells being NG2+ in the CA1, Dorsal Cortex, Corpus Callosum and Fimbrae of GluRB$^{wt/wt}$ and GluRB$^{2lox/2lox}$ mice. Error bars indicate SEM (±). Two-way Anova with Bonferroni post-hoc test used to indicate significant difference. n.s, non-significant. D.Ctx, Dorsal Cortex; CC, Corpus Callosum; Fim, Fimbrae. CTRL, Control; KO, Knockout.

To determine the contribution of the GluRB subunit to OPC maturation, 10 days to 20 days old NG2creER^{TM}BAC:GluR-B$^{2lox/2lox}$:ROSA26/EYFP (KO group) and NG2creER^{TM}BAC:GluR-B$^{wt/wt}$:ROSA26/EYFP (CTRL group) mice were given 0.5 mg Tamoxifen with 1 i.p injection per day for 3 days or 6 days to induce Cre recombination. Gray matter regions of CA1 and dorsal cortex, as well as white matter regions of fimbrae and corpus callosum were examined ~10 days after the last day of TMX induction with NG2-GFP double-immunolabellings to assess the population of NG2 cells among EYFP+ cells.

Reporter positive cells with and without NG2 immunoreactivity (Figure 32A-D, arrowheads, arrows) were observed in all regions under examination. No differences were observed between the control and GluRB knockout experimental groups in the fraction of EYFP+ cells being NG2+ OPCs in the hippocampal CA1 (CTRL, 0.82 ± 0.03, total of 116 EYFP+ cells, n=5 animals; KO, 0.78 ± 0.06, total of 116 EYFP+ cells, n=7 animals; $p > 0.05$, non-significant) or the dorsal cortex (CTRL, 0.79 ± 0.06, total of 131 EYFP+ cells, n=5 animals; KO, 0.72 ± 0.07, total of 226 EYFP+ cells, n=7 animals; $p > 0.05$, non-significant) (Figure 32A,B,E).

Similarly, in the white matter regions too, the population of EYFP+ cells that were NG2+ remained unchanged between the two experimental groups (fimbrae: CTRL, 0.43 ± 0.04, total of 310 EYFP+ cells, n=5 animals; KO, 0.35 ± 0.06, total of 493 EYFP+ cells, n=7 animals; $p > 0.05$, non-significant and corpus callosum: CTRL, 0.46 ± 0.06, total of 226 EYFP+ cells, n=5 animals; KO, 0.51 ± 0.08, total of 293 EYFP+ cells, n=7 animals; $p > 0.05$, non-significant) (Figure 32C,D,E).

4   Discussion

Oligodendroglial fate mapping studies that have relied on transgenic mice expressing Cre recombinase under various oligodendroglial promoters cross-bred to Cre reporter strains, have revealed conflicting results concerning the developmental fate of oligodendroglial precursor cells. These artificially generated oligodendroglial promoter-Cre transgene constructs might not mimic endogenous gene expression. In order to avoid the pitfalls of conventional transgenesis such as- random insertion into the genome, ectopic expression of the transgene, transgene silencing at the inserted locus and potential mosaicism (Feng et al., 2000; Guo et al., 2009; Kang et al., 2010; Zhu et al., 2011), this study employed a knock-in strategy at the 2′,3′-cyclic nucleotide 3′-phosphodiesterase (CNP) gene locus, combined with the Cre-lox system. Mice resulting from the knock-in of Cre into the endogenous CNP locus were inter-bred with two Cre reporter lines: Z/EG and ROSA26/EYFP, to facilitate comparative lineage tracing of oligodendroglial precursors.

The main findings of this study are that: (1) CNP-Cre mediated recombination in both CNP-Cre:Z/EG and CNP-Cre:ROSA26/EYFP lines drives reporter expression in a distinct subpopulation of relatively differentiated oligodendroglial precursor cells (explained in section 4.1); (2) Extensive oligodendrogliogenesis is observed in the CNP-Cre:Z/EG and CNP-Cre:ROSA26/EYFP mice, with EGFP and EYFP expression by all mature myelinating oligodendrocytes; (3) Exclusively in the CNP-Cre:ROSA26/EYFP line, EYFP reporter expression was observed in a small subset of astrocytes in the ventral cortex, as well as in a subpopulation of neurons in the dorsal, ventral and piriform cortices; and (4) Further examination of embryonic reporter expression revealed that the highly sensitive ROSA26/EYFP Cre reporter used in the CNP-Cre:ROSA26/EYFP line, detects transient *Cnp* promoter activity-dependent Cre expression in radial glia-like cells, thereby explaining reporter presence in astrocytes and neurons in this line.

As will be outlined below, I can conclude from my results that oligodendroglial precursors remain committed to the oligodendroglial lineage and do not display multipotency. The unexpected observation of astrocytic and neuronal progeny could be attributed to transient oligodendroglial gene promoter activity in a neural stem cell niche. This is only detected by a sensitive Cre reporter; thereby indicating that choice of Cre reporters introduces a strong bias in fate mapping results.

4.1 Lineage assessment of OPCs

As has been described in length (section 1.2.3.4), OPCs change their gene expression profiles upon differentiation to oligodendrocytes; they cease to express NG2 and PDG-FRα and start the expression of mature oligodendroglial markers such as CNP, GalC PLP to name a few. *In vivo* studies employ these oligodendroglial lineage markers to ascertain whether OPCs display lineage plasticity and possess an astrogliogenic or neurogenic potential, in addition to generating oligodendrocytes.

Cnp promoter driven cell targeting strategies, allow the assessment of oligodendroglial lineage development and function *in vivo*, since transcription of the CNP gene begins during early embryonic developmental stages of the oligodendroglial lineage with an expression pattern similar to that of other oligodendroglial-specific markers. In addition to its well documented expression in the oligodendroglial lineage, CNP-Cre driven reporter expression in a neural stem cell niche, suggests that transient *Cnp* promoter activity could also be present outside of the oligodendroglial lineage (explained in section 4.1.1).

In the CNP-Cre:Z/EG and CNP-Cre:ROSA26/EYFP lines, reporter positive cells were uniformly distributed throughout gray and white matter regions. At early postnatal ages in both experimental groups, not all NG2 cells expressed EGFP or EYFP; thus reporter expression was confined to a subset of OPCs (Figure 14). The CNP gene product-CNPase, occurs only in mature myelinating oligodendrocytes (Sprinkle, 1989). Therefore an OPC that has started to develop towards a mature oligodendrocyte would change its gene expression profile to exhibit *Cnp* promoter activity and display reporter positivity. I term this subset of CNP-Cre expressing oligodendroglial lineage precursors as relatively differentiated or *"late OPCs"*. *Cnp* promoter activity in these late OPCs would make them distinct from the OPC population consisting of comparatively immature or *"early OPCs"* which perhaps have not yet made the decision to develop into oligodendrocytes. These early OPCs would remain unlabelled by CNP-Cre mediated recombination.

Further immunolabelling experiments with markers of "mature" OPCs, immediately prior to differentiation to oligodendrocytes, for e.g. G-protein coupled receptor 17 (GPR17) (Boda et al., 2011) or O1 (Baumann and Pham-Dinh, 2001) could help to ascertain the relatively differentiated phenotype of reporter positive OPCs in this study.

CNP-EGFP transgenic mice have been generated in the past in order to study oligodendroglial lineage development. In these animals, all NG2 cells expressed the reporter, which is in pronounced contrast to the presence of reporter expression in a restricted population of OPCs in my study (Yuan et al., 2002). I attribute this discrepancy to the CNP-EGFP line being a transgenic mouse line in which the artificial *Cnp* promoter is used. In absence of endogenous gene regulatory elements and MicroRNA mediated control, ectopic expression of the CNP gene could drive reporter expression in OPCs that were not labelled in my study with endogenous CNP expression. Differential patterns of reporter expression have also been observed in mouse models using different *Plp* promoter constructs with and without endogenous regulatory sequences (Belachew et al., 2001).

In the present study with the CNP-Cre knock-in line, limited CNP-Cre driven reporter expression in NG2 cells can arise from the following possibilities: (1) Activity of the *Cnp* promoter in a restricted subset of NG2 cells, would result in only this subset being labelled by CNP-Cre mediated recombination; and (2) Extremely low *Cnp* promoter-driven Cre expression levels remaining undetected by the Cre reporter and/or incomplete reporter target excision in a subpopulation of OPCs. Thereby, resulting in the efficiency of CNP-Cre mediated recombination being below 100% in the experimental mouse lines.

It can be ruled out that the efficiency of Cre recombination is not 100% in the CNP-Cre:Z/EG and CNP-Cre:ROSA26/EYFP lines, since EGFP and EYFP labelling is present in all oligodendroglial cells at postnatal ages examined. The proportion of reporter positive cells among NG2 cells was higher in the CNP-Cre:ROSA26/EYFP line as compare to the CNP-Cre:Z/EG line, on account of ROSA26/EYFP being a highly sensitive Cre reporter which detects even low Cre expression levels (discussed in section 4.5). But even in the CNP-Cre:ROSA26/EYFP line only ~60% of NG2 cells elicited reporter positivity, this argues against the possibility that absence of reporter expression in a subset of NG2 cells is due to low *Cnp* promoter driven-Cre expression levels.

These explanations indicate a preferential CNP-Cre mediated reporter labelling in a subset of relatively differentiated oligodendroglial precursors that display *Cnp* promoter activity; I designate this population as *"CNP-Cre expressing late OPCs"*.

4.1.1 Oligodendrocytic promoter expression in radial glia-like cells

A large number of reporter positive cells were detected in the CNP-Cre:ROSA26/EYFP line at embryonic time points (Figure 25), this is consistent with the temporal pattern of expression of *Cnp*, *Pdgfra* and *Dm-20* transcripts at the onset of glial development. *In situ* hybridisation studies report *CNP* mRNA expression in a thin longitudnal zone of the E12.5-E14 diencephalon and spinal cord. *Cnp* transcripts were shown to co-localize in time and space with cells that express mRNA encoding Pdgfra. Transcripts encoding DM-20 detected at E9.5 also had a pattern of expression superimposable on the CNP transcript (Peyron et al., 1997; Yu et al., 1994). At E12.5 EYFP+ cells were found in the VZ of the ventral part of the LGE, and a few scattered cells in the MGE, with a pattern similar to the radial glial marker-RC2 and the pro-neural bHLH transcription factor-Mash1, known to be expressed by radial glial cells (Casarosa et al., 1999; Yun et al., 2002; Hartfuss et al., 2001). This strongly suggested that embryonic reporter positive cells observed in the CNP-Cre:ROSA26/EYFP line could represent a radial glial population. EYFP+ cells had a typical radial glial phenotype with a spindle shaped, elongated cell body and in a few cases a single process extending towards the pial surface. The radial glial phenotype of these cells was further confirmed BLBP immunolabelling (Figure 26). BLBP+/EYFP+ radial glial cells were present at the dorsal, ventral and lateral ventricular walls. In the muCNP-βgeo transgenic mice, β-gal activity has also been reported in radial glial cells; this is indicative of *Cnp* promoter activity in these cells (Chandross et al., 1999; Kurtz et al., 1994). In the present study, the radial glial phenotype of a subset reporter positive cells is indicative that the *Cnp* promoter is active in these neural progenitor cells of the CNS. I term these reporter positive cells as *"Cnp promoter active neural stem cells"*.

Taking together these findings, the following inference can be drawn: apart from its expression in relatively differentiated or *"late OPCs"*, activity of the *Cnp* promoter also labels a more precursor neural stem cell pool in this study: the *"Cnp promoter active neural stem cells"*. This is confirmed from the radial glial phenotype of embryonic reporter positive cells.

4.2 Extensive oligodendrogliogenesis from OPCs

In keeping with the hypothesis that CNP-Cre mediated reporter expression is present in a population of "late OPCs", EGFP and EYFP labelling was present in all mature oli-

godendrocytes at postnatal ages examined in both the CNP-Cre:Z/EG and CNP-Cre:ROSA26/EYFP lines. The presence of EGFP+/EYFP+ mature oligodendrocytes with myelinating processes in the dorsal cortex indicates that CNP-Cre expressing OPCs generate oligodendrocytes in both gray and white matter regions. Radial glial cells expressing *Cnp* promoter activity-dependent EYFP reporter expression are also known to generate oligodendrocytes through an intermediate oligodendrocyte precursor stage (Kriegstein and Alvarez-Buylla, 2009). The oligodendrogliogenic potential of progenitor cells in which the *Cnp* promoter is active, exhibited in this study is in conjunction with *in vitro* studies that employ the CNP-EGFP transgenic mice to show the generation of oligodendrocytes from CNP positive cells (Aguirre and Gallo, 2004; Belachew et al., 2003). Postnatal oligodendrogliogenesis from NG2 progenitors has also been demonstrated (Dimou et al., 2008; Guo et al., 2009; Zhu et al., 2011; Rivers et al., 2008; Kang et al., 2010).

An interesting finding limited to the CNP-Cre:ROSA26/EYFP mice was that in the dorsal cortex at P10 and to a larger extent at P30, there was a considerable population of reporter positive cells that did not co-label either NG2 or CC1 and exhibited a morphology quite distinct from NG2 cells and mature oligodendrocytes. This gave rise to the question whether CNP-Cre expressing OPCs in the gray matter served as putative progenitors to cell types that did not belong to oligodendroglial lineage.

4.3 OPCs do not generate neurons

Amongst the most fiercely debated questions in the field of oligodendroglial biology is whether OPCs serve as neuronal progenitors in the CNS. It has been shown in culture, that NG2 glia exposed to specific environmental signals revert to a multipotent state and generate neurons (Kondo and Raff, 2000). Adult human subcortical white matter cells isolated by *Cnp2* promoter activity generated neurons *in vitro* and in transplanted grafts (Nunes et al., 2003). OPCs from transgenic CNP-EGFP mice were shown to differentiate into neurons *in vitro* and upon transplantation into neurogenic regions of the postnatal brain (Belachew et al., 2003; Aguirre et al., 2004; Aguirre and Gallo, 2004). Recent Cre-lox fate mapping studies also suggest a neurogenic potential of OPCs (Rivers et al., 2008; Guo et al., 2009, 2010).

The current study presents compelling evidence of large scale neurogenesis from *Cnp* promoter active neural stem cells in the dorsal, ventral and piriform cortices (Figure 20).

Reporter positive neurons were classified on the basis of immunoreactivity for NeuN, a ubiquitous mature neuronal marker (Mullen et al., 1992). In some cases, reporter positive cells had the appearance of projection neurons, with large cell bodies and long axons. Importantly, reporter positive neurons were observed exclusively in the CNP-Cre:ROSA26/EYFP line, where EYFP labelling due to *Cnp* promoter activity extends beyond oligodendroglial lineage precursors to a neural stem cell niche.

4.3.1 Radial glia-like cells act as the neurogenic pool

A considerable population of reporter positive radial glial cells identified by morphology and BLBP immunolabellings were observed in the E16 CNP-Cre: ROSA26/EYFP dorso-lateral and ventral ventricular zone, subventricular zone and cortex (Figure 26).

Just prior to neurogenesis, neuroepithelial cells generate radial glia at E9-E10 (Frederiksen and McKay, 1988). It has been shown that radial glia of the dorsal telencephalon (Malatesta et al., 2003) and possibly of all regions, including the ventral forebrain (Anthony et al., 2004; Noctor et al., 2002), pass through a neurogenic phase and are the principal neuronal precursors throughout the CNS.

I speculate in this study that radial glial cells in the ventral and dorsal ventricular zone transiently express the *Cnp* gene, which results in reporter expression in radial glial cells and their progeny. It would be relatively safe to assume that this small subset of *Cnp* promoter active radial glial cells, serves as a source of reporter positive neurons observed in this study; as reporter expression was not observed in neurons in the CNP-Cre:Z/EG line where radial-glia like cells were not EGFP labelled. Also present at the lateral ventricular wall at E16 were EYFP labelled cells that were neither radial-glia like cells nor NG2 cells, it can be assumed that these cells were basal progenitor cells known to be the progeny of radial glial cells and serving as neuronal precursors (Malatesta et al., 2008).

VZ and SVZ progenitors produce neurons destined for different cortical layers from E11.5 to E17.5 in the mouse (Angevine and Sidman, 1961; Caviness and Takahashi,1995; Rakic, 1974). To verify if the embryonic *Cnp* promoter active neural stem cells observed in CNP-Cre:ROSA26/EYFP mice constituted the neurogenic pool; BrdU was administered at E12.5 in an attempt to target the early wave of neurogenesis. A large fraction of EYFP+ neurons in the ventral and piriform cortices co-labelled BrdU after a long ~40 day chase; suggesting that they were generated embryonically from

Cnp promoter active radial glia-like cells (Figure 23). No reporter positive NG2 cells co-labelled BrdU at P30 after a pulse at E12.5 (Figure 24). NG2 cells are generated from progenitor cells that would have been labelled by the E12.5 BrdU injection; it was therefore surprising that no BrdU positivity was found in NG2 cells. It can be speculated that the BrdU label is lost due to repeated cycles of divisions of the NG2 cell, which is an actively mitotic postnatal cell population. It also cannot be ruled out that an NG2 cell that had incorporated BrdU label from its precursor cell upon E12.5 BrdU administration, lost the BrdU label on subsequent divisions and became quiescent postnatally, did trans-differentiate into a neuron. This mode of neurogenesis via trans-differentiation from a quiescent postnatal NG2 cell would ensure the absence of BrdU labelling in it upon postnatal BrdU administration.

Some of the earliest born neurons that originate in the ventral telencephalon from E12.5-E14, migrate tangentially to populate the dorsal cortex (Anderson et al., 2001). Radial glial progenitors of the ventral forebrain generate GABAergic inhibitory neurons, including basal ganglia neurons as well olfactory bulb interneurons, which populate the ventral and piriform cortices respectively; while dorsal forebrain progenitors give rise to glutamatergic neurons at the dorsal cortex (Guillemot, 2005; Kriegstein and Götz, 2003). The ventral forebrain regions where EYFP+BrdU+ neurons were observed (Figure 23) are the anterior amygdaloid area (AA) and anterior amygdaloid nucleus (ACo), where it has been shown that peak neurogenesis occurs from E12.5-E14 (Bayer, 1980). The largest part of the primary olfactory cortex is made up by the piriform cortex, which constitutes the third step in the pathway of odour information processing after the olfactory epithelium and bulb (Suzuki and Bekkers, 2007). A large majority of layer II cells are born at E12 than at E14 or E16 and these E12 born cells differentiate into pyramidal neurons in this trilaminar cortex (Sarma et al., 2011; Bayer, 1986). Thus, peak neurogenesis in the ventral and piriform cortex matches perfectly with the E12.5 BrdU administration strategy used in this study; thereby targeting majority of EYFP+ neurons of these regions. Almost no BrdU labelled neurons were found in the layer II dorsal cortex under examination, this is most likely expected as neurons of the cortical plate (layer II to VI) are generated between E15-E16 (Bayer and Altman, 1990): a time point not targeted by E12.5 BrdU administration, thus resulting in no labelling of late neuronal progenitors. This was also in conjunction with parallel experiments in wild type mice, where E16 BrdU injections primarily labelled these later born neurons in the dorsal cortex (Figure 22). As has been already mentioned, the cortical interneurons gen-

erated in the ventral forebrain migrate tangentially to the dorsal cortex. Therefore, the very small subset of BrdU labelled reporter positive neurons (0.025 ± 0.008) observed in the dorsal cortex upon E12.5 BrdU administration, could possibly account for those neurons that have migrated from the ventral telencephalon.

Postnatal BrdU labelling studies reveal that NG2 cells constitute ~75% of the BrdU positive cells in gray matter regions (Dawson, 2003); thus the absence of any BrdU label in EYFP+ neurons upon postnatal BrdU administration in my study indicates that these are not generated atleast from the major postnatally cycling cell population i.e. NG2+ OPCs. Since no BrdU+EYFP+ neurons were found after four consecutive post-natal days of BrdU labelling, followed by a ~20 day chase; this argues against the generation of the observed reporter neurons from postnatal CNP-Cre expressing OPCs. On the other hand, it can be imagined that postnatally generated neurons were not BrdU labelled in this particular study because: (1) BrdU was pulsed from P10 to P13, perhaps not targeting the time window for postnatal neurogenesis; (2) Alternatively, it can also be that a late postnatal trickle of neurogenesis occurs by trans-differentiation of postmitotic CNP-Cre expressing OPCs; and (3) *Cnp* promoter activity-dependent labelling in adult neural stem cells of the SVZ could be another source of neurons observed only in the CNP-Cre:ROSA26/EYFP line.

If indeed transdifferentiation of CNP-Cre expressing OPCs led to generation of neurons, one would expect to observe reporter positive neurons in the CNP-Cre:Z/EG line as well. However, no reporter positive neurons were observed in the CNP-Cre:Z/EG line, where reporter expression was restricted to cells of the oligodendroglial lineage and did not extend into the neural stem cell niche. Therefore, together with the observation that there was no increase in the number of EYFP+ neurons with age (section 3.3.3.1), postnatal neurogenesis from CNP-Cre expressing OPCs seems improbable. These results demonstrate that embryonic *Cnp* promoter active radial glial precursors and not CNP-Cre expressing OPCs generate neurons. Additional postnatal BrdU pulse chase experiments would need to be combined with littermate control experiments verifying distribution of EYFP+ neurons with age, in order to address the question of postnatal neurogenesis from adult SVZ stem cells.

Postnatal neurogenesis has been reported from OPCs using inducible Cre expression under the *Plp* and *Pdgfra* promoters (Guo et al., 2009; Rivers et al., 2008). While Guo et al. (2009) show neurogenesis from early postnatal *Plp* promoter expressing-

progenitors, Rivers et al. (2008) failed to demonstrate BrdU labelling in their reporter positive neurons and hence, concluded that these neurons were the result of direct trans-differentiation from post-mitotic NG2 cells. It can be argued that with their transgenic constructs these studies labelled neonatal as well as adult SVZ neural stem cells which resulted in the observation of reporter positive neurons.

Neurogenesis was not detected in studies using Cre expression under the *Pdgfra* (Kang et al., 2010), *Cspg4* promoters (Zhu et al., 2008, 2011) and *Olig2* promoters (Dimou et al., 2008). However using another inducible Olig2creER^{TM} line, Ono et al. (2008) demonstrated extensive neurogenesis in the telencephalon by E12.5 Olig2+ precursors. It is worth mentioning that Kang et al. (2010) and Dimou et al. (2008) did observe a few reporter positive neurons in gray matter regions, which they dismissed as ectopic Cre-driven reporter expression in neurons themselves. The presence of BrdU labelling in reporter positive neurons in this study, argues against reporter positivity due to ectopic Cre expression or transient CNP expression by neurons; but rather provides direct evidence of neurogenesis from proliferating *Cnp* promoter active embryonic precursors. However, another possibility cannot be ruled out: neurons were BrdU labelled since they were generated from EYFP negative neuronal precursors targeted by the E12.5 BrdU pulse, and subsequently became EYFP positive due to ectopic Cre expression.

Having observed reporter expression in embryonic neural stem cells in the CNP-Cre: ROSA26/EYFP line, an approach with inducible Cre expression under the NG2 promoter was adopted to specifically answer if oligodendroglial precursors had a neuronal fate.

Extensive neurogenesis was observed in adult P30 NG2creER^{TM}BAC:ROSA26/EYFP mice induced with Cre at late embryonic ages. Reporter positive neurons were observed both in the neocortex and palaeocortex. The radial glial phenotype of embryonic reporter positive cells, lends support to the speculation made in this study, as well as by Richardson et al. (2011), that the NG2 promoter and other oligodendroglial lineage gene, might be transiently switched on in these neural stem cell types, at extremely low levels.Thus, oligodendrocyte promoter-Cre lines cross-bred with the sensitive Cre reporter: ROSA26/EYFP, will ensure that these low oligodendrocyte promoter driven Cre expression levels are detected, leading to reporter expression in these cell types. EYFP reporter expression in neural stem cells would also explain the presence of reporter positivity in neurons.

A similar study by Zhu et al. (2011), using NG2creER^{TM}BAC transgenesis with the Z/EG Cre reporter failed to report any neurogenesis. As opposed to reporter expression in radial glia-like cells at embryonic time points in this study, Zhu et al. (2011) observed that all EGFP+ cells at E19.5 were NG2+. The discrepancies in these results can be due to two separate Cre reporter lines used; re-emphasizing the point that low and transient NG2 promoter expression in neural stem cells can be detected only by the ROSA26/EYFP Cre reporter used in this study. "Leaky" Cre expression in this double transgenic line can also be ruled out, since no reporter positivity was observed in a series of frontal sections through the dorsal, ventral and piriform cortices of control NG2creER^{TM}BAC:ROSA26/EYFP mice at ~P30 that had not been administered with Tamoxifen prior to analysis. The absence of reporter positivity in neurons upon postnatal Cre induction also confirms that only embryonic reporter positive radial glia-like cells and not NG2 cells serve as progenitors of the observed neurons.

4.4   Astrocyte generation from radial glia-like cells rather than from OPCs

In the early 1990's, *in vivo* studies reporting the absence of GFAP+/NG2+ cells (Skoff, 1990; Fulton et al., 1992) alongwith lack of evidence of astrocytic generation from transplanted OPCs (Groves et al., 1993), led many investigators to conclude that the observation by Raff et al. (1983) of the astrogliogenic potential of OPCs was merely a culture artefact (Noble et al., 2005). Almost more than a decade later, direct *in vivo* fate mapping studies have lend support to the observations of Raff et al. (1983) regarding astrocytic generation from OPCs in the normal (Zhu et al., 2008a, 2008b, 2011; Guo et al., 2009) and compromised CNS (Tripathi et al., 2010; Zawadzka et al., 2010).

This study demonstrates EYFP reporter expression by astrocytes exclusively in the CNP-Cre:ROSA26/EYFP line. Reporter positive cells with a highly branched, fine arborisation of bushy processes reminiscent of protoplasmic astrocytes (Bushong et al., 2004), were most prevalent in the ventral forebrain regions at both early and late postnatal ages under examination (Figure 19). While most of the reporter cells that were characterised as astrocytes displayed GFAP immunoreactivity, there were a few GFAP negative cells classified as being astrocytes based on their highly ramified and complex morphology. The ventral forebrain remains the predominant region where reporter positive astrocytes were observed. Reporter positive/GFAP positive cells in the dorsal cortex were not an infrequent occurrence, alongwith the presence of reporter positive fi-

brous astrocytes in the white matter regions of corpus callosum and fimbrae. Reporter positive astrocytes appeared to increase slightly from P6 to P30 and occurred mostly in cohorts of doublets or triplets, indicative of local proliferation of newly generated astrocytes.

The time point of astrocytic generation from *Cnp* promoter active progenitor cells cannot be ascertained with the current set of experiments where Cre is expressed constitutively under the *Cnp* promoter. However, I suggest that the source of astrocytes observed in my study could be radial glial cells in which the *Cnp* promoter as well as other oligodendroglial promoters are active, and not CNP-Cre expressing late OPCs because: (1) Reporter positive astrocytes were only observed in the CNP-Cre:ROSA26/EYFP line in which *Cnp* promoter active radial glia-like cells at the dorso-lateral and ventral ventricular walls were EYFP labelled, and not in the CNP-Cre:Z/EG line in which only CNP-Cre expressing oligodendroglial precursors were labelled. If astrocytes were generated from oligodendroglial precursors then they should have been EGFP labelled also in the CNP-Cre:Z/EG line; and (2) In their experiments with the NG2creER^{TM}BAC:Z/EG line, reporter labelled astrocytes were only observed upon embryonic Tamoxifen induction which also labelled radial-glia like cells, but not when only oligodendroglial lineage precursors were labelled by postnatal TMX induction (Zhu et al., 2011).

Radial glia and SVZ neural stem cells are known to generate astrocytes in gray and white matter telencephalic regions (Voigt, 1989; Mission et al., 1991; Levison et al., 1993; Malatesta et al., 2000). Therefore, I hypothesize that these embryonic *Cnp* promoter active neural stem cell niche served as the astrogliogenic pool in the present study.

However, it is important to note that within the scope of experiments performed in this study, it cannot be ruled out that astrocytes were reporter positive due to the fact that they themselves expressed Cre ectopically.

Zhu et al. (2011) suggest that there exist separate subpopulations of OPCs that are astrogliogenic and oligogenic in the developing brain. Therefore, in their experiments where Cre was induced at E16.5 with TMX injections to NG2creER^{TM}:Z/EG animals, this embryonic "astrogliogenic pool of OPCs" led to reporter positive astrocytes in the ventral forebrain. However, with postnatal (P2 and P60) TMX injections, no EGFP+

astrocytes were observed in the forebrain. This suggests that a subset of OPCs only at late embryonic ages generate ventral forebrain astrocytes.

In studies using artificially generated *Cnp* promoter to drive EGFP expression- CNP-EGFP transgenic line (Yuan et al., 2002), it has been shown that fluorescence-activated cell sorting (FACS) sorted EGFP+ cells displaying CNP gene activity were multipotent and gave rise to astrocytes *in vitro* (Nunes et al., 2003; Belachew et al., 2003). It can be assumed that the artificial *Cnp* promoter used in these studies could drive reporter positivity in a neural stem cell niche. Studies using BAC transgenic Pdgfra-creER^{TM} mice which were Cre induced at P45 (Rivers et al., 2008) and P30 (Kang et al., 2010), failed to report positivity in astrocytes. Another study using Olig2creER^{TM} mice (Dimou et al., 2008) Cre induced at 2.5 month and 6 month of age, has also challenged the astrogliogenic potential of OPCs. The discrepancies in these results are perhaps because these studies investigated the progeny of postnatal OPCs and do not label embryonic OPCs or transient oligodendrocyte promoter-expressing radial glial cells.

4.5   Differences between Cre reporter lines: contribution towards a bias in fate mapping results

Different lineages of progenitors labelled by the CNP-Cre knock-in approach are observed by employing two separate Cre reporter lines used (see Table 2).

% of EGFP+ or EYFP+ cells being:	CNP-Cre cross bred with:	
	Z/EG	**ROSA26/EYFP**
Oligodendrocytes	~73 in Dorsal Cortex ~96 in Corpus Callosum	~24 in Dorsal Cortex ~88 in Corpus Callosum
Astrocytes	< 2 in Ventral Cortex	~12 in Ventral Cortex
Neurons	< 1 in Dorsal Cortex 0 in Ventral Cortex < 1 in Piriform Cortex	~55 in Dorsal Cortex ~40 in Ventral Cortex ~70 in Piriform Cortex

Table 2. Comparative lineage of precursor cells labelled by CNP-Cre mediated recombination with the Z/EG and ROSA26/EYFP Cre reporters.

Oligodendrocytes are the only reporter positive cells detected throughout the gray and white matter regions of CNP-Cre:Z/EG mice. In absolute contrast, with the interbreeding strategy involving ROSA26/EYFP Cre reporter, in addition to oligodendrocytes and a small subset of astrocytes, large number of neurons appear reporter positive.

It is well documented that different Cre reporter lines possess varying recombination efficacies (Richardson et al., 2011), which might contribute extensively in influencing the outcome of lineage tracing results. The present study is the first of its kind that compares and integrates data obtained by using two separate Cre reporter lines in investigating the fate of *"late OPCs"*; thereby providing a clearer understanding of fate mapping data.

It is noteworthy, that of the two mouse lines: CNP-Cre:Z/EG and CNP-Cre:ROSA26/EYFP, reporter positive cell types, namely embryonic radial glial cells, astrocytes and neurons were primarily detected in the latter line which uses the ROSA26/EYFP Cre reporter (Srinivas et al., 2001). Several reasons can be attributed to this differential fate observed between the experimental groups using the two separate Cre reporter lines: (1) Different promoter constructs were used to drive reporter transgene expression, while the Z/EG line uses the strong pCAGGS promoter, EYFP expression in the ROSA26/EYFP line is achieved by targeting the ubiquitously expressed ROSA26 locus. It cannot be ruled out that this could lead to differences in the pattern and levels of reporter transgene expression. Due to different promoter constructs, it could also be that one or the other reporter transgene is preferentially expressed in certain cell types, thereby introducing an unwanted bias in cell type specificity. This can be ruled out to a certain extent in double reporters like the Z/EG line used in this study, wherein overlapping expression patterns of both reporters have been observed (Novak et al., 2000); and (2) The ROSA26/EYFP line (Srinivas et al., 2001) is considered a more sensitive Cre reporter which can detect very low Cre expression levels, which would otherwise remain undetected by the Z/EG line that recombines less efficiently (Novak et al., 2000). For instance, using the NG2creER^{TM} and Pdgfra-creER^{TM} lines, 30 fold and more than 2 fold higher Cre recombination efficacies were achieved when the Z/EG Cre reporter was replaced by the ROSA26/EYFP (Zhu et al., 2011; Kang et al., 2010). It has been suggested that the stoichiometric threshold for Cre expression or the minimal concentration of Cre required in the cell nucleus, below which minimal recombination occurs, is lower for a good recombiner (Richardson et al., 2011). Thus, low and transient expression levels of *Cnp* promoter-driven Cre in embryonic radial glial cells is only "picked

up" by the sensitive ROSA26/EYFP Cre reporter used in the CNP-Cre:ROSA26/EYFP line and remains undetected in the CNP-Cre:Z/EG line. In addition, location of the reporter transgene cassette and the distance between the loxP sites could also be the factors influencing different Cre recombination efficiencies.

The detection of CNP-Cre driven reporter expression in radial glia-like cells, which serve as the source of the observed reporter positive neurons, make the CNP-Cre:ROSA26/EYFP line unsuitable for studying purely oligodendroglial lineage development. On the other hand, the CNP-Cre :Z/EG, results in the detection of reporter positivity only in cells of the oligodendroglial lineage. Therefore, the choice of Cre reporter results in differences in the cell populations being labelled and this is the reason for a stark contrast in the lineage of precursor cells labelled by CNP-Cre mediated recombination.

4.6   Developmental regulation of CNP expression: a possible role of MicroRNAs

Key players of the posttranscriptional silencing machinery- MicroRNAs (miRNAs) are known to be enriched in oligodendroglial lineage cells and have been implicated as critical regulators of oligodendrocyte development and myelination. It has been shown that miR-219, miR-338 and Dicer1 are required for normal oligodendrocyte differentiation and developmental myelination (Dugas et al., 2010; Zhao et al., 2010). Conditional Dicer deletion in oligodendroglial lineage cells using the CNP-Cre mice has also been shown to effect oligodendrocyte cell number (Budde et al., 2010).

In P10 CNP-Cre:Z/EG and CNP-Cre:ROSA26/EYFP mice, reporter positivity was present in a large subset of OPCs. This indicates that in these subsets of reporter positive NG2 cells, Cre recombination under the *Cnp* promoter had taken place; implying that the CNP gene was actively transcribed in these cell populations. However, CNP immmunolabelling revealed that none of the reporter positive NG2 cells in either gray or white matter expressed the CNP protein (Figure 27). This is consistent with the appearance of *Cnp* transcripts in the CNS as early as E12.5 (Peyron et al., 1997), and that the CNP protein is seen only much later to be expressed by differentiating oligodendrocytes (Baumann and Pham-Dinh, 2001).This regulation in the timing of expression of the *Cnp* mRNA and protein hints towards a possible role of miRNAs. The absence of CNP protein in OPCs compared with the broad distribution of its message in these cell

types supports a posttranscriptional control; such that interaction of an miRNA with the CNP mRNA blocks protein translation, and that this inhibitory effect is only removed later in the developmental lineage of the OPC, leading to CNP protein expression in the ensuing mature stages. Similar to the developmental pattern of expression of the CNP gene, PLP mRNA is expressed embryonically, whereas the protein is expressed only much later by myelinating oligodendrocytes postnatally (Baumann and Pham-Dinh, 2001). miR-20a has been reported to regulate PLP gene expression through its 3'UTR (Wang and Cambi, 2012). Therefore, it can be imagined that regulation of CNP expression action of miRNA's, could play a defining role in the early stages of oligodendroglial development.

4.7   AMPA receptor subunit composition in OPCs influences proliferation

Chemical synaptic transmission is not used exclusively for communication between neurons. A wealth of studies in the recent decade has shown that NG2 glia form direct synaptic contacts with both glutamatergic and GABAergic neurons (Paukert and Bergles, 2006; Kukley et al., 2007; Ziskin et al., 2007). The finding that NG2 cells receive both excitatory and inhibitory synaptic input raised the possibility that neuron-glia signalling at the synapse could influence development and cellular properties of OPCs.

A number of studies have previously shown that electrical activity of the axon controls OPC proliferation and myelinogenesis (Gyllensten and Malmfors, 1963; Barres and Raff, 1993; Demerens et al., 1996). Furthermore, *in vitro* experiments show that vesicularly released glutamate influences initial events in myelination (Wake et al., 2011). It is important however to note that these studies modify axonal release to investigate its role in oligodendroglial development, and this could also regulate neuron-neuron interactions in addition to influencing neuron-OPC signalling. On the other hand, in my study I concentrate on the detection site of the neuron-OPC synapse and modify the AMPA receptor subunit- GluRB on the NG2 cell, to ascertain its effect on OPC behaviour and physiology.

The GluRB subunit was genetically ablated only in OPCs by an inducible Cre-lox based experimental approach; and subsequent inter-breeding with a Cre reporter line ensured EYFP labelling of targeted OPCs. 0.5 mg Tamoxifen was administered to GluRB KO and GluRB CTRL experimental groups at P5-P10 for 1 or 3 days and ~2 weeks after the

last TMX injection, animals were given 300 mg/kg BrdU. In the GluRB knockout group, NG2 cells that had lost the GluRB subunit were EYFP labelled, while EYFP labelled NG2 cells in the GluRB control group still possessed the GluRB subunit. The absolute number of reporter positive cells remained unchanged between the control and experimental groups; however, the proportion reporter positive cells that were BrdU+ cells was significantly reduced in the GluRB knockout group (Figure 31). A reduction in proliferation of EYFP labelled cells, which are presumably NG2 cells as they represent the major cycling cell population in the postnatal brain (Dawson, 2003; Psachoulia et al., 2009), while keeping the absolute numbers same, seems confusing. If NG2 cells proliferated less upon GluRB deletion, reduced number of EYFP+ cells should have been observed in the GluRB KO group, unless GluRB ablation changed NG2Cre expression in the KO group. This discrepancy with respect to the observed absolute number of EYFP+ cells can perhaps be attributed to variances due to the Tamoxifen induction protocols, since the TMX injections could greatly influence Cre-mediated EYFP positive cell counts. Therefore, it cannot be said with certainty that the absolute number of EYFP+ cells remained unchanged between the two experimental groups.

The GluRB subunit governs the receptors Ca^{++} permeability, with its presence rendering the receptor Ca^{++} impermeable and its absence leading to an increased Ca^{++} influx into the cell. Keeping this in mind, the present study indicates that removing the GluRB subunit from the OPC, leading to an increased Ca^{++} influx into the cell in response to endogenous neuronal activity-mediated glutamate release; in turn inhibits OPC proliferation. Inhibition of proliferation could initiate the differentiation of an OPC towards the mature oligodendrocyte stage. Kukley et al. (2010) have shown that synaptic input is lost upon differentiation of the OPC towards the mature oligodendroglial state; therefore it can be speculated that an increased Ca^{++} influx upon GluRB removal could lead to a downregulation of synaptic input onto the OPC. Inhibition of OPC proliferation due to GluRB removal-mediated Ca^{++} influx seems consistent when extended to an unpublished observation by our own group where electrical stimulation is in the corpus callosum has been shown to decrease the total number of proliferating cells. It has also previously been demonstrated using cortical OPC cultures, that non-NMDA glutamate receptor agonists inhibit cell proliferation (Gallo et al., 1996).

As has been mentioned above, a decrease in the rate of OPC proliferation upon GluRB removal, could perhaps give rise to the scenario that OPCs in the GluRB knockouts undergo differentiation to generate mature oligodendrocytes. It can be imagined that cell

cycle arrest which would permit the OPC to undertake the differentiation pathway, would also lead to a decrease in the incorporation of BrdU, as observed in the GluRB knockouts. Cell cycle withdrawal by cyclin-dependent kinase (CDK) inhibitor has been shown to facilitate differentiation of OPCs (Casaccia-Bonnefil et al., 1997).

To verify if glutamatergic signalling via the GluRB subunit influences myelination and differentiation of OPCs, the fraction of EYFP+ cells that were NG2 cells was determined. For this P10 to P20 animals of the GluRB KO group and GluRB CTRL group were given 0.5 mg Tamoxifen (single i.p injection for 3 or 6 days) and analysed ~10 days after the last TMX injection. The fraction of reporter positive cells that were NG2+ remained unchanged between the two experimental groups; this would suggest that altering the glutamatergic input by GluRB deletion has no effect on myelination (Figure 32). However, it must be remembered that the read out of differentiation in this study was the fraction of NG2 cells among EYFP+ cells and the population of mature oligodendrocytes among reporter positive cells was not calculated. NG2 cells could have undergone asymmetric division, thus keeping the number of NG2+EYFP+ cells same. Further experiments determining the fraction of mature CC1+ oligodendocytes among reporter positive cells and PLP immunolabellings identifying myelin sheaths, would need to be performed to examine the effect of GluRB subunit on differentiation and myelination.

5   Summary

In this study, I employ a mouse line in which Cre is knocked-in for the 2',3' -cyclic nucleotide 3' –phosphodiesterase (CNP) gene and compare the fates of CNP-Cre expressing OPCs between two Cre reporters: Z/EG and ROSA26/EYFP. CNPase is found only in mature oligodendrocytes; therefore a subpopulation of "late" or relatively differentiated OPCs which have presumably made the decision to differentiate into oligodendrocytes are labelled with this experimental strategy.

In the first section of this study, I present evidence of extensive oligodendrogliogenesis from CNP-Cre expressing OPCs in both experimental lines. I also show a small subset of reporter positive astrocytes and extensive neurogenesis in discrete regions of the CNP-Cre:ROSA26/EYFP line: ~12% of all EYFP+ cells in the ventral cortex represent an astrocytic phenotype with GFAP positivity and 55-70% reporter positive cells in the dorsal, ventral and piriform cortices are NeuN positive neurons. In striking contrast, no EGFP positive astrocytes or neurons are observed in the CNP-Cre:Z/EG line.

In the second section I report *Cnp* promoter activity-dependent reporter labelling in embryonic radial-glia (RG) like cells which are known to display multipotency. I suggest that OPCs remain committed to an oligodendroglial fate and do not display lineage plasticity; while oligodendroglial genes are switched on transiently in RG-like cells at extremely low levels, only to be detected by sensitive Cre reporters. I thereby show that fate mapping studies can be strongly biased by the choice of Cre reporter strains, resulting in stark differences in the progeny of oligodendroglial precursors as observed in this study.

The last part of my thesis, is devoted to elucidating the functional role of the GluRB AMPA receptor subunit in influencing OPC physiology, by availing the GluRB floxed NG2creER^{TM}:GluR-B$^{2lox/2lox}$:ROSA26/EYFP mouse line. I demonstrate that removing the GluRB subunit from the OPC leads to a reduction in OPC proliferation in white matter regions. AMPA receptors are the principal mediators of glutamatergic signalling at the neuron-OPC synapse, and an insight into their effect on OPC development, as presented in this study, will further enhance our understanding of neuron-OPC cross-talk.

6 References

Aguirre A, Gallo V (2004) Postnatal neurogenesis and gliogenesis in the olfactory bulb from NG2-expressing progenitors of the subventricular zone. The Journal of Neuroscience 24:10530–10541.

Aguirre AA, Chittajallu R, Belachew S, Gallo V (2004) NG2-expressing cells in the subventricular zone are type C-like cells and contribute to interneuron generation in the postnatal hippocampus. The Journal of Cell Biology 165:575–589.

Allen FW, Davis FF (1956) A specific phosphodiesterase from beef pancreas. Biochimica et Biophysica Acta 21:14–17.

Alonso G (2005) NG2 proteoglycan-expressing cells of the adult rat brain: possible involvement in the formation of glial scar astrocytes following stab wound. Glia 49:318–338.

Amur-Umarjee SG, Dasu RG, Campagnoni AT (1990) Temporal expression of myelin-specific components in neonatal mouse brain cultures: evidence that 2',3'-cyclic nucleotide 3'-phosphodiesterase appears prior to galactocerebroside. Developmental Neuroscience 12:251–262.

Anderson SA, Marín O, Horn C, Jennings K, Rubenstein JL (2001) Distinct cortical migrations from the medial and lateral ganglionic eminences. Development 128:353–363.

De Angelis DA, Braun PE (1994) Isoprenylation of brain 2',3'-cyclic nucleotide 3'-phosphodiesterase modulates cell morphology. Journal of Neuroscience Research 39:386–397.

De Angelis DA, Braun PE (1996) Binding of 2',3'-cyclic nucleotide 3'-phosphodiesterase to myelin: an in vitro study. Journal of Neurochemistry 66:2523–2531.

Angevine JB, Sidman RL (1961) Autoradiographic study of cell migration during histogenesis of cerebral cortex in the mouse. Nature 192:766–768.

Angevine, J. B., Bodian, D., Coulombre, A. J., Edds, M. V., Hamburger, V., Jacobson, M., Lyser, K. M., Prestige, M. C., Sidman, R. L., Varon, S. and Weiss PA (1970) Embryonic vertebrate central nervous system: revised terminology. The Boulder Committee. The Anatomical record 166:257–261.

Anthony TE, Klein C, Fishell G, Heintz N (2004) Radial glia serve as neuronal progenitors in all regions of the central nervous system. Neuron 41:881–890.

Bansal R, Pfeiffer SE (1985) Developmental expression of 2',3'-cyclic nucleotide 3'-phosphohydrolase in dissociated fetal rat brain cultures and rat brain. Journal of Neuroscience Research 14:21–34.

Bansal R, Pfeiffer SE (1992) Novel stage in the oligodendrocyte lineage defined by reactivity of progenitors with R-mAb prior to O1 anti-galactocerebroside. Journal of Neuroscience Research 32:309–316.

Barres BA, Raff MC (1993) Proliferation of oligodendrocyte precursor cells depends on electrical activity in axons. Nature 361:258–260.

Baumann N, Pham-Dinh D (2001) Biology of oligodendrocyte and myelin in the mammalian central nervous system. Physiological Reviews 81:871–927.

Bayer SA (1980) Quantitative 3H-thymidine radiographic analyses of neurogenesis in the rat amygdala. The Journal of Comparative Neurology 194:845–875.

Bayer SA (1986) Neurogenesis in the rat primary olfactory cortex. International Journal of Developmental Neuroscience 4:251–271.

Bayer SA, Altman J (1990) Development of layer I and the subplate in the rat neocortex. Experimental Neurology 107:48–62.

Bayer SA, Altman J (1991) Development of the endopiriform nucleus and the claustrum in the rat brain. Neuroscience 45:391–412.

Belachew S, Chittajallu R, Aguirre A a, Yuan X, Kirby M, Anderson S, Gallo V (2003) Postnatal NG2 proteoglycan-expressing progenitor cells are intrinsically multipotent and generate functional neurons. The Journal of Cell Biology 161:169–186.

Belachew S, Yuan X, Gallo V (2001) Unraveling oligodendrocyte origin and function by cell-specific transgenesis. Developmental Neuroscience 23:287–298.

Bergles DE, Jabs R, Steinhäuser C (2010) Neuron-glia synapses in the brain. Brain Research Reviews 63:130–137.

Bergles DE, Roberts JD, Somogyi P, Jahr CE (2000) Glutamatergic synapses on oligodendrocyte precursor cells in the hippocampus. Nature 405:187–191.

Bernier L, Alvarez F, Norgard EM, Raible DW, Mentaberry A, Schembri JG, Sabatini DD, Colman DR (1987) Molecular cloning of a 2',3'-cyclic nucleotide 3'-phosphodiesterase: mRNAs with different 5' ends encode the same set of proteins in nervous and lymphoid tissues. The Journal of Neuroscience 7:2703–2710.

Bernier L, Colman DR, D'Eustachio P (1988) Chromosomal locations of genes encoding 2',3' cyclic nucleotide 3'-phosphodiesterase and glial fibrillary acidic protein in the mouse. Journal of Neuroscience Research 20:497–504.

Bevis BJ, Glick BS (2002) Rapidly maturing variants of the Discosoma red fluorescent protein (DsRed). Nature Biotechnology 20:83–87.

Bhat RV, Axt KJ, Fosnaugh JS, Smith KJ, Johnson KA, Hill DE, Kinzler KW, Baraban JM (1996) Expression of the APC tumor suppressor protein in oligodendroglia. Glia 17:169–174.

De Biase LM, Kang SH, Baxi EG, Fukaya M, Pucak ML, Mishina M, Calabresi PA, Bergles DE (2011) NMDA receptor signaling in oligodendrocyte progenitors is not required for oligodendrogenesis and myelination. The Journal of Neuroscience 31:12650–12662.

Bifulco M, Laezza C, Stingo S, Wolff J (2002) 2',3'-Cyclic nucleotide 3'-phosphodiesterase: a membrane-bound, microtubule-associated protein and membrane anchor for tubulin. Pro-

ceedings of the National Academy of Sciences of the United States of America 99:1807–1812.

Bignami A, Eng LF, Dahl D, Uyeda CT (1972) Localization of the glial fibrillary acidic protein in astrocytes by immunofluorescence. Brain Research 43:429–435.

Boda E, Viganò F, Rosa P, Fumagalli M, Labat-Gest V, Tempia F, Abbracchio MP, Dimou L, Buffo A (2011) The GPR17 receptor in NG2 expressing cells: Focus on in vivo cell maturation and participation in acute trauma and chronic damage. Glia 1973:1958–1973.

Braun PE, De Angelis D, Shtybel WW, Bernier L (1991) Isoprenoid modification permits 2',3'-cyclic nucleotide 3'-phosphodiesterase to bind to membranes. Journal of Neuroscience Research 30:540–544.

Braun PE, Lee J, Gravel M (2004) 2´, 3´-Cyclic nucleotide 3´-phosphodiesterase: structure, biology and function, in : Myelin biology and disorders, edited by Lazzarini RA (Elsevier Science, London), 499–522.

Brenner T, Lisak RP, Rostami A, McMorris FA, Silberberg DH (1986) A monoclonal antibody raised to corpus callosum extract reacts with 2',3'-cyclic nucleotide 3'-phosphohydrolase. Journal of Neurochemistry 46:54–60.

Bu J, Banki A, Wu Q, Nishiyama A (2004) Increased NG2(+) glial cell proliferation and oligodendrocyte generation in the hypomyelinating mutant shiverer. Glia 48:51–63.

Budde H, Schmitt S, Fitzner D, Opitz L, Salinas-Riester G, Simons M (2010) Control of oligodendroglial cell number by the miR-17-92 cluster. Development 137:2127–2132.

Bunge RP (1968) Glial cells and the central myelin sheath. Physiol Rev 48:197–251.

Burnashev N, Monyer H, Seeburg PH, Sakmann B (1992) Divalent ion permeability of AMPA receptor channels is dominated by the edited form of a single subunit. Neuron 8:189–198.

Bushong EA, Martone ME, Ellisman MH (2004) Maturation of astrocyte morphology and the establishment of astrocyte domains during postnatal hippocampal development. International Journal of Developmental Neuroscience 22:73–86.

Cai J, Qi Y, Hu X, Tan M, Liu Z, Zhang J, Li Q, Sander M, Qiu M (2005) Generation of oligodendrocyte precursor cells from mouse dorsal spinal cord independent of Nkx6 regulation and Shh signaling. Neuron 45:41–53.

Cameron HA, McKay RD (2001) Adult neurogenesis produces a large pool of new granule cells in the dentate gyrus. The Journal of Comparative Neurology 435:406–417.

Casaccia-Bonnefil P, Tikoo R, Kiyokawa H, Friedrich V, Chao MV, Koff A (1997) Oligodendrocyte precursor differentiation is perturbed in the absence of the cyclin-dependent kinase inhibitor p27Kip1. Genes & Development 11:2335–2346.

Casarosa S, Fode C, Guillemot F (1999) Mash1 regulates neurogenesis in the ventral telencephalon. Development 126:525–534.

Casper KB, McCarthy KD (2006) GFAP-positive progenitor cells produce neurons and oligodendrocytes throughout the CNS. Molecular and Cellular Neurosciences 31:676–684.

Caviness VS, Takahashi T (1995) Proliferative events in the cerebral ventricular zone. Brain & Development 17:159–163.

Chan-Ling T, Chu Y, Baxter L, Weible Ii M, Hughes S (2009) In vivo characterization of astrocyte precursor cells (APCs) and astrocytes in developing rat retinae: differentiation, proliferation, and apoptosis. Glia 57:39–53.

Chandross KJ, Cohen RI, Paras P, Gravel M, Braun PE, Hudson LD (1999) Identification and characterization of early glial progenitors using a transgenic selection strategy. The Journal of Neuroscience 19:759–774.

Chen P, Cai W, Wang L, Deng Q (2008) A morphological and electrophysiological study on the postnatal development of oligodendrocyte precursor cells in the rat brain. Brain Research 1243:27–37.

Chittajallu R, Aguirre A, Gallo V (2004) NG2-positive cells in the mouse white and grey matter display distinct physiological properties. The Journal of Physiology 561:109–122.

Clarke LE, Young KM, Hamilton NB, Li H, Richardson WD, Attwell D (2012) Properties and fate of oligodendrocyte progenitor cells in the corpus callosum, motor cortex, and piriform cortex of the mouse. The Journal of Neuroscience 32:8173–8185.

Dahl D (1981) The vimentin-GFA protein transition in rat neuroglia cytoskeleton occurs at the time of myelination. Journal of Neuroscience Research 6:741–748.

Davidoff MS, Middendorff R, Köfüncü E, Müller D, Jezek D, Holstein AF (2002) Leydig cells of the human testis possess astrocyte and oligodendrocyte marker molecules. Acta Histochemica 104:39–49.

Davidoff MS, Middendorff R, Müller D, Köfüncü E, Holstein AF (1997) Immunoreactivity for glial cell markers in the human testis. Advances in Experimental Medicine and Biology 424:151–152.

Dawson M (2003) NG2-expressing glial progenitor cells: an abundant and widespread population of cycling cells in the adult rat CNS. Molecular and Cellular Neuroscience 24:476–488.

Demerens C, Stankoff B, Logak M, Anglade P, Allinquant B, Couraud F, Zalc B, Lubetzki C (1996) Induction of myelination in the central nervous system by electrical activity. Proceedings of the National Academy of Sciences of the United States of America 93:9887–9892.

Dimou L, Simon C, Kirchhoff F, Takebayashi H, Götz M (2008) Progeny of Olig2-expressing progenitors in the gray and white matter of the adult mouse cerebral cortex. The Journal of Neuroscience 28:10434–10442.

Doetsch F (2003) A niche for adult neural stem cells. Current Opinion in Genetics & Development 13:543–550.

Douglas AJ, Fox MF, Abbott CM, Hinks LJ, Sharpe G, Povey S, Thompson RJ (1992) Structure and chromosomal localization of the human 2',3'-cyclic nucleotide 3'-phosphodiesterase gene. Annals of Human Genetics 56:243–254.

Dreiling CE, Schilling RJ, Reitz RC (1981) 2',3'-cyclic nucleotide 3'-phosphohydrolase in rat liver mitochondrial membranes. Biochimica et Biophysica Acta 640:114–120.

Drummond GI, Iyer N, Keith J (1962) Hydrolysis of ribonucleoside 2',3'-cyclic phosphates by a diesterase from brain. The Journal of Biological Chemistry 237:3535–3539.

Dugas JC, Cuellar TL, Scholze A, Ason B, Ibrahim A, Emery B, Zamanian JL, Foo LC, McManus MT, Barres BA (2010) Dicer1 and miR-219 Are required for normal oligodendrocyte differentiation and myelination. Neuron 65:597–611.

Dyer CA, Benjamins JA (1989) Organization of oligodendroglial membrane sheets. I: Association of myelin basic protein and 2',3'-cyclic nucleotide 3'-phosphohydrolase with cytoskeleton. Journal of Neuroscience Research 24:201–211.

Etxeberria A, Mangin J-M, Aguirre A, Gallo V (2010) Adult-born SVZ progenitors receive transient synapses during remyelination in corpus callosum. Nature Neuroscience 13:287–289.

Fancy SPJ, Chan JR, Baranzini SE, Franklin RJM, Rowitch DH (2011) Myelin regeneration: a recapitulation of development? Annual Review of Neuroscience 34:21–43.

Feng G, Mellor RH, Bernstein M, Keller-Peck C, Nguyen QT, Wallace M, Nerbonne JM, Lichtman JW, Sanes JR (2000) Imaging Neuronal Subsets in Transgenic Mice Expressing Multiple Spectral Variants of GFP. Neuron 28:41–51.

Feng L, Hatten ME, Heintz N (1994) Brain lipid-binding protein (BLBP): A novel signaling system in the developing mammalian CNS. Neuron 12:895–908.

Filley CM (1998) The behavioral neurology of cerebral white matter. Neurology 50:1535–1540.

Fogarty M, Richardson WD, Kessaris N (2005) A subset of oligodendrocytes generated from radial glia in the dorsal spinal cord. Development 132:1951–1959.

Frederiksen K, McKay RD (1988) Proliferation and differentiation of rat neuroepithelial precursor cells in vivo. The Journal of Neuroscience 8:1144–1151.

Fröhlich N, Nagy B, Hovhannisyan A, Kukley M (2011) Fate of neuron-glia synapses during proliferation and differentiation of NG2 cells. Journal of Anatomy 219:18–32.

Fulton BP, Burne JF, Raff MC (1992) Visualization of O-2A progenitor cells in developing and adult rat optic nerve by quisqualate-stimulated cobalt uptake. The Journal of Neuroscience 12:4816–4833.

Gallo V, Mangin J-M, Kukley M, Dietrich D (2008) Synapses on NG2-expressing progenitors in the brain: multiple functions? The Journal of Physiology 586:3767–3781.

Gallo V, Zhou JM, McBain CJ, Wright P, Knutson PL, Armstrong RC (1996) Oligodendrocyte progenitor cell proliferation and lineage progression are regulated by glutamate receptor-mediated K+ channel block. The Journal of Neuroscience 16:2659.

Ge W-P, Yang X-J, Zhang Z, Wang H-K, Shen W, Deng Q-D, Duan S (2006) Long-term potentiation of neuron-glia synapses mediated by Ca2+-permeable AMPA receptors. Science 312:1533–1537.

Genoud S, Lappe-Siefke C, Goebbels S, Radtke F, Aguet M, Scherer SS, Suter U, Nave K-A, Mantei N (2002) Notch1 control of oligodendrocyte differentiation in the spinal cord. The Journal of Cell Biology 158:709–718.

Gillespie CS, Bernier L, Brophy PJ, Colman DR (1990) Biosynthesis of the myelin 2',3'-cyclic nucleotide 3'-phosphodiesterases. Journal of Neurochemistry 54:656–661.

Giulian D, Moore S (1980) Identification of 2':3'-cyclic nucleotide 3'-phosphodiesterase in the vertebrate retina. The Journal of Bological chemistryhemistry 255:5993–5995.

Goldman JE (1993) Both oligodendrocytes and astrocytes develop from progenitors in the subventricular zone of postnatal rat forebrain. Cell I:201–212.

Gravel M, DeAngelis D, Braun PE (1994) Molecular cloning and characterization of rat brain 2',3'-cyclic nucleotide 3'-phosphodiesterase isoform 2. Journal of Neuroscience Research 38:243–247.

Gravel M, Peterson J, Yong VW, Kottis V, Trapp B, Braun PE (1996) Overexpression of 2',3'-cyclic nucleotide 3'-phosphodiesterase in transgenic mice alters oligodendrocyte development and produces aberrant myelination. Molecular and Cellular Neurosciences 7:453–466.

Gravel M, Di Polo A, Valera PB, Braun PE (1998) Four-kilobase sequence of the mouse CNP gene directs spatial and temporal expression of lacZ in transgenic mice. Journal of Neuroscience Research 53:393–404.

Gravel M, Robert F, Kottis V, Gallouzi I-E, Pelletier J, Braun PE (2009) 2',3'-Cyclic nucleotide 3'-phosphodiesterase: a novel RNA-binding protein that inhibits protein synthesis. Journal of Neuroscience Research 87:1069–1079.

Greger IH, Ziff EB, Penn AC (2007) Molecular determinants of AMPA receptor subunit assembly. Trends in Neurosciences 30:407–416.

Groves AK, Barnett SC, Franklin RJ, Crang AJ, Mayer M, Blakemore WF, Noble M (1993) Repair of demyelinated lesions by transplantation of purified O-2A progenitor cells. Nature 362:453–455.

Gudz TI, Komuro H, Macklin WB (2006) Glutamate stimulates oligodendrocyte progenitor migration mediated via an alphav integrin/myelin proteolipid protein complex. The Journal of Neuroscience 26:2458–2466.

Guillemot F (2005) Cellular and molecular control of neurogenesis in the mammalian telencephalon. Current Opinion in Cell Biology 17:639–647.

Guo F, Ma J, McCauley E, Bannerman P, Pleasure D (2009) Early postnatal proteolipid promoter-expressing progenitors produce multilineage cells in vivo. The Journal of Neuroscience 29:7256–7270.

Guo F, Maeda Y, Ko EM, Delgado M, Horiuchi M, Soulika A, Miers L, Burns T, Itoh T, Shen H, Lee E, Sohn J, Pleasure D (2012) Disruption of NMDA receptors in oligodendroglial lineage cells does not alter their susceptibility to experimental autoimmune encephalomyelitis or their normal development. The Journal of Neuroscience 32:639–645.

Guo F, Maeda Y, Ma J, Xu J, Horiuchi M, Miers L, Vaccarino F, Pleasure D (2010) Pyramidal neurons are generated from oligodendroglial progenitor cells in adult piriform cortex. The Journal of Neuroscience 30:12036–12049.

Gyllensten L, Malmfors T (1963) Myelinization of the optic nerve and its dependence on visual function--a quantitative investigation in mice. Journal of Embryology and Experimental Morphology 11:255–266.

Hardy R, Reynolds R (1991) Proliferation and differentiation potential of rat forebrain oligodendroglial progenitors both in vitro and in vivo. Development 111:1061–1080.

Hartfuss E, Galli R, Heins N, Götz M (2001) Characterization of CNS precursor subtypes and radial glia. Developmental Biology 229:15–30.

Hartline DK, Colman DR (2007) Rapid conduction and the evolution of giant axons and myelinated fibers. Current Biology 17:R29–35.

Heaton PA, Eckstein F (1996) Diastereomeric specificity of 2',3'-cyclic nucleotide 3'-phosphodiesterase. Nucleic Acids Research 24:850–853.

Hirano A (1968) A confirmation of the oligodendroglial origin of myelin in the adult rat. The Journal of Cell Biology 4:32–34.

Horner PJ, Power AE, Kempermann G, Kuhn HG, Palmer TD, Winkler J, Thal LJ, Gage FH (2000) Proliferation and differentiation of progenitor cells throughout the intact adult rat spinal cord. The Journal of Neuroscience 20:2218–2228.

Hume RI, Dingledine R, Heinemann SF (1991) Identification of a site in glutamate receptor subunits that controls calcium permeability. Science (New York, NY) 253:1028–1031.

Jabs R, Pivneva T, Hüttmann K, Wyczynski A, Nolte C, Kettenmann H, Steinhäuser C (2005) Synaptic transmission onto hippocampal glial cells with hGFAP promoter activity. Journal of Cell Science 118:3791–3803.

Jessell TM (2000) Neuronal specification in the spinal cord: inductive signals and transcriptional codes. Nature Reviews Genetics 1:20–29.

Kang SH, Fukaya M, Yang JK, Rothstein JD, Bergles DE (2010) NG2+ CNS glial progenitors remain committed to the oligodendrocyte lineage in postnatal life and following neurodegeneration. Neuron 68:668–681.

Kessaris N, Fogarty M, Iannarelli P, Grist M, Wegner M, Richardson WD (2006) Competing waves of oligodendrocytes in the forebrain and postnatal elimination of an embryonic lineage. Nature Neuroscience 9:173–179.

Komitova M, Zhu X, Serwanski DR, Nishiyama A (2009) NG2 cells are distinct from neurogenic cells in the postnatal mouse subventricular zone. The Journal of Comparative Neurology 512:702–716.

Kondo T, Raff M (2000) Oligodendrocyte precursor cells reprogrammed to become multipotential CNS stem cells. Science 289:1754–1757.

Kosaka T, Hama K (1986) Three-dimensional structure of astrocytes in the rat dentate gyrus. The Journal of Comparative Neurology 249:242–260.

Kriegstein A, Alvarez-Buylla A (2009) The glial nature of embryonic and adult neural stem cells. Annual Review of Neuroscience 32:149–184.

Kriegstein AR, Götz M (2003) Radial glia diversity: a matter of cell fate. Glia 43:37–43.

Kukley M, Capetillo-Zarate E, Dietrich D (2007) Vesicular glutamate release from axons in white matter. Nature Neuroscience 10:311–320.

Kukley M, Dietrich D (2009) Kainate receptors and signal integration by NG2 glial cells. Neuron Glia Biology 5:13–20.

Kukley M, Kiladze M, Tognatta R, Hans M, Swandulla D, Schramm J, Dietrich D (2008) Glial cells are born with synapses. The FASEB journal 22:2957–2969.

Kukley M, Nishiyama A, Dietrich D (2010) The fate of synaptic input to NG2 glial cells: neurons specifically downregulate transmitter release onto differentiating oligodendroglial cells. The Journal of Neuroscience 30:8320–8331.

Kurihara T, Monoh K, Sakimura K, Takahashi Y (1990) Alternative splicing of mouse brain 2',3'-cyclic-nucleotide 3'-phosphodiesterase mRNA. Biochemical and Biophysical Research Communications 170:1074–1081.

Kurihara T, Tsukada Y (1967) The regional and subcellular distribution of 2 , 3 -cyclic nucleotide 3 -phosphohydrolase in the central nervous system. Journal of Neurochemistry 14:1167–1174.

Kurihara T, Tsukada Y (1968) 2',3'-Cyclic nucleotide 3'-phosphohydrolase in the developing chick brain and spinal cord. Journal of Neurochemistry 15:827–832.

Kurtz A, Zimmer A, Schnütgen F, Brüning G, Spener F, Müller T (1994) The expression pattern of a novel gene encoding brain-fatty acid binding protein correlates with neuronal and glial cell development. Development 120:2637–2649.

Laezza C, Wolff J, Bifulco M (1997) Identification of a 48-kDa prenylated protein that associates with microtubules as 2',3'-cyclic nucleotide 3'-phosphodiesterase in FRTL-5 cells. FEBS letters 413:260–264.

Lallemand Y, Luria V, Haffner-Krausz R, Lonai P (1998) Maternally expressed PGK-Cre transgene as a tool for early and uniform activation of the Cre site-specific recombinase. Transgenic Research 7:105–112.

Lappe-Siefke C, Goebbels S, Gravel M, Nicksch E, Lee J, Braun PE, Griffiths IR, Nave K-A (2003) Disruption of Cnp1 uncouples oligodendroglial functions in axonal support and myelination. Nature Genetics 33:366–374.

Lee J, Gravel M, Zhang R, Thibault P, Braun PE (2005) Process outgrowth in oligodendrocytes is mediated by CNP, a novel microtubule assembly myelin protein. The Journal of Cell Biology 170:661–673.

Levine JM, Stallcup WB (1987) Plasticity of developing cerebellar cells in vitro studied with antibodies against the NG2 antigen. The Journal of Neuroscience 7:2721–2731.

Levine JM, Stincone F, Lee YS (1993) Development and differentiation of glial precursor cells in the rat cerebellum. Glia 7:307–321.

Levison SW, Chuang C, Abramson BJ, Goldman JE (1993) The migrational patterns and developmental fates of glial precursors in the rat subventricular zone are temporally regulated. Development 119:611–622.

Levison SW, Young GM, Goldman JE (1999) Cycling cells in the adult rat neocortex preferentially generate oligodendroglia. Journal of Neuroscience Research 57:435–446.

Ligon KL, Kesari S, Kitada M, Sun T, Arnett HA, Alberta JA, Anderson DJ, Stiles CD, Rowitch DH (2006) Development of NG2 neural progenitor cells requires Olig gene function. Proceedings of the National Academy of Sciences of the United States of America 103:7853–7858.

Lin S-C, Bergles DE (2003) Physiological characteristics of NG2-expressing glial cells. Journal of Neurocytology 31:537–549.

Lin S-C, Huck JHJ, Roberts JDB, Macklin WB, Somogyi P, Bergles DE (2005) Climbing fiber innervation of NG2-expressing glia in the mammalian cerebellum. Neuron 46:773–785.

Lu QR, Sun T, Zhu Z, Ma N, Garcia M, Stiles CD, Rowitch DH (2002) Common developmental requirement for Olig function indicates a motor neuron/oligodendrocyte connection. Cell 109:75–86.

Lunn KF, Baas PW, Duncan ID (1997) Microtubule Organization and Stability in the Oligodendrocyte. The Journal of Neuroscience 17:4921–4932.

Mabie PC, Mehler MF, Marmur R, Papavasiliou A, Song Q, Kessler JA (1997) Bone morphogenetic proteins induce astroglial differentiation of oligodendroglial-astroglial progenitor cells. The Journal of Neuroscience 17:4112–4120.

Malatesta P, Appolloni I, Calzolari F (2008) Radial glia and neural stem cells. Cell and Tissue Research 331:165–178.

Malatesta P, Hack MA, Hartfuss E, Kettenmann H, Klinkert W, Kirchhoff F, Götz M (2003) Neuronal or glial progeny: regional differences in radial glia fate. Neuron 37:751–764.

Malatesta P, Hartfuss E, Götz M (2000) Isolation of radial glial cells by fluorescent-activated cell sorting reveals a neuronal lineage. Development 127:5253–5263.

Matthias K, Kirchhoff F, Seifert G, Huttmann K, Matyash M, Kettenmann H, Steinhauser C (2003) Segregated expression of AMPA-type glutamate receptors and glutamate transporters defines distinct astrocyte populations in the mouse hippocampus. Journal of Neuroscience 23:1750–1758.

McConnell SK, Kaznowski CE (1991) Cell cycle dependence of laminar determination in developing neocortex. Science 254:282.

Menn B, Garcia-Verdugo JM, Yaschine C, Gonzalez-Perez O, Rowitch D, Alvarez-Buylla A (2006) Origin of oligodendrocytes in the subventricular zone of the adult brain. The Journal of Neuroscience 26:7907–7918.

Miller RH (2002) Regulation of oligodendrocyte development in the vertebrate CNS. Progress in Neurobiology 67:451–467.

Miller RH, Payne J, Milner L, Zhang H, Orentas DM (1997) Spinal cord oligodendrocytes develop from a limited number of migratory highly proliferative precursors. Journal of Neuroscience Research 50:157–168.

Miller RH, Raff MC (1984) Fibrous and protoplasmic astrocytes are biochemically and developmentally distinct. The Journal of Neuroscience 4:585–592.

Mission JP, Takahashi T, Caviness VS (1991) Ontogeny of radial and other astroglial cells in murine cerebral cortex. Glia 4:138–148.

Molyneaux BJ, Arlotta P, Menezes JRL, Macklis JD (2007) Neuronal subtype specification in the cerebral cortex. Nature Reviews Neuroscience 8:427–437.

Monoh K, Kurihara T, Sakimura K, Takahashi Y (1989) Structure of mouse 2', 3'-cyclic-nucleotide 3'-phosphodiesterase gene. Biochemical and Biophysical Research Communications 165:1213–1220.

Monoh K, Kurihara T, Takahashi Y, Ichikawa T, Kumanishi T, Hayashi S, Minoshima S, Shimizu N (1993) Structure, expression and chromosomal localization of the gene encoding human 2',3'-cyclic-nucleotide 3'-phosphodiesterase. Gene 129:297–301.

Mullen RJ, Buck CR, Smith AM (1992) NeuN, a neuronal specific nuclear protein in vertebrates. Development 116:201–211.

Nishiyama A (2007) Polydendrocytes: NG2 cells with many roles in development and repair of the CNS. The Neuroscientist 13:62–76.

Nishiyama A, Chang A, Trapp BD (1999) NG2+ glial cells: a novel glial cell population in the adult brain. Journal of Neuropathology and Experimental Neurology 58:1113–1124.

Nishiyama A, Lin XH, Giese N, Heldin CH, Stallcup WB (1996) Co-localization of NG2 proteoglycan and PDGF alpha-receptor on O2A progenitor cells in the developing rat brain. Journal of Neuroscience Research 43:299–314.

Nishiyama A, Watanabe M, Yang Z, Bu J (2002) Identity, distribution, and development of polydendrocytes: NG2-expressing glial cells. Journal of neurocytology 31:437–455.

Nishiyama A, Yang Z, Butt A (2005) Astrocytes and NG2-glia: what's in a name? Journal of Anatomy 207:687–693.

Nishizawa Y, Kurihara T, Takahashi Y (1981) Immunohistochemical localization of 2', 3'-cyclic nucleotide 3'-phosphodiesterase in the central nervous system. Brain Research 212:219–222.

Nishizawa Y, Kurihara T, Takahashi Y (1982) Immunohistochemical localization of 2', 3'-cyclic nucleotide 3'-phosphodiesterase in the retina. Brain Research 251:384–387.

Noble M, Mayer-Pröschel M, Miller RH (2005) The oligodendrocyte, in: Developmental neurobiology 4th edition, edited by Rao MS and Jacobson M (Plenum Publishers, New York), 151–196.

Noctor SC, Flint AC, Weissman TA, Wong WS, Clinton BK, Kriegstein AR (2002) Dividing precursor cells of the embryonic cortical ventricular zone have morphological and molecular characteristics of radial glia. The Journal of Neuroscience 22:3161–3173.

Novak A, Guo C, Yang W, Nagy A, Lobe CG (2000) Z/EG, a double reporter mouse line that expresses enhanced green fluorescent protein upon Cre-mediated excision. Genesis 28:147–155.

Nunes MC, Roy NS, Keyoung HM, Goodman RR, McKhann G, Jiang L, Kang J, Nedergaard M, Goldman SA (2003) Identification and isolation of multipotential neural progenitor cells from the subcortical white matter of the adult human brain. Nature Medicine 9:439–447.

Ono K, Takebayashi H, Ikeda K, Furusho M, Nishizawa T, Watanabe K, Ikenaka K (2008) Regional- and temporal-dependent changes in the differentiation of Olig2 progenitors in the forebrain, and the impact on astrocyte development in the dorsal pallium. Developmental Biology 320:456–468.

O'Neill RC, Braun PE (2000) Selective synthesis of 2',3'-cyclic nucleotide 3'-phosphodiesterase isoform 2 and identification of specifically phosphorylated serine residues. Journal of Neurochemistry 74:540–546.

O'Neill RC, Minuk J, Cox ME, Braun PE, Gravel M (1997) CNP2 mRNA directs synthesis of both CNP1 and CNP2 polypeptides. Journal of Neuroscience Research 50:248–257.

Paukert M, Bergles DE (2006) Synaptic communication between neurons and NG2+ cells. Current Opinion in Neurobiology 16:515–521.

Paxinos G, Halliday G, Watson C, Koutcherov Y, Wang H (2007) Atlas of the developing mouse brain (Elsevier, Amsterdam).

Peyron F, Timsit S, Thomas JL, Kagawa T, Ikenaka K, Zalc B (1997) In situ expression of PLP/DM-20, MBP, and CNP during embryonic and postnatal development of the jimpy mutant and of transgenic mice overexpressing PLP. Journal of Neuroscience Research 50:190–201.

Polito A, Reynolds R (2005) NG2-expressing cells as oligodendrocyte progenitors in the normal and demyelinated adult central nervous system. Journal of Anatomy 207:707–716.

Pringle NP, Richardson WD (1993) A singularity of PDGF alpha-receptor expression in the dorsoventral axis of the neural tube may define the origin of the oligodendrocyte lineage. Development 117:525–533.

Pringle NP, Yu WP, Guthrie S, Roelink H, Lumsden A, Peterson AC, Richardson WD (1996) Determination of neuroepithelial cell fate: induction of the oligodendrocyte lineage by ventral midline cells and sonic hedgehog. Developmental Biology 177:30–42.

Psachoulia K, Jamen F, Young KM, Richardson WD (2009) Cell cycle dynamics of NG2 cells in the postnatal and ageing brain. Neuron Glia Biology 5:57–67.

Raff MC, Abney ER, Cohen J, Lindsay R, Noble M (1983a) Two types of astrocytes in cultures of developing rat white matter: differences in morphology, surface gangliosides, and growth characteristics. The Journal of Neuroscience 3:1289–1300.

Raff MC, Miller RH, Noble M (1983b) A glial progenitor cell that develops in vitro into an astrocyte or an oligodendrocyte depending on culture medium. Nature 303:390–396.

Rakic P (1974) Neurons in rhesus monkey visual cortex: systematic relation between time of origin and eventual disposition. Science 183:425–427.

Rao MS, Noble M, Mayer-Pröschel M (1998) A tripotential glial precursor cell is present in the developing spinal cord. Proceedings of the National Academy of Sciences of the United States of America 95:3996–4001.

Rasband MN, Tayler J, Kaga Y, Yang Y, Lappe-Siefke C, Nave K-A, Bansal R (2005) CNP is required for maintenance of axon-glia interactions at nodes of Ranvier in the CNS. Glia 50:86–90.

Rastogi SC, Clausen J (1985) Membrane-bound 2',3',-cyclic nucleotide 3'-phosphohydrolase activity of lymphocytes, granulocytes and erythrocytes in multiple sclerosis. Acta Neurologica Scandinavica 71:303–308.

Reynolds R, Hardy R (1997) Oligodendroglial progenitors labeled with the O4 antibody persist in the adult rat cerebral cortex in vivo. Journal of Neuroscience Research 47:455–470.

Reynolds R, Wilkin GP (1988) Development of macroglial cells in rat cerebellum. II. An in situ immunohistochemical study of oligodendroglial lineage from precursor to mature myelinating cell. Development 102:409–425.

Richardson WD, Pringle N, Mosley MJ, Westermark B, Dubois-Dalcq M (1988) A role for platelet-derived growth factor in normal gliogenesis in the central nervous system. Cell 53:309–319.

Richardson WD, Young KM, Tripathi RB, McKenzie I (2011) NG2-glia as multipotent neural stem cells: fact or fantasy? Neuron 70:661–673.

Rivers LE, Young KM, Rizzi M, Jamen F, Psachoulia K, Wade A, Kessaris N, Richardson WD (2008) PDGFRA/NG2 glia generate myelinating oligodendrocytes and piriform projection neurons in adult mice. Nature Neuroscience 11:1392–1401.

Rowitch DH, Kriegstein AR (2010) Developmental genetics of vertebrate glial-cell specification. Nature 468:214–222.

Salzer JL (2003) Polarized domains of myelinated axons. Neuron 40:297–318.

Sarma AA, Richard MB, Greer CA (2011) Developmental dynamics of piriform cortex. Cerebral Cortex 21:1231–1245.

Sauer F (1935) Mitosis in the neural tube. The Journal of Comparative Neurology 62:377–405.

Scherer SS, Braun PE, Grinspan J, Collarini E, Wang D, Kamholz J (1994) Differential regulation of the 2 ' -phosphodiesterase gene during oligodendrocyte development. Cell 12:1363–1375.

Sheedlo HJ, Doran JE, Sprinkle TJ (1984) An investigation of 2':3'-cyclic nucleotide 3'-phosphodiesterase (EC 3.1.4.37, CNP) in peripheral blood elements and CNS myelin. Life Sciences 34:1731–1737.

Shimshek DR, Jensen V, Celikel T, Geng Y, Schupp B, Bus T, Mack V, Marx V, Hvalby Ø, Seeburg PH, Sprengel R (2006) Forebrain-specific glutamate receptor B deletion impairs spatial memory but not hippocampal field long-term potentiation. The Journal of Neuroscience 26:8428–8440.

Skoff RP (1990) Gliogenesis in rat optic nerve: astrocytes are generated in a single wave before oligodendrocytes. Developmental Biology 139:149–168.

Snyder DS, Zimmerman TR, Farooq M, Norton WT, Cammer W (1983) Carbonic anhydrase, 5'-nucleotidase, and 2',3'-cyclic nucleotide-3'-phosphodiesterase activities in oligodendrocytes, astrocytes, and neurons isolated from the brains of developing rats. Journal of Neurochemistry 40:120–127.

Spassky N, Goujet-Zalc C, Parmantier E, Olivier C, Martinez S, Ivanova A, Ikenaka K, Macklin W, Cerruti I, Zalc B, Thomas JL (1998) Multiple restricted origin of oligodendrocytes. The Journal of Neuroscience 18:8331–8343.

Sprinkle TJ (1989) 2',3'-cyclic nucleotide 3'-phosphodiesterase, an oligodendrocyte-Schwann cell and myelin-associated enzyme of the nervous system. Critical Reviews in Neurobiology 4:235–301.

Sprinkle TJ, Lanclos KD, Lapp DF (1992) Assignment of the human 2',3'-cyclic nucleotide 3'-phosphohydrolase gene to chromosome 17. Genomics 13:877–880.

Sprinkle TJ, McMorris FA, Yoshino J, DeVries GH (1985) Differential expression of 2':3'-cyclic nucleotide 3'-phosphodiesterase in cultured central, peripheral, and extraneural cells. Neurochemical Research 10:919–931.

Sprinkle TJ, Zaruba ME, McKhann GM (1978) Activity of 2',3'-cyclic-nucleotide 3'-phosphodiesterase in regions of rat brain during development: quantitative relationship to myelin basic protein. Journal of Neurochemistry 30:309–314.

Srinivas S, Watanabe T, Lin CS, William CM, Tanabe Y, Jessell TM, Costantini F (2001) Cre reporter strains produced by targeted insertion of EYFP and ECFP into the ROSA26 locus. BMC Developmental Biology 1:4.

Stallcup WB, Beasley L (1987) Bipotential glial precursor cells of the optic nerve express the NG2 proteoglycan. The Journal of Neuroscience 7:2737–2744.

Stegmüller J, Werner H, Nave K-A, Trotter J (2003) The proteoglycan NG2 is complexed with alpha-amino-3-hydroxy-5-methyl-4-isoxazolepropionic acid (AMPA) receptors by the PDZ glutamate receptor interaction protein (GRIP) in glial progenitor cells. Implications for glial-neuronal signaling. The Journal of Biological Chemistry 278:3590–3598.

Stingo S, Masullo M, Polverini E, Laezza C, Ruggiero I, Arcone R, Ruozi E, Dal Piaz F, Malfitano AM, D'Ursi AM, Bifulco M (2007) The N-terminal domain of 2',3'-cyclic nucleotide 3'-phosphodiesterase harbors a GTP/ATP binding site. Chemical Biology & Drug Design 70:502–510.

Sturrock RR (1980) Myelination of the mouse corpus callosum. Neuropathology and Applied Neurobiology 6:415–420.

Sugimoto Y, Taniguchi M, Yagi T, Akagi Y, Nojyo Y, Tamamaki N (2001) Guidance of glial precursor cell migration by secreted cues in the developing optic nerve. Development 128:3321–3330.

Suzuki N, Bekkers JM (2007) Inhibitory interneurons in the piriform cortex. Clinical and Experimental Pharmacology & Physiology 34:1064–1069.

Timsit S, Martinez S, Allinquant B, Peyron F, Puelles L, Zalc B (1995) Oligodendrocytes originate in a restricted zone of the embryonic ventral neural tube defined by DM-20 mRNA expression. The Journal of Neuroscience 15:1012–1024.

Tong X, Li X, Zhou B, Shen W, Zhang Z, Xu T, Duan S (2009) Ca(2+) signaling evoked by activation of Na(+) channels and Na(+)/Ca(2+) exchangers is required for GABA-induced NG2 cell migration. The Journal of Cell Biology 186:113–128.

Trapp BD, Bernier L, Andrews SB, Colman DR (1988) Cellular and subcellular distribution of 2',3'-cyclic nucleotide 3'-phosphodiesterase and its mRNA in the rat central nervous system. Journal of Neurochemistry 51:859–868.

Trapp BD, Nishiyama A, Cheng D, Macklin W (1997) Differentiation and death of premyelinating oligodendrocytes in developing rodent brain. The Journal of Cell Biology 137:459–468.

Tripathi RB, Rivers LE, Young KM, Jamen F, Richardson WD (2010) NG2 glia generate new oligodendrocytes but few astrocytes in a murine experimental autoimmune encephalomyelitis model of demyelinating disease. The Journal of Neuroscience 30:16383–16390.

Vallstedt A, Klos JM, Ericson J (2005) Multiple dorsoventral origins of oligodendrocyte generation in the spinal cord and hindbrain. Neuron 45:55–67.

Ventura R, Harris KM (1999) Three-dimensional relationships between hippocampal synapses and astrocytes. The Journal of Neuroscience 19:6897–6906.

Verkhratsky A, Steinhäuser C (2000) Ion channels in glial cells. Brain Research Reviews 32:380–412.

Vogel U, Thompson R (1988) Molecular structure, localization, and possible functions of the myelin-associated enzyme 2 , 3 -cyclic nucleotide 3 -phosphodiesterase. Journal of Neurochemistry 50:1667–1677.

Voigt T (1989) Development of glial cells in the cerebral wall of ferrets: direct tracing of their transformation from radial glia into astrocytes. The Journal of Comparative Neurology 289:74–88.

Voyvodic JT (1996) Cell death in cortical development: How much? Why? So what? Neuron 16:693–696.

Wake H, Lee PR, Fields RD (2011) Control of local protein synthesis and initial events in myelination by action potentials. Science 333:1647–1651.

Wang E, Cambi F (2012) MicroRNA expression in mouse oligodendrocytes and regulation of proteolipid protein gene expression. Journal of Neuroscience Research 90:1701–1712.

Warf BC, Fok-Seang J, Miller RH (1991) Evidence for the ventral origin of oligodendrocyte precursors in the rat spinal cord. The Journal of Neuroscience 11:2477–2488.

Weissbarth S, Maker HS, Raes I, Brannan TS, Lapin EP, Lehrer GM (1981) The activity of 2',3'-cyclic nucleotide 3'-phosphodiesterase in rat tissues. Journal of Neurochemistry 37:677–680.

Whitfeld PR, Heppel LA, Markham R (1955) The enzymic hydrolysis of ribonucleoside-2':3' phosphates. The Biochemical journal 60:15–19.

Xiang Z, Chen M, Ping J, Dunn P, Lv J, Jiao B, Burnstock G (2006) Microglial morphology and its transformation after challenge by extracellular ATP in vitro. Journal of Neuroscience Research 83:91–101.

Yin X, Peterson J, Gravel M, Braun PE, Trapp BD (1997) CNP overexpression induces aberrant oligodendrocyte membranes and inhibits MBP accumulation and myelin compaction. Journal of Neuroscience Research 50:238–247.

Yu WP, Collarini EJ, Pringle NP, Richardson WD (1994) Embryonic expression of myelin genes: evidence for a focal source of oligodendrocyte precursors in the ventricular zone of the neural tube. Neuron 12:1353–1362.

Yuan X, Chittajallu R, Belachew S, Anderson S, McBain CJ, Gallo V (2002) Expression of the green fluorescent protein in the oligodendrocyte lineage: a transgenic mouse for developmental and physiological studies. Journal of Neuroscience Research 70:529–545.

Yuan X, Eisen AM, McBain CJ, Gallo V (1998) A role for glutamate and its receptors in the regulation of oligodendrocyte development in cerebellar tissue slices. Development 125:2901–2914.

Yun K, Fischman S, Johnson J, Hrabe de Angelis M, Weinmaster G, Rubenstein JLR (2002) Modulation of the notch signaling by Mash1 and Dlx1/2 regulates sequential specification and differentiation of progenitor cell types in the subcortical telencephalon. Development 129:5029–5040.

Zawadzka M, Rivers LE, Fancy SPJ, Zhao C, Tripathi R, Jamen F, Young K, Goncharevich A, Pohl H, Rizzi M, Rowitch DH, Kessaris N, Suter U, Richardson WD, Franklin RJM (2010) CNS-resident glial progenitor/stem cells produce Schwann cells as well as oligodendrocytes during repair of CNS demyelination. Cell Stem Cell 6:578–590.

Zhao C, Deng W, Gage FH (2008) Mechanisms and functional implications of adult neurogenesis. Cell 132:645–660.

Zhao X, He X, Han X, Yu Y, Ye F, Chen Y, Hoang T, Xu X, Mi Q-S, Xin M, Wang F, Appel B, Lu QR (2010) MicroRNA-mediated control of oligodendrocyte differentiation. Neuron 65:612–626.

Zhu X, Bergles DE, Nishiyama A (2008a) NG2 cells generate both oligodendrocytes and gray matter astrocytes. Development 135:145–157.

Zhu X, Hill RA, Dietrich D, Komitova M, Suzuki R, Nishiyama A (2011) Age-dependent fate and lineage restriction of single NG2 cells. Development 138:745–753.

Zhu X, Hill RA, Nishiyama A (2008b) NG2 cells generate oligodendrocytes and gray matter astrocytes in the spinal cord. Neuron Glia Biology 4:19–26.

Ziskin JL, Nishiyama A, Rubio M, Fukaya M, Bergles DE (2007) Vesicular release of glutamate from unmyelinated axons in white matter. Nature Neuroscience 10:321–330.

Erklärung

Hiermit erkläre ich, dass ich die vorliegende Doktorarbeit selbständig angefertigt habe. Es wurden nur die in der Arbeit ausdrücklich benannten Quellen und Hilfsmittel be-nutzt. Wörtlich oder sinngemäß übernommenes Gedankengut habe ich als solches kenntlich gemacht.

_____   _____

Ort, Datum   Unterschrift